



LiBRARY Michigan State University

This is to certify that the

dissertation entitled
A model of the human upper extremity
and its application to a baseball
pitching motion

presented by

Byeong Hwa Ahn

has been accepted towards fulfillment of the requirements for

Ph.D. degree in Physical Education and Exercise Science

Major professor

Date 3/11/91

A Section of the second section of the section of th

PLACE IN RETURN BOX to remove this checkout from your record. TO AVOID FINES return on or before date due.

DATE DUE	DATE DUE	DATE DUE	
	AUG 1 5 2009 5		
क्षित्रश्च स्थ			
007 ₀₅			

MSU is An Affirmative Action/Equal Opportunity Institution

A MODEL OF THE HUMAN UPPER EXTREMITY AND ITS APPLICATION TO A BASEBALL PITCHING MOTION

Ву

Byeong Hwa Ahn

A DISSERTATION

Submitted to
Michigan State University
in partial fulfillment of the requirements
for the degree of

DOCTOR OF PHILOSOPHY

Department of Physical Education and Exercise Science

ABSTRACT

A MODEL OF THE HUMAN UPPER EXTREMITY AND ITS APPLICATION TO A BASEBALL PITCHING MOTION

By

Byeong Hwa Ahn

The purposes of the study were to create a mathematical model of the human upper extremity and to apply the model to the acceleration phase of the fast baseball pitching motion. Angular trajectories at the elbow and wrist joints in the fast baseball pitching were generated experimentally by a three-dimensional cinematographic technique and theoretically by simulation and optimization techniques.

The mathematical model was applied to generate

a) angular trajectories that closely matched the

experimental trajectories at the elbow and wrist joint and

b) optimal angular trajectories that maximize the velocity

of the hand at the release of the ball. The mathematical

model was also used to investigate the roles of elbow and

wrist joint muscles in baseball pitching.

The model of the human upper extremity, created in this study was considered to closely simulate the experimental angular trajectories at the elbow and wrist joint in the pitching motion.

The hand velocity at the release of the ball was approximately 80 percent of the experimental result when the resultant elbow joint torque was set to zero, approximately 95 percent of the experimental result when the resultant wrist joint torque was set to zero, and approximately 75 percent of the experimental result when both the resultant elbow and wrist joint torques were set to zero.

Velocity of the ball at release in pitching was primarily generated by body parts other than the upper extremity. Therefore, the optimal angular trajectory of the pitching arm that can be obtained from simulation and/or optimization is not the true optimal angular trajectory unless the motion of the other body parts is optimal.

Dedicated to my mom and dad who modeled for me
the importance of hardwork toward
a far-reaching goal.

ACKNOWLEDGMENTS

I am gratefully indebted to my wife, Hyunsook, for her moral support, lasting patience and invaluable assistance throughout the whole years of Ph.D. study at Michigan State University. I doubt whether I could have completed this degree without her. I express my appreciation to my parents-in-law for their encouragement and continued patience for so many years. I feel sorry for my lovely son, Kwangchan. I was not a good dad!

I wish to thank the members of my committee for their efforts. I would particularly like to express my appreciation to Dr. Brown for his friendship and for providing a research assistantship through the Youth Sports Institute and to Dr. Mase for helping to formulate the mathematical model.

Special thanks to Mr. Bob Wells who helped me to setup the experimental equipment and to Mr. Dan O'Brien who served as a subject and gave me valuable comments on the practical aspect of baseball pitching.

I wish to extend my sincere appreciation and thanks to the unforgettable individuals who helped me in various ways while I was in the United States; Dr. Widule who always lives in my mind as a teacher and friend and Mr. and Mrs.

Gillengerten who were friendly in helping my wife and I.

I do wish to acknowledge my friends; Dan Wilson, Kicheon Lee, Kihong Kim, and Yongjin Yoon.

TABLE OF CONTENTS

<u>.g</u>	age
LIST OF TABLES	x
LIST OF FIGURES	хi
<u>Chapter</u>	
I. INTRODUCTION	1
Statement of the problem	7 7
II. REVIEW OF RELATED LITERATURE	11
I. Biomechanical Aspects of the Upper Extremity. A. Elbow Joint and Forearm 1. Analysis of motion 2. Prime flexors and extensors of the elbow and pronators and supinators of the forearm B. Wrist Joint 1. Analysis of motion 2. Prime flexors and extensors of the wrist II. Optimization and Simulation in Biomechanics A. Optimization in Biomechanics B. Simulation in Biomechanics III. Throwing A. Baseball Pitching B. Electromyographic Study of Elbow and Wrist Joint Muscles in the Throwing Motion	11 11 13 16 16 16 16 18 19 20
III. METHODS	24
I. Rigid-body Dynamics of the Upper ExtremityA. Bones of Upper ExtremityB. Axes of Rotation for Upper Extremity	24
segments	26 29

	D. Euler's Angles and Transformation	
	Matrices	31
	E. Position Vectors, Linear Velocities,	
		35
		37
	G. Lagrange's Equations for Upper Extremity	
		38
	H. Generalized Forces	4 C
	I. Location of Center of Mass and Mass	
		42
		45
		45
	Moments of inertia of forearm	45
	3. Moments of inertia of the radius bone.	46
		49
TT		50
тт.		
		52
	B. Selection of Muscle Model	52
	C. Moment Arms	61
	1. Moment arms with respect to elbow	
		62
		U Z
	2. Moment arms with respect to wrist	
		63
	D. Muscle Length	64
	1. Length of muscles with respect to	
		65
	2. Length of muscles with respect to elbow	-
	joint angle and/or wrist joint angle	65
T17 CT1	MILLANTON AND ODMINICAMION	7.
14. 21	MULATION AND OPTIMIZATION	70
I.	Determination of Constants and Parameter	
	Values	70
		70
		72
		79
		79
	2. Experimental trajectories	92
		93
TT.		97
		01
TTT.	Optimization	U
V. RES	SULTS AND DISCUSSION 1	04
Т.	Experimental Results	04
	A. Velocities of the Ball and Hand at	0 4
		_
		04
	B. Kinematics of the Elbow and Wrist Joints	
	during the Acceleration Phase 1	05
		_

	C. Kinematics of the Forearm during the	
	Acceleration	110
II.	Simulation Results	111
	Conclusion	129
III.	Recommendations	131
BIBLI	OGRAPHY	133

LIST OF TABLES

<u>Table</u>		pac	<u>ie</u>
3-1.	Segmental mass distribution as ratios to total body mass		42
3-2.	Location of the center of segmental mass from the proximal end as ratios of total segment lengths	• •	43
3-3.	Coefficients for the center of segmental mass and mass distribution	• •	44
3-4.	Coefficients for the moments of inertia of the upper arm	• •	45
3-5.	Coefficients for the moments of inertia of the forearm	• •	45
4-1.	Length and weight measurements from the subject	• •	71
4-2.	Width measurements from the subject	• •	71
4-3.	Circumference measurements from the subject	• •	72
4-4.	Muscle structure	• •	75
4-5.	Fiber angle	• •	76
4-6.	Physiological cross-sectional area (mm ²) of muscles		78
4-7.	Constants of passive joint torque function		96

LIST OF FIGURES

Figure	<u>e</u>	age
1-1.	Elbow angle	8
1-2.	Wrist angle	10
3-1.	Anterior view of the skeletal system of the right upper extremity	25
3-2.	Anterior view of the skeletal system of the right upper arm	27
3-3.	Anterior view of the skeletal system of the right forearm and hand	28
3-4.	Mathematical model of the upper extremity	30
3-5.	Euler angles	32
3-6.	Frustum of right circular cone	47
3-7.	Model of the hand and ball	51
3-8.	Prime elbow flexor muscles	53
3-9.	Prime elbow extensor muscles	54
3-10.	Prime elbow and wrist flexors and forearm pronator muscles	55
3-11.	Prime elbow and wrist extensors and forearm supinator muscles	56
3-12.	Model for approximating supinator muscle length variations	68
4-1.	Anatomical geometry of the subject's forearm	74
4-2.	Calibration structure	81
4-3.	Targets on the upper extremity	82
4-4	Geometry of the upper arm targets	85

4-5.	Spatial geometry of the upper arm targets	86
4-6.	Simplified block diagram of the simulation of one muscle	100
5-1.	Experimental angular trajectory of the elbow joint during the acceleration phase	106
5-2.	Experimental angular trajectory of the wrist joint during the acceleration phase	106
5-3.	Experimental angular velocity at the elbow during the acceleration phase	108
5-4.	Experimental angular velocity at the wrist during the acceleration phase	108
5-5.	Experimental angular trajectory of the forearm for pronation-supination during the acceleration phase	110
5-6.	Simulated and experimental angular trajectories of the elbow joint during the acceleration phase	113
5-7.	Simulated and experimental angular trajectories of the wrist joint during the acceleration phase	113
5-8.	Simulated resultant elbow joint torque during the acceleration phase	115
5-9.	Simulated resultant wrist joint torque during the acceleration phase	115
5-10.	Optimal and simulated angular trajectories of the elbow joint during the acceleration phase	117
	Optimal and simulated angular trajectories of the wrist joint during the acceleration phase	117
5-12.	Simulated resultant elbow joint torque and optimal resultant elbow joint torque for optimal angular trajectory of the elbow joint during the acceleration phase	118
5-13.	Simulated resultant wrist joint torque and optimal resultant wrist joint torque for optimal angular trajectory of the wrist joint during the acceleration phase	118
5-14.	Control parameter pattern of the elbow joint extensor muscles during the acceleration phase	120

5-15.	Control parameter pattern of the elbow joint flexor muscles during the acceleration phase	120
5-16.	Control parameter pattern of the wrist joint flexor muscles during the acceleration phase	121
5-17.	Control parameter pattern of the wrist joint extensor muscles during the acceleration phase	121
5-18.	Predicted angular trajectory of the elbow joint during an acceleration phase of 0.0325 seconds	124
5-19.	Predicted angular trajectory of the wrist joint during an acceleration phase of 0.0325 seconds	124
5-20.	Predicted resultant elbow joint torque during an acceleration phase of 0.0325 seconds	125
5-21.	Predicted resultant wrist joint torque during an acceleration phase of 0.0325 seconds	125
5-22.	Simulated angular trajectory of the elbow joint and predicted angular trajectory of the elbow joint with the resultant elbow joint torque set to zero	127
5-23.	Simulated angular trajectory of the wrist joint joint and predicted angular trajectory of the wrist joint with the resultant wrist joint torque set to zero	127
5-24.	Simulated angular trajectory of the elbow joint and predicted angular trajectory of the elbow joint with the resultant joint torques of both the elbow and wrist joints set to zero	128
5-25.	Simulated angular trajectory of the wrist joint and predicted angular trajectory of the wrist joint with the resultant joint torques of both the elbow and wrist joints set to zero	128

CHAPTER I

INTRODUCTION

Biomechanics is the application of mechanics to biology (Fung, 1981). Biomechanics as an area common to mechanics, materials, physical medicine, orthopaedic surgery, dentistry, prosthetics, rehabilitation, injury prevention, ergonomics, sports, and others is interwoven and thus difficult to define (Fung, 1972; Huiskes, 1982).

It is colored differently by its many fields of application and the backgrounds of its disciplinaries. It partly overlaps sciences such as biomaterials, medical physics and biophysics, physiology, and functional anatomy. It can be regarded as a subbranch of biomedical engineering (or bioengineering) and a branch of biomechanical engineering. What biomechanics is or becomes depends on the spirits and efforts of those who sail under its flag, rather than a rigid application of definitions. (Huiskes, 1982, p. ix)

Biomechanics applied to the analysis of gross human motions such as walking, running, and sports activities can be studied by the principle of rigid-body dynamics, that is typically solved by the inverse dynamics or direct dynamics approach (Crowninshield, 1980; King, 1984). The inverse dynamics problem computes resultant muscular forces and moments from observed kinematics and/or measured external forces (Zatsiorsky, 1978; Crowninshield and Brand, 1980; Zajac and Gordon, 1989). This inverse dynamics problem

has been applied extensively to the study of sports skills since the studies of Plagenhoef (1966, 1968, 1971) and Dillman (1970, 1971). The application of this inverse dynamics approach to sport motions, however, has a serious drawback. It is descriptive. It analyzes only existing movement patterns because the input is the data that are recorded from existing motions.

The direct dynamics approach computes kinematics, with muscular forces or moments prescribed. It is predictive. The predictive approach of modeling is stronger or better than the descriptive approach since it is especially useful for identifying and examining causal factors influencing human performance and finding the best movement pattern (Redfield and Hull, 1986). The direct dynamics problem that is theory-oriented can be solved by simulation or optimization.

Currently, most of the research in sports biomechanics, for training and coaching high performance athletes, is conducted in a descriptive or comparative manner (Nigg, 1982). Dillman (1985) stated that:

present biomechanical evaluations are generally conducted by comparing an athlete's style to the best in the world. The assumption of these comparative analyses is that elite athletes through years and years of practice have optimized their performance and that their techniques can serve as criteria in the evaluation of skill. (p. 108)

Sprigings (1986) pointed out the limitation of this comparative approach as follows:

The biomechanist would be in a very good position to help up-and-coming athletes by comparing their movement patterns to those that are successfully employed by highly skilled performers. But, when it came to trying to help the elite athlete, he would be at a The biomechanist would have no way of knowing loss. whether the elite athlete's technique could be improved, since his present analytical methods require comparison with someone of significantly higher skill level in order to provide the insight into what is possible. The only solution to this very real problem in present-day sport biomechanics is mathematically to model the human body so that subsequent forward dynamic computer simulation can be performed. (p. 5)

Hatze (1984) also raised criticism of the research approach currently being employed. He stated that the vast majority of motion analyses carried out today should be called 'motion descriptions' or 'motion comparisons'. True motion analysis would imply that inferences can be made based on neural control processes and performance criteria that generated the observed motion.

Recently, biomechanical studies in sports have become more directed toward modeling (Hubbard and Barlow, 1980; Nigg, 1982). However, most studies of the optimization or simulation of human movements, including sports skills, have used resultant muscular torques as input without directly considering muscle mechanics as part of the model (Ghosh and Boykin, 1976; Hubbard and Barlow, 1980). The optimization or simulation of human motion, without considering individual muscles that may be able to explain individual differences in movement patterns in sports skills, may not be enough to improve the highly skilled athlete's performance though it is suitable for the gross motion

studies such as automobile crash response, aerospace related problems, and other engineering applications.

Variations in human motion stem from both anatomical and physiological differences. These variations may be very important factors in determining individual differences in movement patterns associated with performances of sports skills. Amis (1978) and Amis et al. (1979), in their studies of four cadaver limbs, reported wide variations in the size ratios of muscles from limb to limb, while the musculo-skeletal geometry was basically similar from limb to limb. Very few investigators, however, have included the muscular control mechanisms in their models because of the difficulties in constructing control models of skeletal muscle (Hatze, 1980).

In order to gain insight into how to improve the highly skilled athlete's performance, sports biomechanics badly needs delicate control models of skeletal muscle. Hatze has pioneered this area of study with the development of a mathematical model of the human musculo-skeletal system and a control model of skeletal muscle behavior based upon physiological phenomena (Dillman, 1985). His model successfully optimized or simulated the kicking motion and the take-off phase of the long jump (Hatze, 1975, 1976, 1977, 1981, 1983).

The human body is the most sophisticated and dynamic system in the world. Formulation of a dynamic model that acts as a real human being may be beyond human ability.

It is also theoretically impossible to validate completely a model under all test conditions because the purpose of a mathematical model is the prediction of behavior in unknown situations (Panjabi, 1979). There is, however, no doubt that dynamic mathematical models of the human body will play a very significant role in understanding how the body moves (Peindl and Engin, 1987).

Dynamic modeling is one of the most interesting and challenging areas of biomechanics. With improvements in models of skeletal muscle and the musculo-skeletal system and the development of biomedical instrumentation, dynamic modeling is getting closer to the simulation of human motion. The development of biomedical instrumentation, such as nuclear magnetic resonance (NMR), that can measure individual-specific anatomical and physiological characteristics, will play a very important role in practically supporting the application of a theoretical model to the coaching and training of athletes.

Dynamic modeling of baseball pitching, one of the most dynamic and fascinating human motions, may be useful for training and coaching baseball pitchers to improve pitching ability and to study injury prevention, if it can be done. Baseball pitching is accomplished by a sequential interaction of the body segments, through a link system from the foot to the throwing hand (Pappas et al., 1985; Moynes et al., 1986). A mathematical model of a baseball pitcher could represent the whole body or be restricted to the

throwing arm (Hubbard and Barlow, 1980). A mathematical model of the whole body, including individual muscles, is incredibly complicated and lengthy (Hatze, 1981). It is beyond the scope of this study.

The shoulder complex is the most complicated and least successfully modeled among the major joints of the human It is composed of four joints (sternoclavicular, acromioclavicular, scapulothoracic, and glenohumeral) (Kent, 1971; Dvir and Berme, 1978; Engin and Chen, 1986). Twentyone muscles act on the shoulder complex. Among these muscles, twelve are connected to the body from the scapula (Högfors et al., 1987). The glenohumeral joint, the socalled shoulder joint, is the most mobile of all joints in Its movements can not be separated from those the body. of the shoulder complex because all joints and bones in the shoulder complex function interdependently to generate arm There is also a paucity of information on the movement. dynamic modeling of the shoulder complex. Therefore, the scope of this study will be limited to the motion of the elbow and wrist joints of the pitching arm, under the condition that the influence of other parts of body on pitching is considered as input data and can be obtained by three-dimensional cinematographic techniques.

The application of optimization theory to find optimal trajectory of a sport motion, that is essential for training an athlete, is one of the major objectives of sports biomechanics (Hatze, 1981). However, dynamic optimization

theory is still in the developing stage because of the limitations of optimization methods currently applied in analyzing such complex systems as human motions that are highly nonlinear and large in dimension (Zatsiorsky, 1978; Hatze, 1981, 1984).

STATEMENT OF THE PROBLEM

The purposes of this study were to a) create a mathematical model of the human upper extremity that is applicable to most gross human upper extremity motions and b) apply the model to the baseball pitching motion, trying to find the optimal angular trajectories of the elbow and wrist joints to maximize the velocity of the pitching hand at the release of the ball.

DEFINITIONS OF TERMS

The following terms, that are frequently used in this dissertation, are defined to assist the reader.

Acceleration phase of the baseball pitching motion - A movement of the pitching arm from the maximum external rotation of the upper arm to the release of the ball.

Anatomical position - A position in which the body is erect, facing the observer, and arms are at the side with the palms of the hands facing forward.

Angular trajectory - A changing pattern of the angle of the elbow or wrist with respect to time.

Carrying angle - A angle formed between the longitudinal axis of the humerus and the longitudinal axis of the forearm when the upper extremity is in the anatomical position.

Elbow angle - ψ_2 in Figure 1-1.

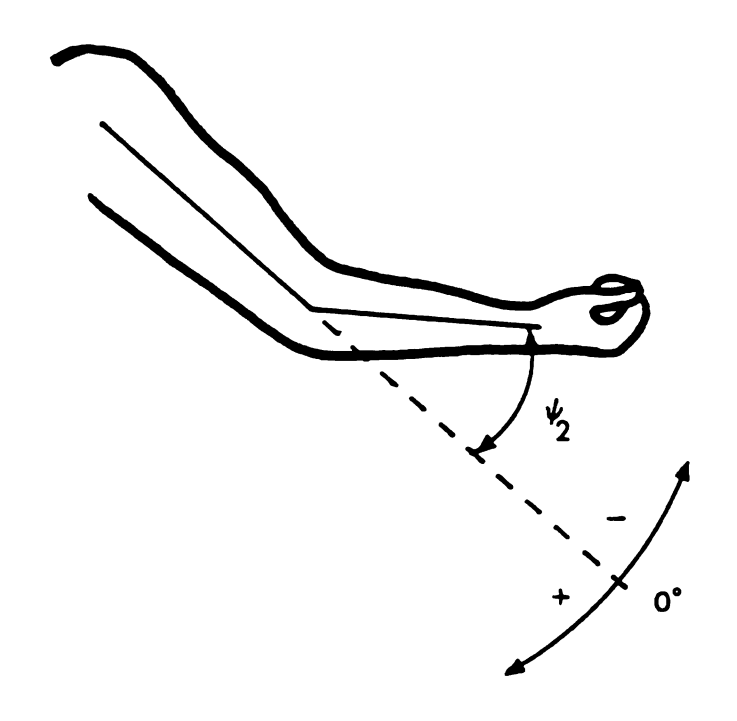


Figure 1-1. Elbow angle.

<u>Elbow extension</u> - A movement that increases the angle between the upper arm and the forearm.

Elbow flexion - A movement that decreases the angle between the upper arm and the forearm.

<u>Experimental angular trajectory</u> - An angular trajectory obtained experimentally from the subject.

<u>Forearm pronation</u> - An inward rotation of the forearm.

<u>Forearm supination</u> - An outward rotation of the forearm.

<u>Instantaneous center of rotation</u> - The immovable point generated at an instant time by one segment of a rigid-body rotating about an adjacent segment.

Optimal angular trajectory - An angular trajectory generated by simulation or optimization so that the velocity of the pitching hand at the release of the ball is maximized.

<u>Predicted angular trajectory</u> - An angular trajectory obtained from simulation.

Radio-ulna deviation - A movement of the hand from anatomical position either away from the body (thumb side leading) or toward the body (little finger side leading).

<u>Simulated angular trajectory</u> - An angular trajectory generated so that a predicted angular trajectory closely matches the experimental angular trajectory.

Tracking parameters - Distances, velocities, and the accelerations of the upper arm that were obtained from the cinematographic analyses to describe the subject's pitching motion.

Upper arm - The humerus bone and its surrounding soft tissue between the shoulder and elbow. It should be noted that the 'arm', technically meaning the humerus bone and its surrounding soft tissue in medical terminology, is called the upper arm in this dissertation.

Wrist angle - ψ_4 in Figure 1-2.

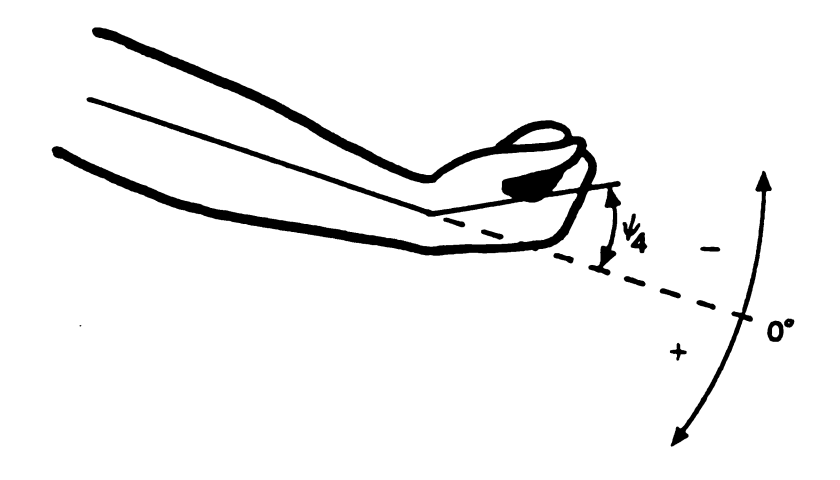


Figure 1-2. Wrist angle.

<u>Wrist extension</u> - A return movement from the wrist flexion.

<u>Wrist flexion</u> - A movement in which the palmar surface of the hand approaches the anterior surface of the forearm.

CHAPTER II

REVIEW OF RELATED LITERATURE

- I. BIOMECHANICAL ASPECTS OF THE UPPER EXTREMITY
- A. Elbow Joint and Forearm

1. Analysis of motion

The forearm has two degrees of freedom:

flexion-extension and pronation-supination (Morrey et al.,
1976; Chao et al., 1980; Cochran, 1982; Torzilli, 1982;

Engin and Chen, 1987). The axis of rotation of elbow

flexion-extension (see Figure 3-2) passes through the

centers of the humeral trochlea and capitulum (Morrey et
al., 1976; Chao and Morrey, 1978; London and Pedro, 1981;

Torzilli, 1982).

The instantaneous centers of rotation for elbow flexion-extension lies within an area 3 mm in diameter (Morrey et al., 1976; Chao and Morrey, 1978; London, 1981). The curved portions of the trochlea and capitulum are considered to be circular in cross section (Youm et al., 1979; Shiba and Sorbie, 1985). Therefore, the concept of the single axis of rotation for elbow flexion-extension is supported by most investigators (Morrey et al., 1976; Chao and Morrey, 1978; Youm et al., 1979; London, 1981; Cochran, 1982; Torzilli, 1982).

The axis of rotation for elbow flexion-extension is slightly oblique to the longitudinal axis of the humerus. The long axis of the ulna deviates laterally and distally from the long axis of the humerus as the elbow joint is fully extended. The carrying angle formed between the long axis of the humerus and the long axis of the forearm varies during flexion-extension. It has been controversely reported that the carrying angle varies linearly (Morrey and Chao, 1976; Chao and Morrey, 1978; Youm et al., 1979) or sinusoidally (Amis et al., 1977; Youm, 1980) during elbow flexion-extension. On the other hand, London (1981) stated that the carrying angle remains constant throughout the whole range of elbow flexion. The carrying angle may depend on individual variation. The carrying angle lies within 15 degrees in males (Morrey and Chao, 1976; Amis et al., 1977; London, 1981; An et al., The range of elbow flexion-extension is limited by 1985). the geometry of the joint surfaces and surrounding bone, by passive supporting structures represented by the collateral, capsular and other ligaments and by the active muscular structures represented by muscles and tendons (Cochran, 1982). The range of elbow flexion-extension is approximately 150 degrees (Rasch and Burke, 1978; Boone and Azen, 1979; Youm et al., 1979; Cochran, 1982).

The axis of rotation for forearm pronation-supination (see Figure 3-3) passes through the centers of the head of

radius and the head of the ulna (Youm et al., 1979;
Cochran, 1982; Tajima, 1985). The range of forearm
pronation-supination has been reported to be between 115
degrees and 175 degrees (Youm et al., 1979; Kapanji, 1982;
Torzilli, 1982).

The motion of forearm pronation-supination is independent of elbow flexion-extension (Chao and Morrey, 1978; Youm et al., 1979; Torzilli, 1982). The axes of elbow flexion-extension and forearm pronation-supination are not orthogonal to each other except when the carrying angle is zero (Chao et al., 1980).

Though the two motions, elbow flexion-extension and forearm pronation-supination, do not interfere with each other, the long axis of the forearm rotates about five degrees internally during early flexion of the elbow joint and about five degrees externally during terminal flexion of the elbow joint (Morrey and Chao, 1976).

2. Prime flexors and extensors of the elbow and pronators and supinators of the forearm

Among elbow joint muscles, the biceps brachii, brachialis, and brachioradialis are considered to be the major flexors and most studies on the role of elbow flexors are concentrated on these muscles (Basmajan and Latif, 1957; Logan, 1970; Bouisset et al., 1976; Rasch and Burke, 1978; Youm, 1980; Cochran, 1982; An et al., 1983; Van Zuylen et al., 1988). Braune and Fischer (1889) cited by Bouisset

et al. (1976) stated that these three prime elbow flexors represent approximately 85 percent of the total flexion torque. On the other hand, based on moment arm measurements, An et al. (1981) demonstrated that the biceps brachii, brachialis, brachioradialis, and extensor carpi radialis are the major elbow flexors. However, Cnockaert et al. (1975) considered the biceps brachii, brachialis, brachioradialis, pronator teres, and extensor carpi radialis longus as the elbow flexor group.

The main elbow extensor is the triceps brachii muscle (Travill, 1962; Logan, 1970; Rasch and Burke, 1978; Cochran, 1982). On the other hand, the anconeus muscle initiates and maintains elbow extension, and is responsible for the fine control of movement (Pauly et al., 1967). Based on the moment arm measurements, An et al. (1981) showed that the triceps brachii, flexor carpi ulnaris, and anconeus are the major elbow extensors.

The main pronator muscle of the forearm is the pronator quadratus (Rasch and Burke, 1978). Supination of the forearm is primarily performed by the supinator muscle (Basmajian and Latif, 1957; Rasch and Burke, 1978).

Basmajian and Latif (1957) showed that the short and long heads of the biceps have similar electromyographic (EMG) activity during elbow flexion-extension although the long head is more active than the short head during the various movements.

The length of the biceps brachii increases as the

forearm moves from supination to pronation (Provins and Salter, 1967; Cnockaert et al., 1975). This muscle contributes to the elbow flexion in a range from 60 to 150 degrees (Ismail and Ranatunga, 1978).

The brachialis is the workhorse for elbow joint flexion (Basmajian and Latif, 1957). This muscle is consistently active during flexion of the elbow joint in most movements (Basmajian and Latif, 1957; An et al., 1983). It was also reported to be markedly active during quick flexion at the elbow joint (Basmajian and Latif, 1957). Among the major elbow joint flexors (biceps, brachialis, and brachioradialis), the brachialis is the only muscle that is not changed in length during the pronation-supination of the forearm (Provins and Salter, 1954).

The brachioradialis has a small cross sectional area but a large moment arm (Amis et al., 1979). This muscle can produce fast movement such as a rapid whip-like action (Basmajian and Latif, 1957; Pauly et al., 1967; Youm, 1980). The length of the brachioradialis also varies during pronation-supination of the forearm (Cnockaert et al., 1975).

The anconeus and three heads of the triceps brachii contract simultaneously when elbow joint extension is performed rapidly (Pauly et al., 1967). The triceps brachii is a very powerful muscle in the upper extremity (Amis et al., 1979).

B. Wrist Joint

1. Analysis of motion

The axes of rotation for flexion-extension and for radio-ulna deviation of the hand relative to the forearm pass through the head of capitate bone (MacConail, 1941; Andrews and Youm, 1979; Volz, 1979; Brumbaugh et al., 1982). The loci of the instantaneous centers for both flexion-extension and radio-ulna deviation remain within a circle with about a 1 mm radius (Andrews and Youm, 1979). Therefore, the wrist joint is considered to be a simple hinge joint. According to Brumbaugh et al. (1982), these axes are nearly perpendicular and intersected at the center of wrist motion.

2. Prime flexors and extensors of the wrist

Prime muscles for wrist flexion are the flexor carpi ulnaris and flexor carpi radialis and for wrist extension are the extensor carpi ulnaris, extensor carpi radialis longus, and extensor carpi radialis brevis (Youm et al., 1976, 1978; Rasch and Burke, 1978; Ekenstam et al., 1984; Tolbert et al., 1985).

II. OPTIMIZATION AND SIMULATION IN BIOMECHANICS

A. Optimization in Biomechanics

Optimization technique has been applied to gross human motions since the 1970's. Among human motions, the gait pattern has been extensively studied via optimization

technique (Chao and Rim, 1973; Chow and Jacobson, 1971, 1974; Seireg and Arvikar, 1975; Hardt, 1978; Pedotti et al., 1978; Crowninshield and Brand, 1981; Patriarco et al., 1981; Davy and Audu, 1987).

Gait, associated with normal daily activity, does not require maximum effort. Therefore, the purpose of optimization techniques, applied to gait patterns, is to minimize objective functions such as mechanical energy (Chow and Jacobson, 1971, 1974), the sum of muscle forces, and joint moments (Seireg and Arvikar, 1975; Pedotti et al., 1978; Patriarco et al., 1981). In this kind of optimization problem, the most important matter is to define a physiologically rationalized optimal criterion in order that an optimal solution is biologically meaningful (Hardt, 1978; Peotti et al., 1978; Crowninshield and Brand, 1981).

On the other hand, many sports activities need a maximum effort from athletes to minimize time or maximize distance. Therefore, the objective function depends upon the goal of each sport event. Optimization problems presented by Hatze (1975) and Ghosh and Boykin (1976) were directed at minimizing execution time in a kicking action and performance time in a kip-up maneuver on a horizontal bar, respectively. The flight distance of a ski jumper, after take-off, was maximized by Remizov (1984). The objective function that Hatze (1981) maximized for the long jumper was velocity at the take-off.

Some optimization studies have employed linear

programming technique (Seireg and Arvikar, 1975; Hardt, 1978), but most studies were formulated by non-linear optimization techniques (Chow and Jacobson, 1971, 1974; Chao and Rim, 1973; Ghosh and Boykin, 1976; Hatze, 1976; Crowninshield and Brand, 1981; Remizov, 1984; Davy and Audu, 1987). Hardt (1978), who investigated walking patterns, studied leg muscle forces by a linear programming technique. He concluded that discrepancies between computed results and experimental data may be due to the simplistic treatment of the muscle and the inherent limitations of the linear programming algorithm.

Gross human motions, in daily activities as well as in sports activities, can be characterized as a mathematically non-linear and physically dynamic system. In order to describe human motion with non-linear and dynamic properties, non-linear dynamic optimization techniques are considered to be the most proper theory (Chow and Jacobson, 1971, 1974; Ghosh and Boykin, 1976; Hatze, 1976; Davy and Audu, 1987).

B. Simulation in Biomechanics

The major advantage of using simulation of motion to study sport skills is that one can experiment with variations of the maneuver before attempting to teach it to an athlete (Ramey and Yang, 1981).

Simulation studies, that have been published, may be classified into three categories: type of model, application

of model, and muscle involvement. The types of models that have been presented are: three segment rigid-body model (Hubbard and Barlow, 1980), nine segment rigid-body model (Ramey and Yang, 1981), 12 segment rigid-body model (Young, 1970), and 15 segment rigid-body model (Gallenstein, 1973; Aleshinsky and Zatsiorsky, 1978; Hatze, 1981). Simulation has been applied to various sports skills: free-fall phase of the long jump (Ramey and Yang, 1981), kick patterns in swimming (Gallenstein, 1973), walking pattern (Aleshinsky and Zatsiorsky, 1978), bar clearing maneuver in pole vaulting (Hubbard and Barlow, 1980), and take-off phase of the long jump (Hatze, 1981). Muscular dynamics was not an integral part of these simulation studies except for the study by Hatze (1981). Hatze's model was two-dimensional. Currently, a three-dimensional model of the entire human body, including all prime muscles, has not been seen because of its extreme complexity.

III. THROWING

There exists a common pattern among most overarm throwing motions such as baseball pitching and throwing, tennis serving, water polo throwing, handball throwing, volleyball spiking, javelin throwing, and football throwing, (Lindner, 1971; Cooper and Glassow, 1976; Anderson, 1979; Atwater, 1979; Toyoshima and Hoshikawa, 1983; Whiting et al., 1985; Jöris et al., 1985; Elliott et al., 1986).

The so-called "kinetic link" principle governing

throwing motions is very clearly described by Kreighbaum and Barthels (1985) (p. 594-599). The delicate difference of each throwing pattern in various sport skills may be due to the difference in the size of the object being thrown, object weight, purpose of throwing, and rules of the sport. In order to contrast and to compare various overhand throwing pattens, the movement is often divided into common phases: preparatory phase, cocking phase, acceleration phase, and follow-through (Richardson, 1983; Pappas et al., 1985; Moyness et al., 1986; Gowan et al., 1987).

A. Baseball Pitching

Baseball pitching is initiated by swinging the hand upward to an overhead position while turning the trunk away from the throwing direction and shifting the body weight from the striding foot to the pivot foot. Preparatory phase or wind-up begins with these initial movements of the pitcher and ends when the ball leaves the gloved hand. This wind-up motion varies from pitcher to pitcher (Hay, 1978; Atwater, 1979; Wickstrom, 1983; Pappas et al., 1985; Jobe et al., 1986).

The cocking phase starts as the ball leaves the gloved hand and ends when the maximum external rotation of the shoulder is reached. After the ball is released from the gloved hand, the pitching arm is swung backward and downward. From the instant the striding foot contacts the ground, the upper arm is abducted, horizontally adducted,

and externally rotated until the maximum external rotation is reached. Maximum external rotation of the shoulder is limited by the passive restraints of the glenohumeral capsule and ligaments (Moynes, 1986; Gowan et al., 1987). The forearm is forced to rotate backward and downward until it is nearly horizontal in the backward direction and the elbow joint is extended to approximately a right angle as the angular velocity of the trunk reaches its peak (Hay, 1978; Atwater, 1979; Wickstrom, 1983; Pappas et al., 1985; Feltner and Dapena, 1986; Moynes et al., 1986; Gowan et al., 1987). During this cocking phase, the forward rotation of the pelvis is followed by the forward rotation of the upper trunk (Atwater, 1979; Pappas et al., 1985).

The acceleration phase starts with the forward movement of throwing arm from the maximum external rotation of the shoulder and ends with ball release from the hand. This phase is begun by three actions: continuing trunk rotation, rapid elbow extension, and shoulder medial rotation The upper arm is internally rotated, (Atwater, 1979). slightly adducted and horizontally abducted. The forearm is pronated and finally the wrist is flexed just before ball release (Atwater, 1979; Felter and Dapena, 1986; Gowan et al., 1987). The angular velocities of the pelvis, upper trunk, upper arm, forearm, and hand reached their peak in a sequential order (Atwater, 1979).

Follow-through starts with ball release and ends as all motion is terminated (Jobe et al., 1983; Jobe et al., 1984;

Pappas et al., 1985). After ball release, the upper arm continues to rotate internally and begins to abduct and adduct horizontally (Feltner and Dapena, 1986). The follow-through is important for control, and the prevention of injury (Gibson and Elliott, 1987). The follow-through phase varies, depending on the techniques of the pitchers (Moynes et al., 1986; Gowan et al., 1987).

B. Electromyographic Study of Elbow and Wrist Joint Muscles in the Throwing Motion

EMG patterns give information regarding which muscles are activated in a certain phase of the throwing motion.

EMG patterns also can be used to estimate muscle control parameters as input to simulation and optimization study.

The biceps brachii muscle showed peak activity with flexion of the elbow joint during the late phase of cocking (Moynes et al., 1986; Gowan et al., 1987). The biceps showed low activation during acceleration. Triceps activity was strong throughout the acceleration phase that is accompanied by rapid elbow extension (Jobe et al., 1984). Peak biceps activity occurred during the follow-through phase to decelerate the rapidly extending elbow (Jobe et al., 1984). The biceps brachii muscle, contributed primarily to position the throwing arm for the delivery of the pitch, with greater activity during the cocking phase and less activity during accelerate the throwing arm

forward with stronger EMG activity evident during the acceleration phase and less activity during the cocking phase (Gowan et al., 1987).

Forearm muscles including the brachioradialis, flexor carpi radialis, extensor carpi radialis longus, extensor carpi radialis brevis, and supinator demonstrated low to moderate EMG activity during all phases of pitching (Sisto et al., 1987).

CHAPTER III

METHODS

This chapter is divided into two parts, rigid-body dynamics of the upper extremity and muscular dynamics of the upper extremity.

I. RIGID-BODY DYNAMICS OF THE UPPER EXTREMITY

The upper arm, forearm, and hand, consisting of soft tissues and body fluids as well as bones, are considered as rigid-bodies. In this study, the radius and ulna are treated as separate rigid-bodies. Therefore, the upper extremity is modeled as a four segment rigid-body dynamic system.

A. Bones of Upper Extremity

Before proceeding with modeling, the bony structure of the human upper extremity is briefly reviewed. A similar review may be found in various anatomy books.

The bones of upper extremity consist of the humerus in the upper arm, the ulna and radius in the forearm, the eight carpals in the wrist, the five metacarpals in the palm, and the 14 phalanges in the five digits (see Figure 3-1). The upper arm is supported by the two bones of the shoulder

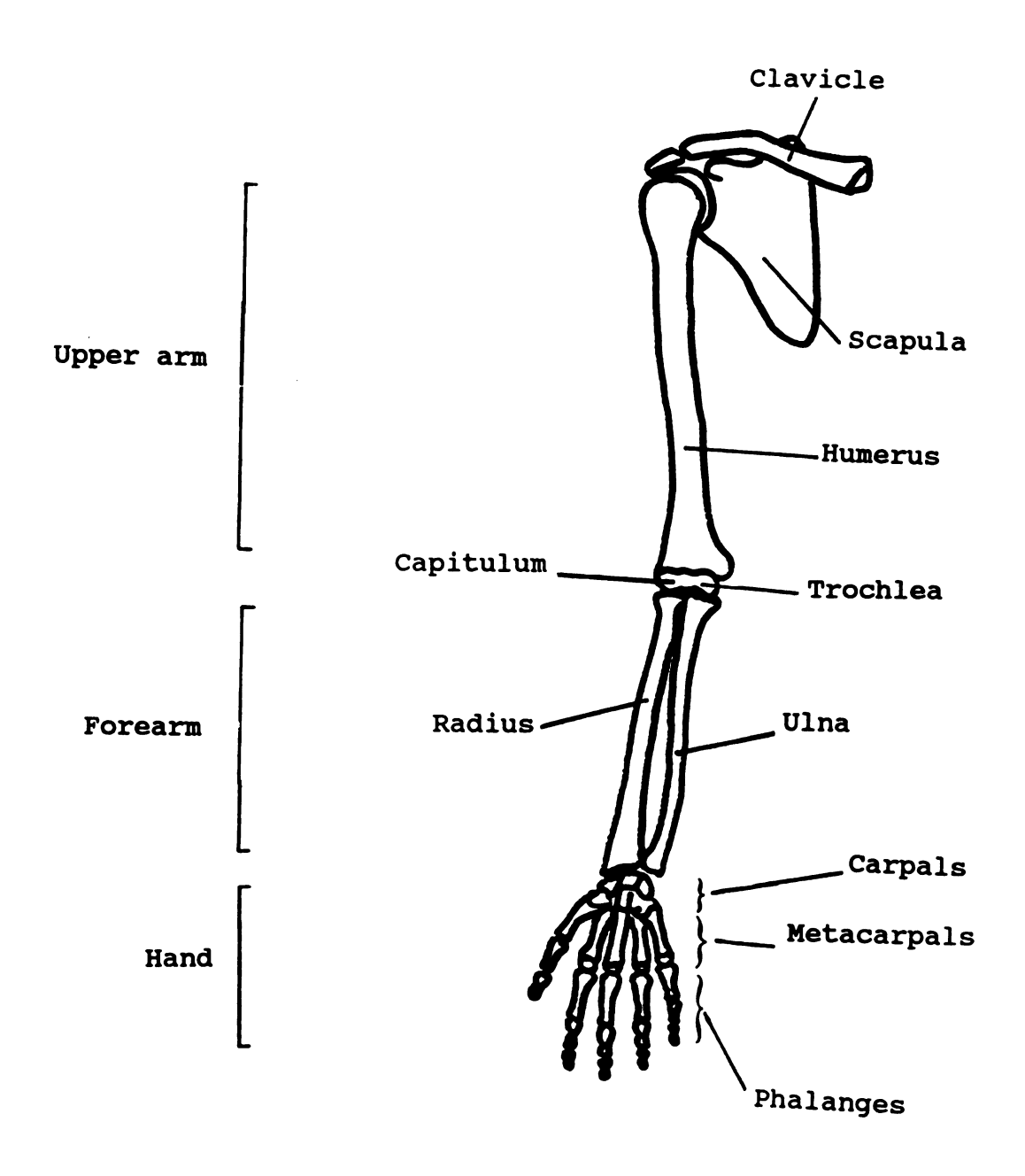


Figure 3-1. Anterior view of the skeletal system of the right upper extremity.

girdle, the scapula and clavicle.

The humerus is the longest and largest bone of the upper extremity. It articulates proximally with the glenoid fossa of the scapula at the shoulder and distally with the radius and ulna at the elbow (see Figure 3-2).

The radius, which is the shorter and more lateral of the two bones of the forearm, articulates with the capitulum of the humerus proximally, the carpal bones distally, and the radial notch of the ulna medially (see Figures 3-2 and 3-3).

The ulna is the longer and more medial bone of the two in the forearm. The proximal end of the ulna consists of the trochlear notch, that fits over the trochlea of the humerus and the radial notch, that articulates with the head of the radius (see Figure 3-3). The distal end of the ulna includes a small rounded head and a small conical styloid process that projects downward.

B. Axes of Rotation for Upper Extremity Segments

The axis of rotation of the humerus passes through the center of the humeral head and the center of the trochlea (Morrey, 1976; Youm, 1980) (see Figure 3-2). The axis of rotation for flexion-extension at the elbow passes through the centers of the capitulum and the trochlea (Chao et al., 1980; Torzilli, 1982) (see Figure 3-2). The axis of rotation for forearm pronation-supination is directed along a line joining the center of the head of the radius and the

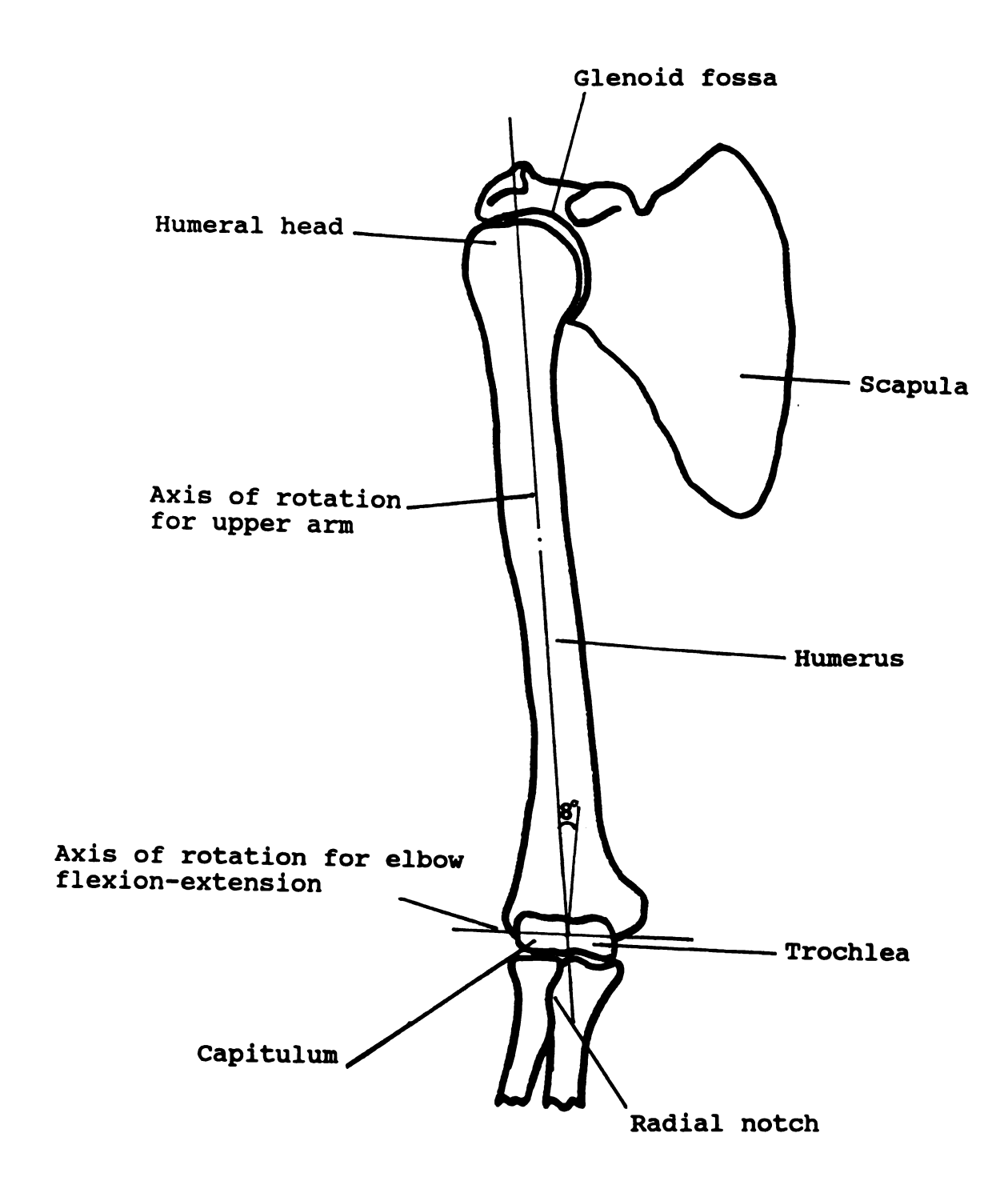


Figure 3-2. Anterior view of the skeletal system of the right upper arm.

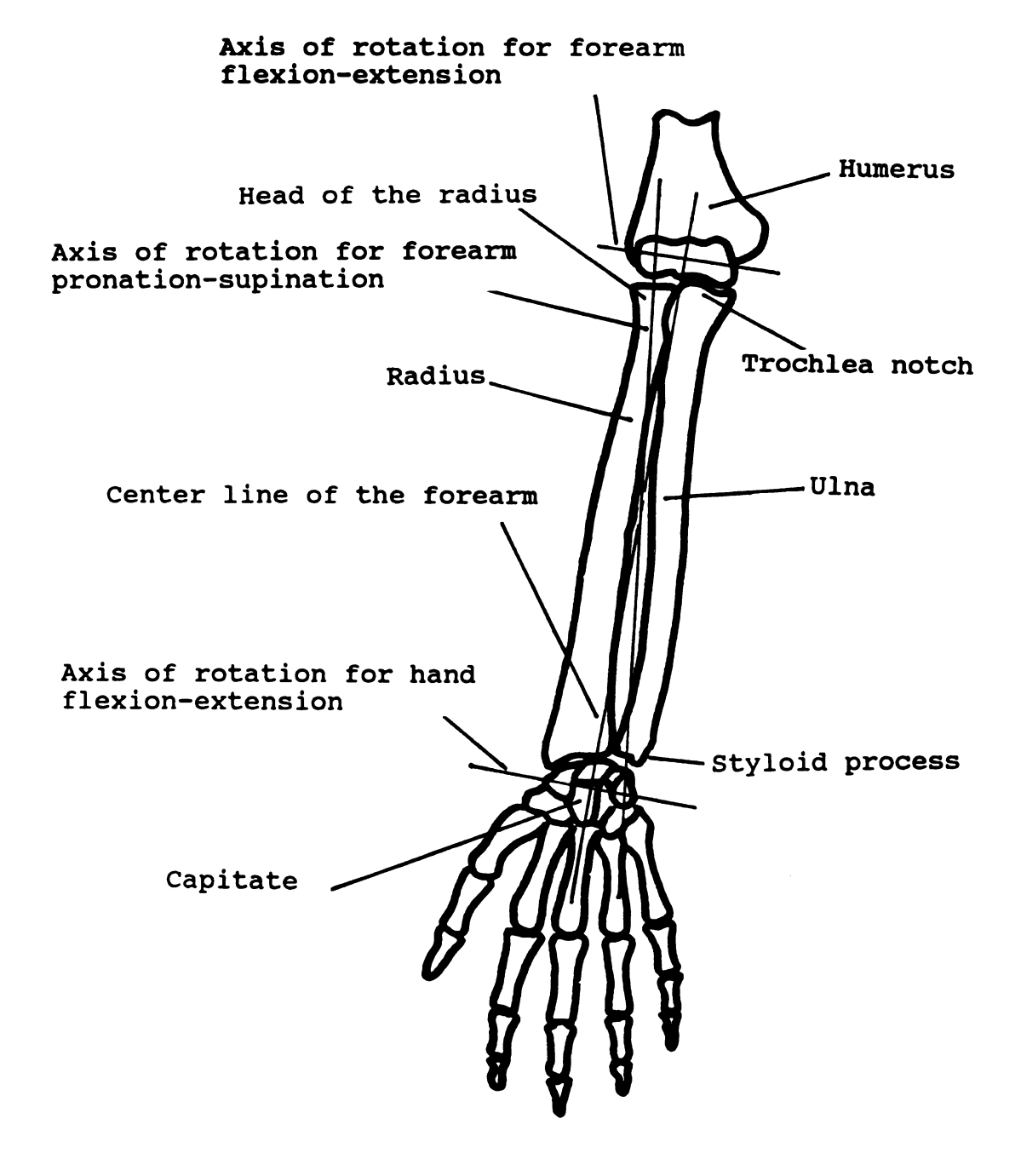


Figure 3-3. Anterior view of the skeletal system of the right forearm and hand.

distal end of the ulna (Morrey and Chao, 1976; Torzilli, 1982; Tajima, 1985) (see Figure 3-3). The axis of rotation for wrist flexion-extension that passes through the head of the capitate may be considered to be at a right angle to the axis of rotation for forearm pronation—supination. Note that in this current study the wrist joint has been assumed not to have radial—ulna deviation since in the baseball pitching motion being considered, such a deviation is negligible.

C. Geometry of the Human Upper Extremity

The human upper extremity has been commonly modeled as a three component rigid-body system (upper arm, forearm, and hand) when the model does not involve muscles (Chao et al., 1980; Langrana, 1981) or when only two-dimensional motions involving muscles are considered (Hatze,1981). Three-dimensional motion, involving muscular activity, may not be accurately modeled by three segments consisting of the upper arm, forearm, and hand; forearm rotation should not be considered as a single rigid-body motion. Therefore, in this study, the human upper extremity was modeled as a four segment rigid-body system consisting of the upper arm, forearm without radius, radius, and hand (see Figure 3-4).

The cartesian coordinate system OXYZ is taken as the inertial frame with the origin O located at some fixed point as shown in Figure 3-4. The cartesian coordinate axes O_i X_i Y_i Z_i (i = 1 to 4) whose origins are located at the mass

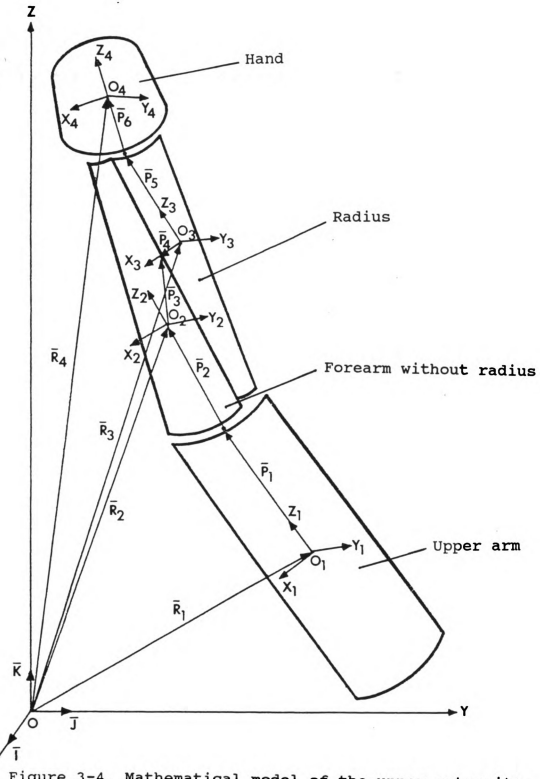


Figure 3-4. Mathematical model of the upper extremity.

center of each segment are the body-fixed coordinate systems of the upper arm, the forearm without radius, the radius, and the hand, respectively. Subscripts i=1, 2, 3, and 4 represent the upper arm, forearm without radius, radius, and hand, respectively. The vectors \overline{R}_i (i=1 to 4) are position vectors from the origin of the inertial frame to the respective origins of the body-fixed coordinate axes. The vectors \overline{P}_j (j=1 to 6) are internal position vectors with components along the body-fixed axes of the individual segments as shown in Figure 3-4.

In this model, the rotational motions permitted are elbow flexion-extension; forearm pronation-supination; wrist flexion-extension; and axial rotation, adduction-abduction, and flexion-extension of the upper arm. In addition, each segment will have a translation of its center of mass.

Therefore, each segment will have linear and angular kinematic components, in general. In this study, however, the upper extremity motion was tracked by experimental data obtained from high speed film. Therefore, the linear and angular kinematic components of this segment are considered to be known.

D. Euler's Angles and Transformation Matrices In order to describe the orientation of each segment, ZYX convention of Euler's angle is employed as shown in the Figure 3-5 (Goldstein, 1980). Transformation matrices $[E_i]$ (i = 1 to 4), relating any set of body axes to its

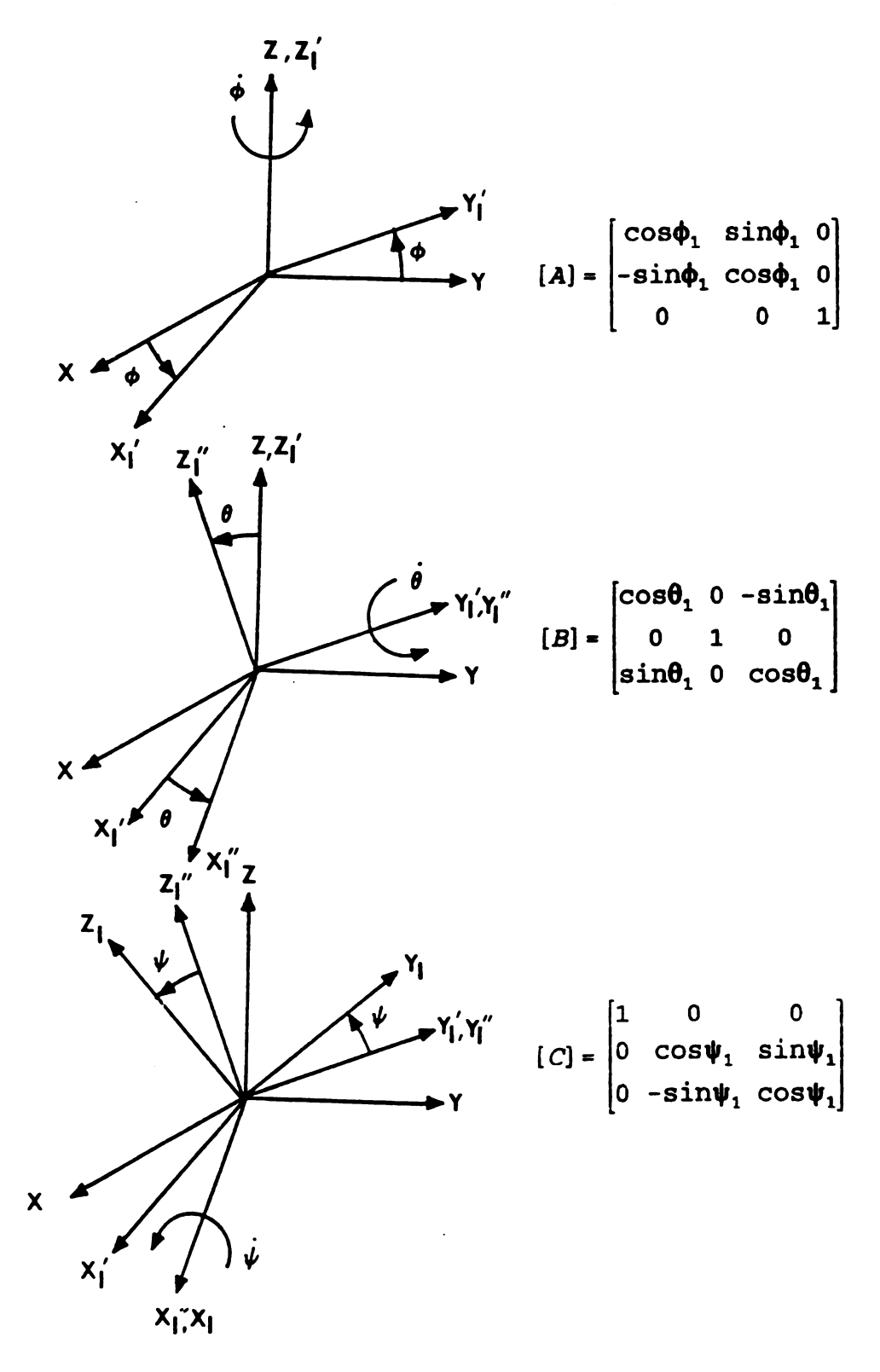


Figure 3-5. Euler angles.

neighboring set in terms of Euler's angles, are defined as follows.

The transformation matrix $[E_1]$ of the upper arm segment relative to the inertial frame is $[E_1] = [C][B][A]$, so that components of any vectors (\overline{A}_1) expressed in the body-fixed reference O_1 , X_1 , Y_1 , Z_1 are given in the inertial frame (\overline{A}_i) by $\overline{A}_i = [E_1]^{-1} \overline{A}_1$, where $[E_1] =$

$$\begin{bmatrix} \cos\theta_1\cos\phi_1 & \cos\theta_1\sin\phi_1 & -\sin\theta_1\\ \sin\psi_1\sin\theta_1\cos\phi_1-\cos\psi_1\sin\phi_1 & \sin\psi_1\sin\theta_1\sin\phi_1+\cos\psi_1\cos\phi_1 & \cos\theta_1\sin\psi_1\\ \cos\psi_1\sin\theta_1\cos\phi_1+\sin\psi_1\sin\phi_1 & \cos\psi_1\sin\theta_1\sin\phi_1-\sin\psi_1\cos\phi_1 & \cos\theta_1\cos\psi_1 \end{bmatrix}$$

$$(3-1)$$

Transformation matrices, $[E_2]$, $[E_3]$ and $[E_4]$, are defined similarly to $[E_1]$. Transformation matrix $[E_2]$ of the forearm without radius relative to the upper arm segment can be reduced since the ulna doesn't rotate with respect to the Y_1 and Z_1 axes. This means that θ_2 and ϕ_2 are zero. Therefore, θ_2 and ϕ_2 are constants and

$$[E_{2}] = \begin{bmatrix} C_{1} & C_{2} & C_{3} \\ C_{4}\sin\psi_{2} - C_{5}\cos\psi_{2} & C_{6}\sin\psi_{2} + C_{7}\cos\psi_{2} & C_{8}\sin\psi_{2} \\ C_{4}\cos\psi_{2} + C_{5}\sin\psi_{2} & C_{6}\cos\psi_{2} - C_{7}\sin\psi_{2} & C_{8}\cos\psi_{2} \end{bmatrix}$$
(3-2)

$$C_1$$
- $\cos\theta_2\cos\phi_2$, C_2 - $\cos\theta_2\sin\phi_2$, C_3 - $-\sin\theta_2$, C_4 - $\sin\theta_2\cos\phi_2$, C_5 - $\sin\phi_2$, C_6 - $\sin\theta_2\sin\phi_2$, C_7 - $\cos\phi_2$, C_8 - $\cos\theta_2$.

The radius segment relative to the forearm without radius has only a single degree of freedom, rotation with respect to the Z_2 axis. Thus, θ_3 and ψ_3 are zero because θ_3 and ψ_3 are constants and the transformation matrix $[E_3]$ can be reduced as follows:

$$[E_3] = \begin{bmatrix} C_9 \cos \phi_3 & C_9 \sin \phi_3 & -C_{10} \\ C_{11} \cos \phi_3 - C_{12} \sin \phi_3 & C_{11} \sin \phi_3 + C_{12} \cos \phi_3 & C_{13} \\ C_{14} \cos \phi_3 + C_{15} \sin \phi_3 & C_{14} \sin \phi_3 - C_{15} \cos \phi_3 & C_{16} \end{bmatrix}$$
(3-3)

where

$$C_9 - \cos\theta_3$$
, $C_{10} - \sin\theta_3$, $C_{11} - \sin\theta_3 \sin\psi_3$, $C_{12} - \cos\psi_3$, $C_{13} - \cos\theta_3 \sin\psi_3$, $C_{14} - \sin\theta_3 \cos\psi_3$, $C_{15} - \sin\psi_3$, $C_{16} - \cos\theta_3 \cos\psi_3$.

The hand actually has two degrees of freedom (flexion-extension and radio-ulna deviation). However, in fastball pitching in baseball, radio-ulna deviation may be ignored (O'Brien, 1990). With this assumption, ϕ_4 and θ_4 are zero. Therefore, ϕ_4 and θ_4 are constants and the

transformation matrix $[E_4]$ of the hand's motion can be defined as follows:

$$[E_4] = \begin{bmatrix} C_{17} & C_{18} & C_{19} \\ C_{20} \sin\psi_4 - C_{21} \cos\psi_4 & C_{22} \sin\psi_4 + C_{23} \cos\psi_4 & C_{24} \sin\psi_4 \\ C_{20} \cos\psi_4 + C_{21} \sin\psi_4 & C_{22} \cos\psi_4 - C_{23} \sin\psi_4 & C_{24} \cos\psi_4 \end{bmatrix}$$
(3-4)

where

$$C_{17} - \cos\theta_4 \cos\phi_4$$
, $C_{18} - \cos\theta_4 \sin\phi_4$, $C_{19} - -\sin\theta_4$, $C_{20} - \sin\theta_4 \cos\phi_4$, $C_{21} - \sin\phi_4$, $C_{22} - \sin\theta_4 \sin\phi_4$, $C_{23} - \cos\phi_4$, $C_{24} - \cos\theta_4$.

Inverses and transposes of these matrices are equal since all are orthogonal transformations. Thus, $[E_i]^{-1} = [E_i]^T$ (i = 1 to 4).

E. Position Vectors, Linear Velocities, and Linear Accelerations

The position vectors \overline{R}_i (i = 1 to 4) for each segment relative to the inertial coordinate frame (see Figure 3-4) may be given as follows: $\overline{R}_i = R_{xi} \overline{I} + R_{yi} \overline{J} + R_{zi} \overline{K}$, where \overline{I} , \overline{J} , and \overline{K} are respective unit vectors of inertial X, Y, and Z axes and R_{xi} , R_{yi} , and R_{zi} are components of position vector R_i (i = 1 to 4). Matrix notation of each position vector is given here.

$$\overline{R}_{1} = [x_{1}, y_{1}, z_{1}]^{T},$$

$$\overline{R}_{2} = \overline{R}_{1} + [E_{1}]^{-1} \overline{P}_{1} + [E_{1}]^{-1} [E_{2}]^{-1} \overline{P}_{2},$$

$$\overline{R}_{3} = \overline{R}_{1} + [E_{1}]^{-1} \overline{P}_{1} + [E_{1}]^{-1} [E_{2}]^{-1} (\overline{P}_{2} + \overline{P}_{3})$$

$$+ [E_{1}]^{-1} [E_{2}]^{-1} [E_{3}]^{-1} \overline{P}_{4}, \text{ and}$$

$$\overline{R}_{4} = \overline{R}_{1} + [E_{1}]^{-1} \overline{P}_{1} + [E_{1}]^{-1} [E_{2}]^{-1} (\overline{P}_{2} + \overline{P}_{3})$$

$$+ [E_{1}]^{-1} [E_{2}]^{-1} [E_{3}]^{-1} (\overline{P}_{4} + \overline{P}_{5})$$

$$+ [E_{1}]^{-1} [E_{2}]^{-1} [E_{3}]^{-1} [E_{4}]^{-1} \overline{P}_{6}.$$
(3-5)

From Figure 3-4, the components of the internal position vectors, \overline{P}_j (j = 1 to 6), can be represented as follows:

$$\overline{P}_{1} = [0, 0, P_{1z}]^{T},
\overline{P}_{2} = [0, 0, P_{2z}]^{T},
\overline{P}_{3} = [P_{3x}, 0, P_{3z}]^{T},
\overline{P}_{4} = [P_{4x}, 0, 0]^{T},
\overline{P}_{5} = [0, 0, P_{5z}]^{T}, and
\overline{P}_{6} = [0, 0, P_{6z}]^{T}.$$
(3-6)

Non-zero components of the internal position vectors in equations 3-6 are constants that can be measured from subjects and will be described in the following section. Linear velocities and linear accelerations, \bar{R}_i , \bar{R}_i (i=1 to 4), of the segments can be obtained from the first time derivative and the second time derivative of position vectors, \bar{R}_i (i=1 to 4), can be expressed in the inertial coordinate system, respectively.

F. Angular Velocities

Angular velocities ($\overline{\omega}_{ib}$ (i = 1 to 4)) along the respective body-fixed coordinate axes are given in terms of Euler's angles (Goldstein, 1980). However, in the motion considered here, the angular velocity components can be reduced on the basis of the restrictions explained in section D.

$$\overline{\omega}_{1b} = \begin{bmatrix}
\dot{\psi}_1 - \dot{\phi}_1 \sin \theta_1 \\
\dot{\theta}_1 \cos \psi_1 + \dot{\phi}_1 \cos \theta_1 \sin \psi_1 \\
-\dot{\theta}_1 \sin \psi_1 + \dot{\phi}_1 \cos \theta_1 \cos \psi_1
\end{bmatrix}, \tag{3-9}$$

$$\overline{\omega}_{2b}$$
- $[\dot{\psi}_2, 0, 0]^T$, (3-10)

$$\overline{\omega}_{3b}$$
 = $[-C_{10}\dot{\phi}_3, C_{13}\dot{\phi}_3, C_{16}\dot{\phi}_3]^T$, (3-11)

$$\overline{\omega}_{4b}^{-} [\dot{\psi}_4, 0, 0]^T,$$
(3-12)

where

$$C_{10} = \sin\theta_3$$
 , $C_{13} = \cos\theta_3 \sin\psi_3$, and $C_{16} = \cos\theta_3 \cos\psi_3$.

Angular velocities ($\overline{\omega}_i$ (i = 1 to 4)) of segments, that are generated by the whole system, relative to body-fixed axes, are given as follows:

$$\overline{\omega}_{1} = \overline{\omega}_{1b},$$

$$\overline{\omega}_{2} = [E_{2}] \overline{\omega}_{1} + \overline{\omega}_{2b},$$

$$\overline{\omega}_{3} = [E_{3}] \overline{\omega}_{2} + \overline{\omega}_{3b}, \text{ and}$$

$$\overline{\omega}_{4} = [E_{4}] \overline{\omega}_{3} + \overline{\omega}_{4b}.$$
(3-13)

G. Lagrange's Equations for Upper Extremity Motion

The total kinetic energy (KE) and potential energy (PE)

of a system of four rigid-bodies (see Figure 3-4) are given respectively by:

$$KE - \frac{1}{2} \sum_{i=1}^{n} m_{i} \bar{R}_{i}^{2} + \frac{1}{2} \sum_{i=1}^{n} \overline{\omega}_{i}^{T} [I_{i}] \overline{\omega}_{i}, \quad n-1, 4$$
(3-14)

where $[I_i]$ is moment of inertia matrix at the respective center of mass (m_i) about body-fixed coordinate axes and

$$PE - \sum_{i=1}^{n} m_i g \overline{R}_{iz}, n=1,4$$
 (3-15)

where \overline{R}_{iz} are Z - components of position vectors (\overline{R}_i) relative to the inertial coordinate system.

Among nine generalized coordinates for translation and orientation of the system of four rigid-bodies, six generalized coordinates $(x_1, y_1, z_1, \phi_1, \theta_1, \psi_1)$ for the upper arm motion are tracked by experimental data. The remaining three generalized coordinates $(\psi_2$ for elbow flexion-extension, ϕ_3 for forearm pronation-supination, and ψ_4 for wrist flexion-extension) are considered as variables.

By definition, the Lagrangian function L equals **KE** - **PE**, from which Lagrange's equations of motion are defined by:

$$\frac{d}{dt} \left(\frac{\partial L}{\partial \dot{q}_{m}} \right) - \frac{\partial L}{\partial q_{m}} - Q_{m} \tag{3-16}$$

where $\mathbf{q}_{\mathbf{m}}$ (m = 1 to 3) are generalized coordinates and $\mathbf{Q}_{\mathbf{m}}$ are generalized forces (see section H for a discussion on generalized forces). The generalized coordinates are assigned as $\mathbf{q}_1 = \psi_2$, $\mathbf{q}_2 = \phi_3$, and $\mathbf{q}_3 = \psi_4$.

Lagrange's equation can be written in matrix form as

$$[\mathbf{A}]\ddot{\mathbf{q}} = \mathbf{B} + \mathbf{Q} \tag{3-17}$$

in which [A] is the matrix of coefficients for the generalized acceleration \ddot{q} , \ddot{B} is a column vector containing all remaining terms with signs reversed, and Q is column vector of generalized forces. Coefficient matrix [A] is a function of \ddot{q} and \ddot{b} is a function of \ddot{q} and \ddot{q} .

Finally, three second-order differential equations can be obtained by computing the inverse matrix [A]⁻¹ of the coefficient matrix [A].

$$\ddot{\overline{\mathbf{q}}} = [\mathbf{A}]^{-1}[\overline{\mathbf{B}} + \overline{\mathbf{Q}}] \tag{3-18}$$

The actual derivation of these equations is easy but extremely lengthy as commonly observed in multi-body dynamics (Young, 1970). Therefore, this derivation will be omitted here. Instead, these equations were entered

into the computer algorithm for simulation and optimization.

H. Generalized Forces

Generalized forces in equation 3-16 may be classified into two categories, active muscular torques and passive joint torques (Hatze, 1977). In three-dimensional analysis, the components of muscular torques are, in general, not directed along the respective angular velocity vectors (Hatze, 1981). In this case, the components of torques need to be decomposed to the directions of the angular velocity vectors.

In this study, the elbow and wrist joints were assumed to have one degree of freedom. The lines of pull of 12 prime muscles, that cross the elbow or the wrist joint, are reasonably parallel to both the upper arm and forearm segments. Therefore, it was assumed that the actual components of muscular torques are the generalized components of generalized forces of Lagrange's equation.

"The passive joint moment arises from the deformation of all tissues which surround the joint including skin, ligaments, tendons, relaxed muscles, etc." (Mansour and Audu, 1986). The passive joint torque consists of the passive elastic and the passive viscous component (Hayes and Hatze, 1977; Yoon and Mansour, 1982). The passive elastic torque (PET) provides the natural limit of joint movements in a dynamic simulation of the mathematical model of human body (Hatze, 1975, 1976; Hayes and Hatze, 1977). Throughout

the mid-range of the motion, the passive elastic joint torque is very small and approximately constant. On the other hand, as the limit of the joint is approached at both ends, the torque increases sharply. Researchers (Hatze, 1981; Yoon and Mansour, 1982; Elgin and Chen, 1987) have proposed different functions to mathematically express the passive elastic joint torque. In this dissertation, a double exponential function that was proposed by Audu and Davy (1985) was adopted.

$$PET(\theta) - C_1 \exp(-C_2(\theta - \theta_1)) - C_3 \exp(-C_4(\theta_2 - \theta))$$
(3-19)

where

 θ = joint angle (rad),

 C_1 , C_2 , C_3 , C_4 = constants and

 θ_1 , θ_2 = angular constants (rad).

The passive viscous joint torque (PVT), that is a function of both the joint angle and angular velocity, was adopted from the function proposed by Hayes and Hatze (1977). The function is given by:

$$PVT(\theta, \dot{\theta}) = C(\theta) \dot{\theta} \quad (Nm)$$
 (3-20)

where

 θ = joint angle (rad) and

 $C(\theta)$ = angular damping coefficient (Nms/rad).

I. Location of Center of Mass and Mass Distribution

Human segmental mass distribution and the location of
the center of a segmental mass have been studied for over a
century. Tables 3-1 and 3-2 are summaries of studies on
segmental mass distribution and the location of the center
of mass.

Table 3-1. Segmental mass distribution as ratios to total body mass.

Investigator	S	Sample	Segment		
			arm	forearm	hand
Harless(1860)	2	cadavers	0.032	0.017	0.009
Braune and Fischer(1889)	3	cadavers	0.033	0.021	0.0085
Braune and Fischer(1892)	2	cadavers	0.0293		
Dempster(1955)	8	cadavers	0.027	0.016	0.006
Dempster(1955)	39	living males	0.0342	0.0182	0.0059
Clauser McConville and Young(1969)	14	cadavers	0.026	0.016	0.007
Zatsiorsky and Seluyanov(1985)	100	living males	0.0271	0.0163	0.006

Among the studies listed in the Tables 3-1 and 3-2, the regression equation proposed by Zatsiorsky and Seluyanov in 1985 was adopted for the current research because anthropometric dimensions needed in their regression equation could be easily obtained from measurements on a living subject. In order to use their regression

equation, anthropometric measurement of the subject was conducted. Anthropometric data are given in Chapter IV.

Table 3-2. Location of the center of segmental mass from the proximal end as ratios of total segment lengths.

Investigator	Sample	Segment		
		arm	forearm	hand
Harless(1860)	1 cadavers	0.427	0.417	0.361
Braune and Fischer(1889)	3 cadavers	0.47	0.421	
Bernstein(1936)	76 living males	0.466	0.412	
Dempster(1955)	8 cadavers	0.436	0.43	0.506
Clauser, McConville and Young(1969)	13 cadavers	0.513	0.39	0.48
Zatsiorsky and Seluyonov(1983)	100 living males	0.45	0.427	0.369
Martin, Mungiole, Marzke and Longhill (1989a)	2 arms 4 forearms (cadavers)	0.45	0.434	

The regression equation proposed by Zatsiorsky and Seluyanov (1983, 1985) is given by:

$$y = b_0 + b_1 x_1 + b_2 x_2 + b_3 x_3$$
 (3-21)

where for the upper arm

 x_1 = length of the upper arm (cm),

 x_2 = circumference of the relaxed arm (cm), and

$$x_3 = (D_1 + D_2) / 2$$

 D_1 = lower diameter of upper arm (cm) and

 D_2 = lower diameter of the forearm (cm)

and where for the forearm

 $x_1 = length of the forearm (cm),$

 x_2 = width of the hand (cm), and

 $x_3 = (D_1 + D_2 + D_3) / 3,$

where

 D_1 = the least circumference of the distal forearm,

D₂ = middle circumference of the forearm (cm), and

D₃ = maximum circumference of the proximal
 forearm (cm).

Regression coefficients b_0 , b_1 , b_2 , and b_3 for the center of mass and segmental mass distribution are given in Table 3-3.

Table 3-3. Coefficients for the center of segmental mass and mass distribution.

Segments	b ₀	b ₁	b ₂	b ₃
upper arm m. * C.M. **	- 2.580	0.0471	0.1040	0.0651
	- 2.004	0.5660	0.0560	- 0.0160
forearm m.	- 2.040	0.0500	- 0.0049	0.0870
C.M.	0.732	0.5880	- 0.0857	- 0.0187

* m = mass

** C.M. = center of mass

J. Computation of Moments of Inertia

1. Moments of inertia of the upper arm

The regression equation for moments of inertia of the upper arm is the same as equation 3-21. Regression coefficients b_0 , b_1 , b_2 , and b_3 for I_{xx} , I_{yy} , and I_{zz} are given in the Table 3-4.

Table 3-4. Coefficients for the moments of inertia of the upper arm.

Inertia	. p ⁰	b ₁	b ₂	b ₃
I _{xx}	- 331	10.3	5.5	5.6
I _{yy}	- 359	10.2	6.4	8.5
I _{yy}	- 106	0.4	3.8	4.6

2. Moment of inertia of forearm

The form of the regression equation for the forearm is the same as equation 3-21. Regression coefficients b_0 , b_1 , b_2 , and b_3 for I_{xx} , I_{yy} , and I_{zz} of the forearm are given in Table 3-5. Moments of inertia of the forearm without radius can be computed from moments of inertia of the forearm and moments of inertia of the radius bone described in the following section.

Table 3-5. Coefficients for the moments of inertia of the forearm.

Inertia	b ₀	b ₁	b ₂	b ₃
I _{xx} I _{yy}	- 220.0 - 229.0 - 39.2	7.06 7.12 0.56	- 0.082 - 0.049 - 0.972	4.544 5.066 1.996

3. Moments of inertia of the radius bone

Moments of inertia for the radius bone are currently not available. The radius bone is shaped like a narrow right frustum. Therefore, it may be assumed that the radius is a frustum of a right circular cone (see Figure 3-6). The centroid of the frustum is located at a distance d from the bottom.

$$d = \frac{h}{4} \frac{R_L^2 + 2R_L R_S + 3R_S^2}{R_L^2 + R_L R_S + R_S^2}$$
(3-22)

where

h = height of the frustum,

 R_s = proximal radius of the frustum, and

 R_l = distal radius of the frustum.

Moments of inertia about the axes X, Y, and Z through the center of mass are given by Hanavan (1964) as:

$$I_{xx} - I_{yy} - m[\frac{m}{\rho h}TA + h^2TB]$$
 (3-23)

where

$$TA = \frac{9}{20\pi} \frac{1 + a + a^2 + a^3 + a^4}{b^2},$$

$$TB = \frac{3}{80} \frac{1 + 4a + 10a^2 + 4a^3 + a^4}{b^2},$$

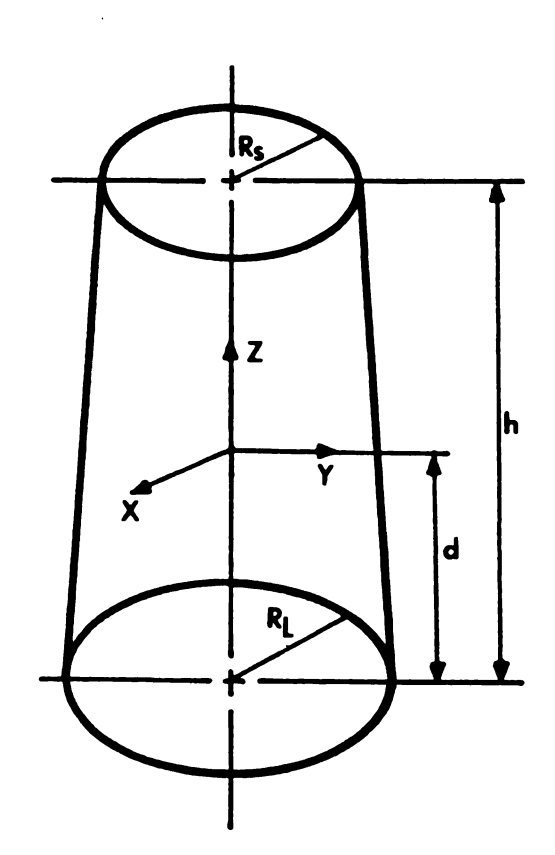


Figure 3-6. Frustum of right circular cone.

$$a = R_s / R_t$$

$$b = 1 + a + a_2$$

h = height of the frustum,

m = mass

and

$$I_{zz} = \frac{3m}{10} \frac{R_L^5 - R_S^5}{R_L^3 - R_S^3}.$$
 (3-24)

Mass (m) can be computed by equation 3-25. According to Rodrigue and Gagnon (1983), the density (ρ) of radius bone measured from 12 male cadavers was 1.43 g/cm³.

$$m = \frac{\pi \rho R_L^2 h}{3} \left(1 + \frac{R_S}{R_L} + \left(\frac{R_S}{R_L} \right)^2 \right)$$
 (3-25)

These moments of inertia are written with respect to the principal axes of the frustum. The axis of rotation of the radius, however, passes through the center of the distal end of the ulna and the center of the proximal end of the radius. The moments of inertia of the radius about the principal axes can be transformed to the axis that is parallel to the rotational axis by the following equation (Pletta and Frederick, 1964):

$$\tilde{I}_{qr} - a_{qi}a_{ri}I_{ij} \tag{3-26}$$

a; = direction cosines and

 I_{ij} = moments of inertia about the principal axes.

If it may be assumed that the longitudinal axes of the forearm pronation-supination and the radius bone are in the same plane, direction cosines can be obtained from the rotation about the y_3 -axis. The elements a_{ij} are given as follows:

$$\begin{bmatrix} a_{ij} \end{bmatrix} = \begin{bmatrix} \cos\theta & 0 & -\sin\theta \\ 0 & 1 & 0 \\ \sin\theta & 0 & \cos\theta \end{bmatrix}$$
(3-27)

where

 θ = inclination between the longitudinal axes of the radius and the forearm pronation-supination.

4. Moments of inertia of hand and ball

One approximation for determining the moment of inertia of the hand is that it may be considered as a sphere (Hanavan, 1964). Moments of inertia, I_{xx} , I_{yy} , and I_{zz} of a sphere are given by

$$I_{xx} - I_{yy} - I_{zz} - \left(\frac{2}{5}\right)mr^2$$
 (3-28)

m = mass of the sphere and

r = radius of the sphere.

It was assumed that the sphere of a baseball placed in the hand intersects at approximately one half of the radius of the sphere formed by the hand (see Figure 3-7). portion of the hand in contact with the ball is considered Moments of inertia of this ellipsoid as an ellipsoid. will be extremely small. Therefore, the sphere assumption Moments of inertia at the center of may still be valid. mass of the combined hand and ball can be computed by the parallel axis theorem. These moments of inertia are not principal moments of inertia as easily seen from Figure 3-7. Products of inertia, with respect to some axes, however, are nearly zero. Therefore, it may be reasonably assumed that these moments of inertia are the principal moments of inertia.

II. MUSCULAR DYNAMICS OF THE UPPER EXTREMITY

In the muscular dynamics of the upper extremity, the muscular system as a force generator was studied.

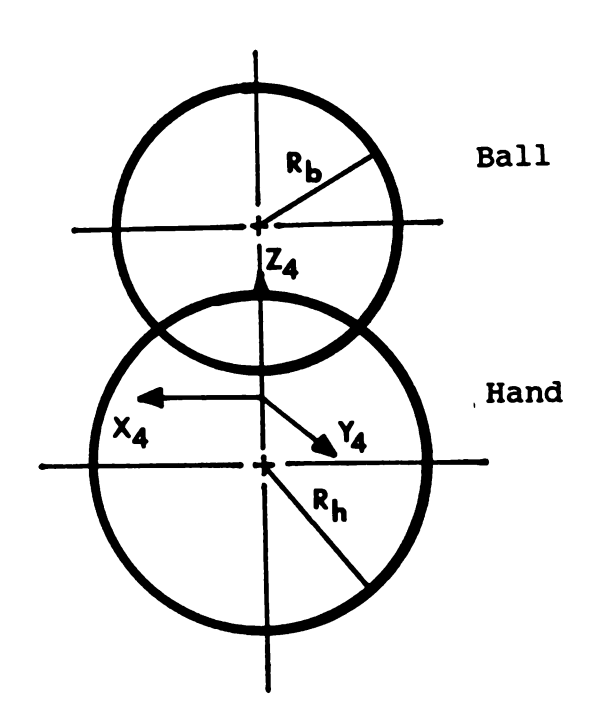


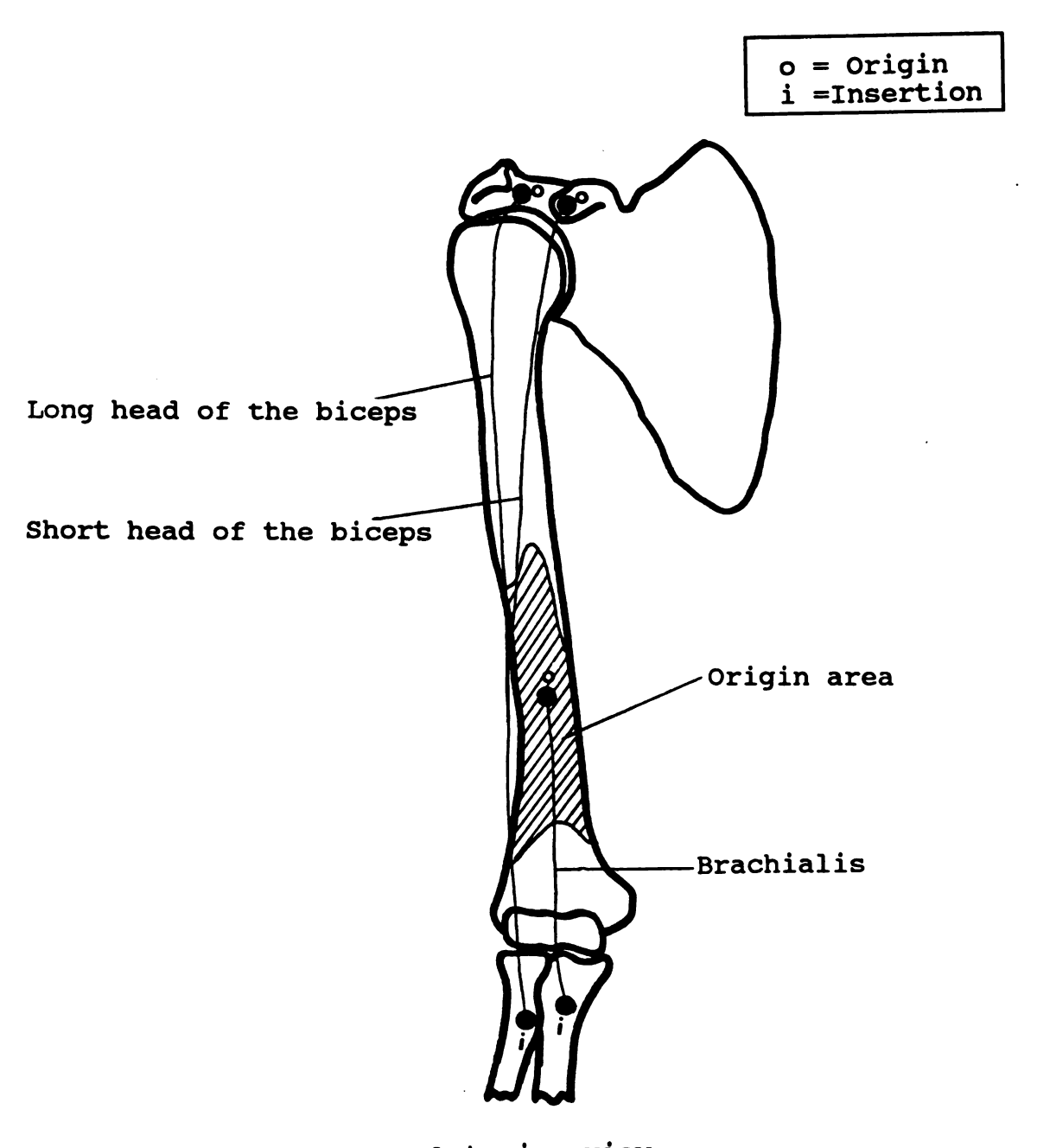
Figure 3-7. Model of the hand and ball.

A. Prime Muscles

Based on the review of literature, the following 14 muscles are considered to be prime muscles for elbow flexion-extension, forearm pronation-supination, and wrist flexion-extension: 1. Prime muscles for elbow flexion long head of biceps, short head of biceps, brachialis, and brachioradialis: 2. Prime muscles for elbow extension long head of triceps, lateral head of triceps, and medial head of triceps: 3. Prime muscles for forearm pronationsupination - pronator quadratus and supinator; muscles for wrist flexion - flexor carpi ulnaris and flexor carpi radialis; and 5. Prime muscles for wrist extension extensor carpi ulnaris, extensor carpi radialis longus, and extensor carpi radialis brevis. Origins and insertions of these 14 prime muscles are shown in the Figures 3-8 through Each head of the biceps and triceps was treated separately because each head of the biceps and triceps is functionally different.

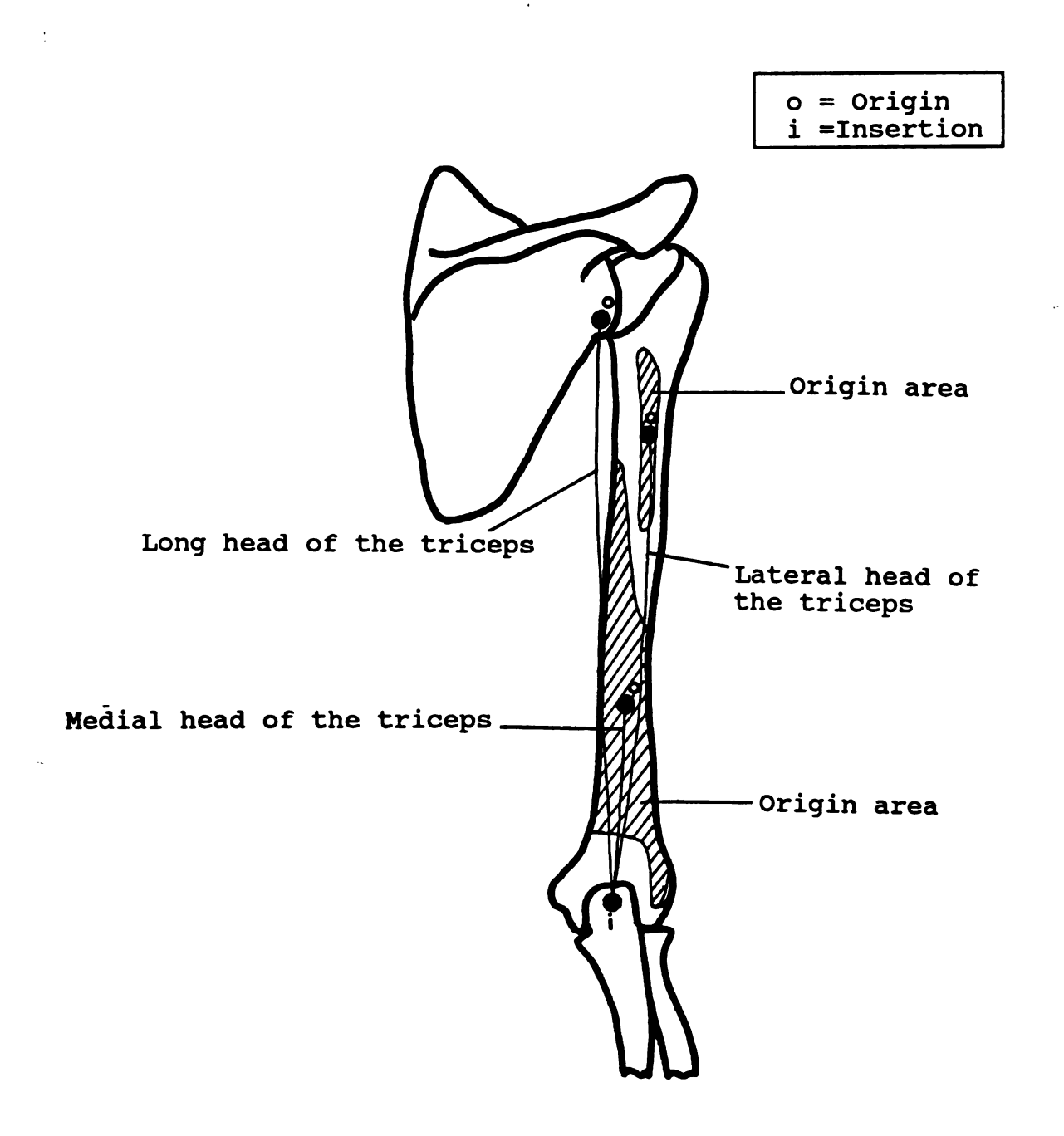
B. Selection of Muscle Model

Based on the sliding filament theory of muscle contraction, size principle, and currently existing physiological and biomechanical data on muscles, Hatze (1981) derived five differential equations governing muscle dynamics and successfully simulated the kicking motion and the take-off phase of the long jump. His muscle model has several significant advantages over other existing muscle



Anterior view

Figure 3-8. Prime muscles for elbow flexion.



Posterior view

Figure 3-9. Prime muscles for elbow extension.

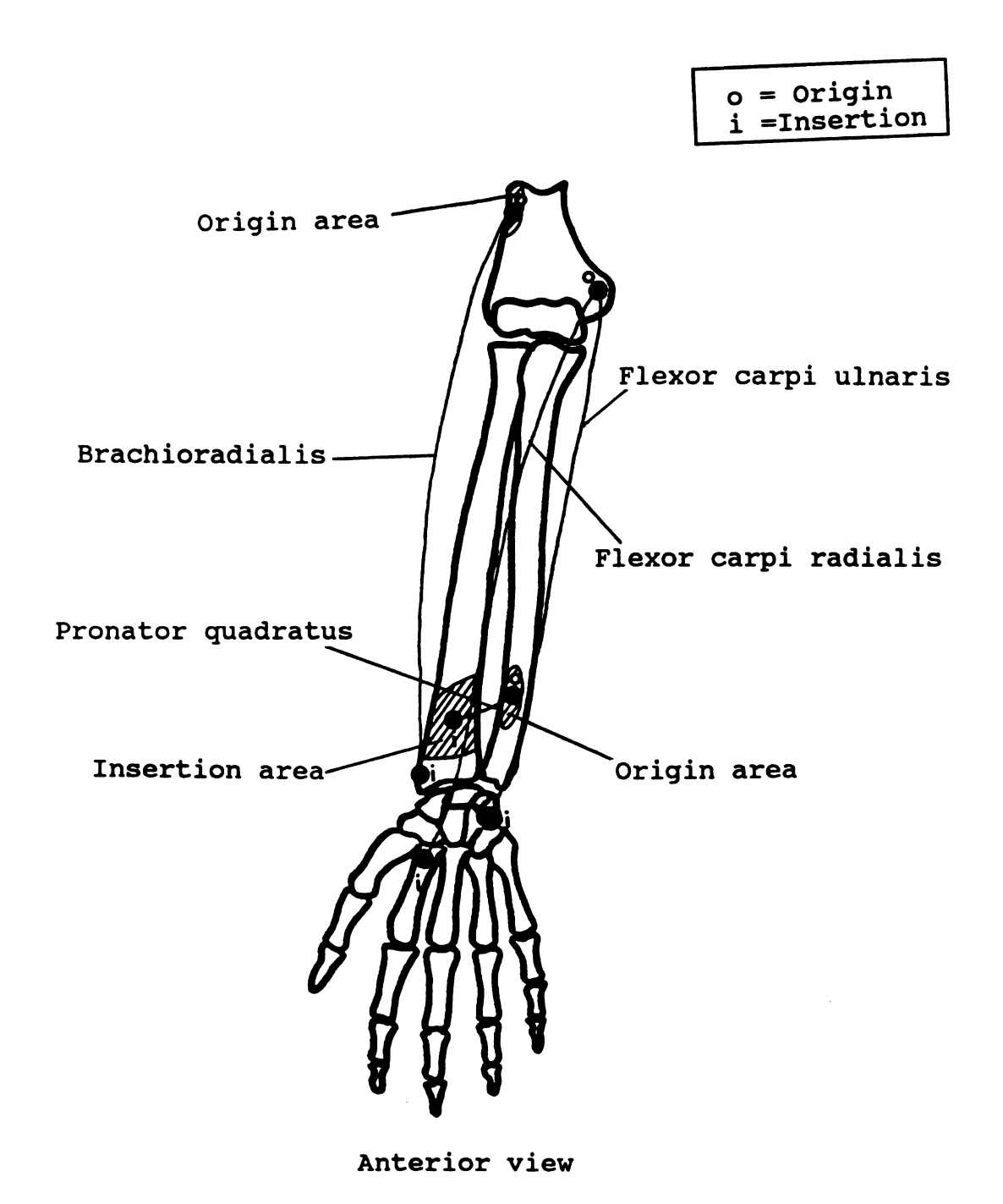


Figure 3-10. Prime muscles for elbow and wrist flexion and forearm pronation.

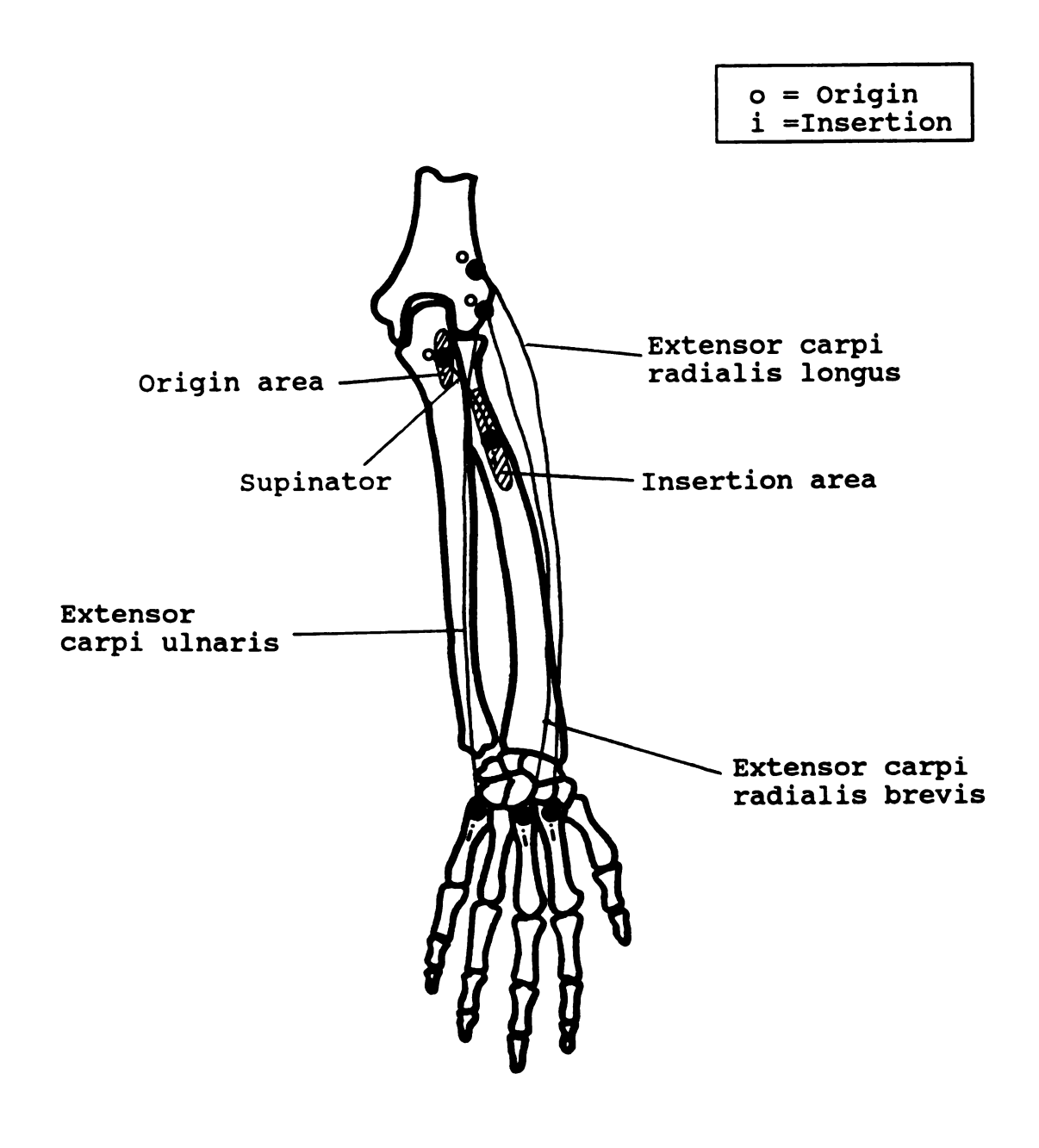


Figure 3-11. Prime muscles for elbow and wrist extension and forearm supination.

models. First, his muscle model includes control parameters, stimulation rate and the rate of motor unit recruitment. Second, his model involves subject-specific physiological parameters that may be able to explain individual differences in movement patterns. Third, his model has been used successfully to simulate human motion in kicking and the take-off phase of the long jump.

In this author's opinion, Hatze's model is currently the best-suited muscle model for the purpose of simulation as studied in the present dissertation. Hatze's muscle model, however, has one serious disadvantage, complexity of its equations. Its equations are highly non-linear. Therefore, Hatze's model brings problems related to instability during simulation and/or optimization and results in a great amount of computing time.

Hatze's five most recent equations (1981) are rewritten here without any modification. Readers interested in learning more about Hatze's muscle model should read his book (1981) and articles on the topic.

$$\dot{n} = \hat{n}z \tag{3-29}$$

$$\dot{r} = -\hat{n}z \frac{r - w^{-}\delta}{r + \delta} - (1 + w^{-}) \frac{m(n,r)r}{10^{-3}m(n,r) + (\phi/k_{2}c)^{2}}$$
(3-30)

$$\psi - m(n) \left[cv - \psi \right] + w^* z \overline{c} \hat{n} \frac{1 - \exp\{\rho_o(\xi) (\psi - \phi)\}}{\rho_o(\xi) (1 - \exp\{-\overline{c}n - \overline{\delta}\})}$$

$$- (1 + w^-) m(n, r) \phi$$
(3-31)

$$\dot{\varphi} = -m(n,r) \varphi - w^{-} \left[m(n) \varphi \left(\frac{cV}{\psi + \overline{\delta}} - 1 \right) - z\overline{c}\hat{n} \frac{1 - \exp\{\rho_{o}(\xi) (\varphi - \psi)\}}{\rho_{o}(\xi) (\exp\{\overline{c}r + \overline{\delta}\} - 1)} \right]$$
(3-32)

$$\xi = \frac{1}{S} \left[\frac{1}{a_3} \arcsin \left(-\frac{1}{a_2} \right) \right]$$

$$\ln \left(\frac{k(\xi) e}{b_2 \left[F^{SE} / F + b_1 k_1(\xi) \right]} - a_1 \right) - 1/2 \right]$$
(3-33)

The state variables in Hatze's equations are n, r, ψ , φ and ξ , that denote respectively the normalized populations of stimulated (n) and semi-active (r) motor units, Caconcentrations of stimulated (ψ) and semi-active (φ) populations, and the normalized length of the lumped contractile element (ξ). The control parameters, z and v, are the normalized rate of motor unit recruitment and the normalized average stimulation rate, respectively.

Functions in his equations, m(n,r), m(n), $\rho_o(\xi)$, $k(\xi)$, and $k_1(\xi)$, are defined as follows:

$$m(n,r) = \frac{1}{1 - \exp(-\overline{c}r)} \left[\frac{e_{11}(\overline{c}A_2 / A_3 - \overline{c}(n+r))}{A_2 - A_3(n+r)} - \frac{\exp(-\overline{c}r)}{A_2 - A_3n} e_{11}(\overline{c}A_2 / A_3 - \overline{c}n) \right], \qquad (3-34)$$

$$m(n) = \frac{1}{\exp(\overline{c}n) - 1} \left[\frac{\exp(\overline{c}n)}{A_2 - A_3 n} e_{11} (\overline{c}A_2 / A_3 - \overline{c}n) - \frac{e_{11} (\overline{c}A_2 / A_3)}{A_2} \right], \qquad (3-35)$$

$$\rho_{o}(\xi) = 53300 \frac{\xi^{s} - 1}{(\xi / \xi)^{s} - 1}, \tag{3-36}$$

$$k(\xi) = \exp\{-\left[\frac{\xi - 1}{S_k}\right]^2\},$$
 (3-37)

$$k_1(\xi) = 2 - \exp\{\delta_{\epsilon}(\xi - 1)\}.$$
 (3-38)

Function ϵ is given by:

$$e - e_n + e_r + e_o$$
 (3-39)

where

$$\epsilon_n - q(\xi, \psi) \left[\exp(\overline{c}n) - 1 \right] / \left[\exp(\overline{c}) - 1 \right],$$
(3-40)

$$\epsilon_r - q(\xi, \varphi) \left[\exp(\overline{c}n + \overline{c}r) - \exp(\overline{c}n) \right]$$

$$/ \left[\exp(\overline{c}) - 1 \right], \qquad (3-41)$$

$$\epsilon_{o} - q_{o} \left[\exp(\overline{c}) - \exp(\overline{c}n + \overline{c}r) \right] / \left[\exp(\overline{c}) - 1 \right]$$
 (3-42)

and where

$$q(\xi, \psi) = \frac{q_0 + [\rho(\xi)\psi]^2}{1 + [\rho(\xi)\psi]^2},$$
 (3-43)

$$q(\xi, \varphi) = \frac{q_0 + [\rho(\xi)\varphi]^2}{1 + [\rho(\xi)\varphi]^2}.$$
 (3-44)

Function 8 is given as follows:

$$S = (e_n S(n) + e_r S(n, r) + e_o S_o) / e$$
(3-45)

where

$$S(n) = \frac{\acute{a}_2}{B} - \frac{\acute{a}_3}{B} n(0.568 + 0.2307n), \qquad (3-46)$$

$$S(n,r) = \frac{a_2}{B} - \frac{a_3}{B}(n + 0.568r + 0.2307r^2),$$
 (3-47)

$$S_{0} = \frac{\dot{a}_{2}}{B} - \frac{\dot{a}_{3}}{B} [n + r + 0.568(1 - n - r) + 0.2307(1 - n - r)^{2}]. \tag{3-48}$$

Functions w and w are defined as follows:

$$w^{+}(z) = 1$$
, $w^{-}(z) = 0$, for $z > 0$;
 $w^{+}(z) = 0$, $w^{-}(z) = 0$, for $z = 0$; and
 $w^{+}(z) = 0$, $w^{-}(z) = -1$, for $z < 0$. (3-49)

Detailed derivations and explanations of these equations, functions, and nomenclature can be found Hatze's book "Myocybernatic control models of skeletal muscle", and numerous articles and technical reports.

C. Moment Arms

Based on graphs from Amis' dissertation (1978), moment arm functions of prime muscles with respect to joint angles were derived by the method of least squares. This method seeks to minimize the sum of the squares of the difference between the function and the tabulated data values.

The size of the cadaver arm used in Amis' study is different from that of the subject in this study. Width between trochlea and capitulum and the length of radius seen clearly from both Amis' scaled figure and x-rays taken from the subject for this study were measured to find a scaling factor. The scaling ratios for width and length were 1.26 and 1.24, respectively. Therefore, an average scaling factor of 1.25 was used to multiply Amis' data before adopting these values for this study.

Moment arm data were divided into a few separate regions depending on characteristics of data such as periodicity, exponential tendency, and symmetry. Then, several orders of polynomials were tried to find the closest polynomial function to the tabulated data. Cholesky's method (Shoup, 1984) with partial pivoting was adopted to solve the system of linear equations.

The followings are polynomial equations for prime muscles. Moment arms and joint angles are given in meters and degrees.

1. Moment arms (TA) with respect to elbow joint angle (ψ_2) in degrees.

Biceps:

$$TA(\psi_2) = 0.025 \text{ for } 0 \le \psi_2 \le 35$$
 (3-50)
 $TA(\psi_2) = -6.192E-03 + 8.845E-04 \psi_2 + 1.279E-06 \psi_2^2$

- 3.418E-08
$$\psi_2^3$$
 for $\psi_2 > 35$ (3-51)

Brachialis:

$$TA(\psi_2) = 0.02 \text{ for } 0 \le \psi_2 \le 47$$
 (3-52)

$$TA(\psi_2) = -8.027E-03 + 6.571E-04 \psi_2 - 9.274E-07 \psi_2^2$$

- 1.170E-08 ψ_2^3 for $\psi_2 > 47$ (3-53)

Brachioradialis:

$$TA(\psi_2) = 0.027 \text{ for } 0 \le \psi_2 \le 20$$
 (3-54)

$$TA(\psi_2) = 1.301E-02 + 5.973E-04 \psi_2$$

for 20 <
$$\psi_2 \le 130$$
 (3-55)

$$TA(\psi_2) = 0.092 + 8.929E-05 \psi_2 \text{ for } \psi_2 > 130$$
 (3-56)

Triceps:

$$TA(\psi_2) = 2.942E-02 + 1.946E-04 \psi_2$$

- $4.048E-06 \psi_2^2$ for $0 \le \psi_2 \le 60$ (3-57)

$$TA(\psi_2) = 2.229E-02 + 1.849E-04 \psi_2$$

- 1.760E-06
$$\psi_2^2$$
 for 60 < $\psi_2 \le 115$ (3-58)

$$TA(\psi_2) = 0.020 \text{ for } \psi_2 > 115$$
 (3-59)

2. Moment arms (TA) with respect to wrist joint angle (ψ_4) in degrees.

Amis (1978) considered moment arms of the flexor carpi ulnaris, flexor carpi radialis, extensor carpi radialis longus, extensor carpi radialis brevis, and extensor carpi ulnaris muscles as constants. On the other hand, Brand (1985) reported that moment arms of these muscles at the wrist vary depending on not only joint angle but also the position of the hand. According to Brand (1985), the moment arm of the extensor carpi ulnaris of the pronated hand is smaller than that of the supinated hand. reported variations in moment arms, depending on joint angle and the position of hand, are very small. Therefore, it may be reasonably assumed, for simulation purposes, that moment arms of muscles crossing the wrist joint are constants for all wrist angles. Constant moment arms scaled from Amis' dissertation (1978) are given as follows.

Flexor carpi radialis:

$$TA(\psi_{\Delta}) = 0.013 \tag{3-60}$$

Flexor carpi ulnaris:

$$TA(\psi_{\lambda}) = 0.020 \tag{3-61}$$

Extensor carpi radialis longus:

$$TA(\psi_{\lambda}) = 0.01 \tag{3-62}$$

Extensor carpi radialis brevis:

$$TA(\psi_{\lambda}) = 0.015 \tag{3-63}$$

Extensor carpi ulnaris:

$$TA(\psi_{\lambda}) = 0.007 \tag{3-64}$$

D. Muscle Length

Muscle length can be represented as a function of the In general, a muscle length function is joint angle. computed from the simple geometry of a joint structure, with assumptions of a straight line of pull of the muscle and a circular shape of the joint structure (Frigo and Pedotti, 1978; Youm, 1980; Torzilli, 1982; Audu, 1985; Seireg and Arvikar, 1989). The muscle paths, however, are not generally in a straight line (Jensen and Davy, 1975; Amis et al., 1979; Hatze, 1980; An et al., 1984). The curved nature of the muscle lines may be able to provide the best estimation of the line of muscle action and be more accurate than a straight line in approximating muscle length (An et Hatze (1981) computed a muscle length function of the triceps muscle based on sequential x-ray pictures taken from a subject at various angles of the elbow joint.

In the present study, based on Amis' scaled figure representing muscle lines, the origins and the insertions of muscles, muscle lengths were measured at various joint angles. Polynomial equations for muscle length variations as functions of joint angles were derived by the method of least squares. Muscle length variations in meters and degrees, depending on joint angle, are given as follows:

1. Length of muscles (ML) with respect to elbow joint angle (ψ_2) .

Long head of triceps:

 $ML(\psi_2) = 0.276 + 5.3059E-04 \psi_2 - 9.0322E-07 \psi_2^2$ (3-65) Lateral head of triceps :

 $ML(\psi_2) = 0.251 + 5.4609E-04 \psi_2 - 1.1430E-06 \psi_2^2$ (3-66) Medial head of triceps :

 $ML(\psi_2) = 0.102 + 4.8016E-04 \psi_2 - 6.4858E-07 \psi_2^2$ (3-67) Brachioradialis:

 $ML(\psi_2) = 0.370 - 3.7650E-04 \psi_2 - 4.1071E-06 \psi_2^2$ (3-68) Biceps:

 $ML(\psi_2) = 0.382 - 4.6377E - 04 \psi_2 - 1.7969E - 06 \psi_2^2$ (3-69) Brachiais:

$$ML(\psi_2) = 0.137 - 2.1631E-04 \psi_2 - 1.7113E-06 \psi_2^2$$
 (3-70)

2. Length of muscles (ML) with respect to elbow joint angle (ψ_2) and/or wrist joint angle (ψ_4) .

Lengths of muscles that cross the wrist joint were determined by combining Amis' figure and measurements taken from x-rays of the subject because Amis' figure didn't include the hand.

Flexor carpi ulnaris:

 $ML(\psi_4) = 0.305 + 2.4412E-04 \psi_4 - 6.8369E-07 \psi_4^2$ (3-71) Flexor carpi radialis :

$$ML(\psi_4) = 0.3385 + 2.4412E-04 \psi_4 - 6.8369E-07 \psi_4^2 (3-72)$$

Extensor carpi radialis longus:

$$ML(\psi_2, \psi_4) = 0.355 - 3.2503E - 04 \psi_2 - 1.0968E - 06 \psi_2^2$$

- 3.7843E - 04 \psi_4 - 1.4190E - 06 \psi_4^2 (3-73)

Extensor carpi radialis brevis :

 $ML(\psi_4) = 0.3188 - 3.7843E-04 \psi_4 - 1.4190E-06 \psi_4^2$ (3-74) Extensor carpi ulnaris :

 $ML(\psi_4) = 0.3013 - 3.7843E-04 \psi_4 - 1.4190E-06 \psi_4^2$ (3-75) Pronator quadratus :

$$ML(\psi_{\lambda}) = 0.047 + 1.6813E-04 \psi_{\lambda}$$
 (3-76)

Among the 14 muscles, the long and short head of biceps, long head of triceps, flexor carpi ulnaris, flexor carpi radialis, extensor carpi radialis longus and brevis, and extensor carpi ulnaris cross two joints. These joints are either the gleno-humeral and elbow joints or the elbow and wrist joints. Thus, these are called two joint The locations of origins of the two heads of the biceps and the long head of triceps are very close to the gleno-humeral joint. Therefore, muscle length variations of these muscles, depending on gleno-humeral joint motion, may be very small because the gleno-humeral joint is relatively stationary during the acceleration phase of the baseball pitching motion that was being studied. these reasons, these two joint muscles are considered in this study to be one joint muscles (considered to only cross the elbow joint).

The flexor carpi radialis and flexor carpi ulnaris muscles arise by the common flexor tendon from the medial epicondyle of the humerus (see Figure 3-10). The extensor carpi radialis brevis and extensor carpi ulnaris take their origin from the lateral epicondyle of the humerus by the common extensor tendon (see Figure 3-11). These common flexor and extensor tendons are located lateral and close to the elbow joint. In the literature, these four muscles are commonly regarded as the wrist joint flexors and Because the origins of these four muscles are extensors. located close to the elbow joint, they may be able to be considered as a one joint muscle (considered to only cross the wrist joint) without a loss of accuracy.

The extensor carpi radialis longus, however, arises from the distal one-third of the lateral supracondylar ridge of the humerus and from the intermuscular septum (see Figure 3-11). This origin is far from the elbow joint.

Therefore, the extensor carpi radialis longus muscle was treated as a two-joint muscle (considered to cross both the elbow and the wrist joint) and is appropriately represented in equation 3-73.

It is difficult to measure the length variation of the supinator muscle from x-ray or Amis' (1978) scaled figure because this muscle is obliquely wound around the shaft of radius bone. Therefore, based on the geometrical shape of the ulna and radius as seen in Figure 3-12, the length variations of supinator muscle in meters was approximated as

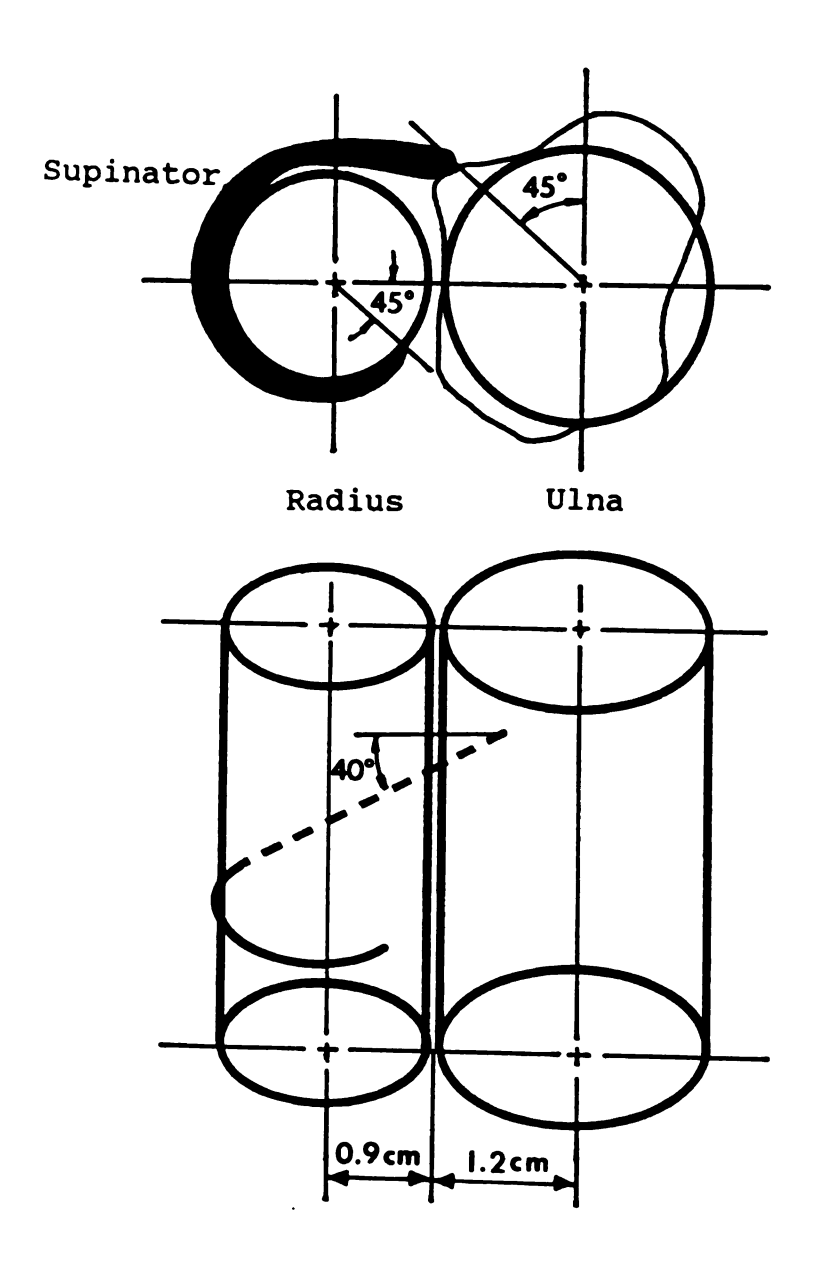


Figure 3-12. Model for approximating supinator muscle length variations.

follows:

supinator:

$$ML(\phi_3) = 0.0763 - 0.0173\phi_3$$
 (3-77)

where

 ϕ_3 = forearm pronation-supination angle in radians.

Currently, the centroids of muscle paths are approximated from the study of cadavers. The error inherent in substituting data from cadavers for living subjects may be resolved in the near future if non-invasive computerized scanning techniques such as NMR become available for use.

CHAPTER IV

SIMULATION AND OPTIMIZATION

In Chapter III, three second-order differential equations were derived to describe a four segment rigid-body dynamics system. In order to simulate the acceleration phase of the baseball pitching motion with these three differential equations and Hatze's muscle equations, all parameters needed as input to these equations were determined prior to simulation and optimization. In this chapter, anthropometric, anatomical, motion-related, and muscular parameters, that were not presented in Chapter III, are described. Based on these parameters, simulation and optimization were performed.

- I. DETERMINATION OF CONSTANTS AND PARAMETER VALUES
- A. Anthropometric Measurements

The primary purpose of anthropometric measurements in simulation of human motion is the calculation of moments of inertia, centers of segmental masses, and segmental mass distributions.

Using a sliding and a spreading calipers and an inelastic tape measure, various anatomical dimensions were measured as recommended in the Anthropometric

Standardization Reference Manual (Lohman, et al., 1988).

Tables 4-1 through 4-3 contain anthropometric data obtained from the subject in the current study.

Table 4-1. Length and weight measurements from the subject.

Weight(kg)	Height(cm)	Arm(cm)	Forearm(cm)	Hand(cm)
90.05	94.05	38.3	33.1	21.2

* Landmarks for determining length:

arm length: from superiolateral aspect of the acromion process of the scapula to posterior surface of the olecranon process of the ulna

forearm length: from the most posterior point overlying
the olecranon process to the most distal
palpable point of the styloid process of
the radius

hand length: from styloid process of the radius to the tip of the middle finger

Table 4-2. Width measurements from the subject.

Portion of Body Segment		Upper Arm(cm)	Forearm(cm)	Hand(cm)
proximal	m-1 *	10.8	7.8	11.6
	a-p**	13.1	7.6	4.6
middle	m-l	8.7	9.3	8.5
	a-p	9.7	6.8	2.6
distal	m-l	7.8	5.8	7.8
	a-p	7.8	4.3	2.0

* m-l: medial-lateral

** a-p : anterior-posterior

Table 4-3. Circumference measurements from the subject	Table 4-3. Circumfer	rence measuremen	ts from	the	subject	5 .
--	----------------------	------------------	---------	-----	---------	------------

Portion of Body Segment	Upper Arm(cm)	Forearm(cm)	Hand(cm)
proximal	42.2(below axilla)	30.0	27.5
middle	33.3		20.4
distal	28.2	17.4	17.8

Regression equations proposed by Zatsiorsky and Seluyanov (1983, 1985) were used to calculate segmental parameters of the subject. Computed segmental masses of the upper arm and the forearm were 3.16 kg and 1.6 kg, respectively. The locations of mass centers of the upper arm and the forearm were 21.42 cm and 19.36 cm from the distal end of their segment, respectively. Principal moments of inertia of the upper arm at the center of mass about the body-fixed coordinate system were $I_{xx} = 0.02873 \text{ kg.m}^2$, $I_{xy} = 0.03065 \text{ kg.m}^2$, and $I_{,,} = 0.00685 \text{ kg.m}^2$. Principal moments of inertia of the forearm at the center of mass about the body-fixed coordinate system were I = 0.0121 kg.m², $I_{w} = 0.0126 \text{ kg.m}^2$, and $I_{zz} = 0.00222 \text{ kg.m}^2$. Moments of inertia at the center of mass of the combined hand and ball were $I_{xx} = I_{w} = 0.00125 \text{ kg.m}^2 \text{ and } I_{yy} = 0.00121 \text{ kg.m}^2.$

B. Anatomical Parameters

Four x-ray pictures, consisting of an anterior and a lateral view of the upper arm and the forearm, were taken at

the Clinical Center of Michigan State University. Subject-specific anatomical dimensions of the upper arm and the forearm, that were needed as input data in the study, were measured from x-ray pictures as shown in the Figure 4-1. Cartesian coordinate of internal position vectors (see Figure 3-4) in centimeters were $\mathbf{p_1} = (0, 0, 21.1)$, $\mathbf{p_2} = (0, 0, 12.2)$, $\mathbf{p_3} = (-1.7, 0, 7.4)$, $\mathbf{p_4} = (1.4, 0, 0)$, $\mathbf{p_5} = (0, 0, 11.4)$, and $\mathbf{p_6} = (0, 0, 11.0)$. Angle values (see Figure 3-5) in degrees as defined in the Chapter III were $\phi_2 = 0.0$, $\theta_2 = 8.0$, $\theta_3 = 7.0$, $\psi_3 = 0.0$, $\phi_4 = 0.0$, and $\theta_4 = 7.0$.

Cadaver measurements were also conducted to obtain muscle-tendon length ratios of the prime muscles studied because these values could not be obtained from the subject. The lengths of muscles and tendons from two male cadaver arms (one arm dissected from the anterior view and the other arm dissected from the posterior view) were measured with a steel tape measure. From these two cadavers, muscletendon ratios of the long head of the biceps, short head of the biceps, brachialis, brachioradialis, flexor carpi radialis, flexor carpi ulnaris, extensor carpi radialis longus, extensor carpi radialis brevis, and extensor carpi ulnaris were 0.28/0.72, 0.66/0.31, 0.37/0.07, 0.60/0.30, 0.59/0.49, 0.90/0.18, 0.36/0.81, 0.38/0.79, and 0.60/0.47, It should be mentioned that it is not known respectively. how appropriate the anthropometric measurements from the two cadaver arms were with respect to the subject used in this

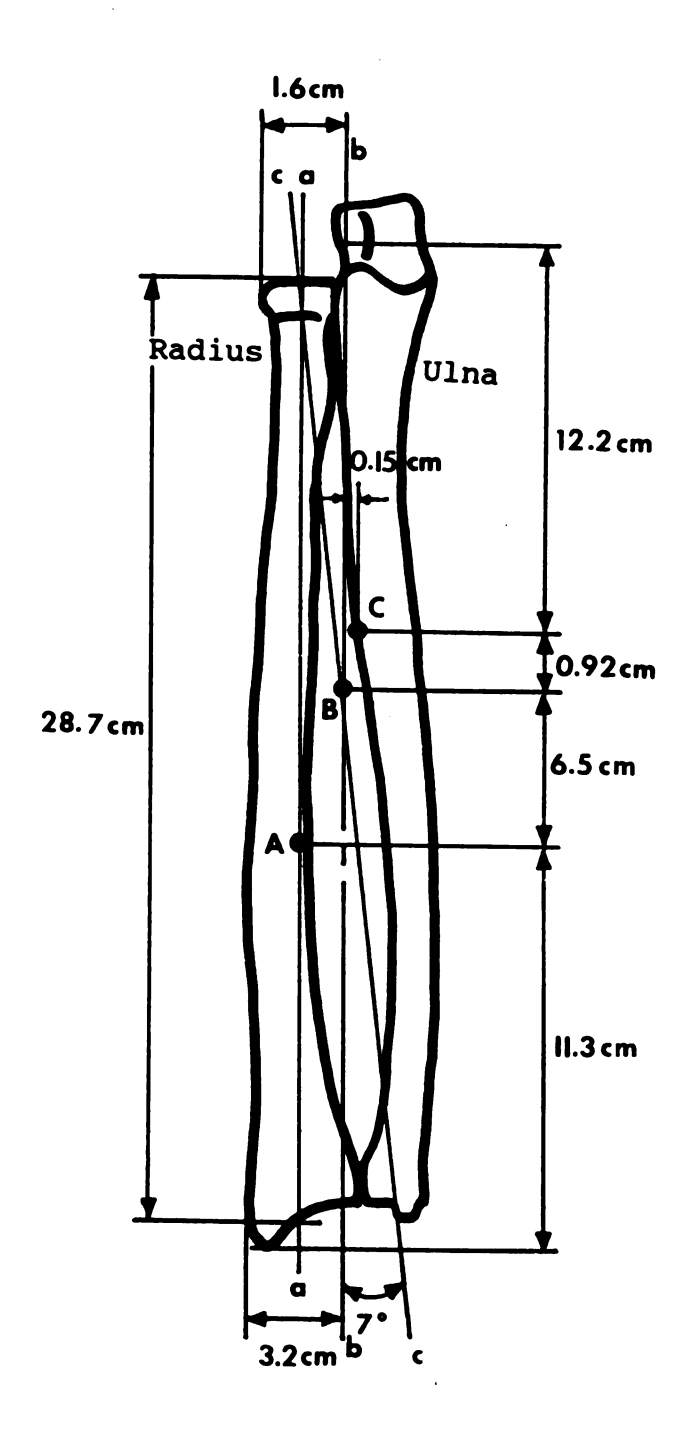


Figure 4-1. Anatomical geometry of the subject's forearm.

study.

Based on fiber length and layer thickness data, fiber angles of pennate muscles relative to line of pull were computed using the following formula as suggested by Amis (1978):

fiber
$$\angle - \sin^{-1}\left(\frac{layer\ thickness}{fiber\ length}\right)$$

Fiber structures, fiber angles and cross-sectional areas of four muscular cadaver limbs adopted from Amis' dissertation (1978) are shown in the Table 4-4, Table 4-5, and Table 4-6.

Table 4-4. Muscle structure (From Amis' dissertation(1978), "Biomechanics of the upper limb, and design of an elbow prosthesis").

Muscle	Cadaver	Cadaver	Cadaver	Cadaver
	1	2	3	4
BI(long) BI(short) BRR TR(long) TR(medial) TR(lateral) BR FCU FCR ECU	PF * UP ** UP UP UP PF BP ***	PF UP UP UP UP PF UP UP BP	PF UP PF UP UP PF BP UP BP	PF UP PF UP UP UP PF UP BP
ECRL	BP	BP	BP	BP
ECRB	UP	UP	BP	UP
PQ	PF	PF	PF	PF
SP	PF	PF	PF	PF

^{*} PF = parallel fiber

^{**} UP = unipennate muscle

^{***} BP = bipennate muscle

Each muscle of four cadavers studied by Amis (1978) had the same fiber structure except for the flexor carpi ulnaris and the extensor carpi radialis brevis. In the present study, the flexor carpi ulnaris and the extensor carpi radialis brevis were treated as unipennate and bipennate, respectively. Other muscles were treated as being the same fiber structure as shown in Table 4-4.

Table 4-5. Fiber angle (rad) (From Amis' dissertation(1978), "Biomechanics of the upper limb, and design of an elbow prosthesis").

Muscle	Cadaver 1	Cadaver 2	Cadaver	Cadaver 4	Average
BI(long)	0.0	0.0	0.0	0.0	0.0
BI(short)	2.5	3.0	4.7	2.9	3.3
BRR	0.0	0.0	0.0	0.0	0.0
TR(long)	18.5	17.8	15.7	17.1	17.3
TR(medial)	10.9	8.6	13.2	9.6	10.6
TR(lateral)	10.8	14.2	11.9/ 8.5	20.9	14.5/ 2.1
BR	0.0	0.0	0.0	0.0	0.0
FCU	5.7/5.7	2.9	9.6/1.8	10.2	7.1/1.9
FCR	13.0	6.8	8.6	13.7	10.5
ECU	5.0/3.9	4.0/5.2	8.5/6.8	3.4/6.2	5.2/5.5
ECRL	4.9/1.9	3.9/1.5	6.4/3.7	5.5/2.2	5.2/2.3
ECRB	7.8	6.4	9.4/3.5	7.9	7.9/0.9
PQ	0.0	0.0	0.0	0.0	0.0
SP	0.0	0.0	0.0	0.0	0.0

Maximum muscle fiber angle of the long fibers and minimum muscle fiber angle of the short fibers are needed in Hatze's muscle model if the muscle considered is a pennate muscle. These angles, however, are very difficult to measure without the help of dissection specialists and several fresh Additionally, there is no guarantee that these values would match that of the living subject used in this Therefore, under the quideline of the average study. fiber angles reported in Table 4-5, maximum and minimum fiber angles of pennate muscles were estimated from actual photographs of dissected muscles shown in anatomy books (Vidic and Suarez, 1984; Clemente, 1987). Respective maximum and minumum angles, in radians, of the long head of the triceps, medial head of the triceps, lateral head of the triceps, flexor carpi ulnaris, flexor carpi radialis, extensor carpi ulnaris, extensor carpi radialis longus, and extensor carpi radialis brevis were 1.40/1.13, 1.53/1.24, 1.46/1.18, 1.501/1.396, 1.449/1.344, 1.518/1.449, 1.553/1.449, and 1.536/1.466, respectively.

Physiological cross-sectional areas of muscles were needed to estimate the initial guesses of muscular forces in the optimization algorithm for muscular parameter estimation that is explained in section E of this chapter.

Physiological cross-sectional areas of muscles, muscletendon length ratios, and fiber angles for pennate or multipennate muscles may be obtained by Nuclear Magnetic Resonance (NMR) directly from a living subject (Freimanis,

1989).

Table 4-6. Physiological cross-sectional area (mm²) of muscles (From Amis' dissertation (1978), "Biomechanics of the upper limb, and design of an elbow prosthesis").

Muscle	Cadaver 1	Cadaver 2	Cadaver 3	Cadaver 4	Average
BI(long)	297	244	413	305	315
BI(short)	178	178	396	256	252
BRR	140	76	322	158	174
TR(long)	1563	1418	2044	1760	1696
TR(medial)	1491	712	1446	1283	1233
TR(lateral)	1237	1061	1542	1055	1233
BR	269	405	949	602	556
FCU	537	361	497	662	539
FCR	242	178	294	377	273
ECU	283	228	472	316	325
ECRL	239	196	330	326	273
ECRB	434	237	472	244	347
PQ	252	333	280	288	288
SP	247	200	395	222	266

Magnetic Resonance Imaging (MRI): a) offers a direct visualization of soft tissue structures, (It has recently been recognized as a significant contribution to the evaluation of the musculoskeletal system.) b) provides more convenient planes of view, such as transverse, sagittal, coronal, and oblique, than other methods for evaluating the structure of muscle. c) is completely non-invasive with no known health risks because it does not

require exposing subjects to ionizing radiation (Roth, 1984; Hillman et al., 1986; Bloem et al., 1988; Harms and Greenvay, 1988; Kieft and Bloem, 1988). NMR, however, was not available for this current study.

C. Motion-Related Parameters

1. Tracking parameters

As mentioned in the Chapter I, the baseball pitching motion is accomplished by a sequential interaction of all body segments, through a link system from the foot to the throwing hand. This project was restricted to the pitching arm. Therefore, the influence of other parts of body on the pitching motion was taken into account as input parameters to simulate the actual pitching motion performed by the whole body. These parameters are called tracking parameters in this project.

The contribution of other body segments to the pitching motion is transmitted to the pitching hand through the upper arm, connected to the trunk at the gleno-humeral joint.

Tracking parameters of the upper arm are translational and rotational position vectors and their first and second time derivatives at the center of mass relative to the inertial coordinate system. To determine these tracking parameters, a three-dimensional cinematographic experiment was conducted at the Center for the Study of Human Performance at Michigan State University.

A calibration structure consisting of four aluminum

poles with surveyor's cord on which three ping pong balls per cord was set up in the pitching area (see Figure 4-2). A calibration space was determined by the locations of the ping pong balls placed on each corner of a rectangle. Distances between the ping pong balls were adjusted so that the pitching arm motion could be viewed from two cameras and filmed as large as possible within the calibration space. Then, distances of the edges of the rectangle and distances between ping pong balls were measured (see Figure 4-2). The calibration structure was filmed. The digitized coordinates of the calibration structure became the calibration file.

One half inch (1.27 cm) pompom balls were placed on bony landmarks of the pitching arm of the subject as targets for digitization. Bony landmarks were identified by palpation. Targets, forming an arbitrary triangle, were placed on the upper arm, forearm, and hand to determine a segment-fixed reference frame (see Figure 4-3). This is hereafter called a film coordinate system. These triads were placed on either side of the joints. Joint targets were also placed on the center of both ends of each segment (see Figure 4-3).

In order to film the pitching motion in the laboratory, a portable pitching mound was prepared. One camera was placed lateral and one placed lateral-posterior to the plane of the pitching motion for a better viewing of targets (see Figure 4-2). The inclusion angle of the optical axes of

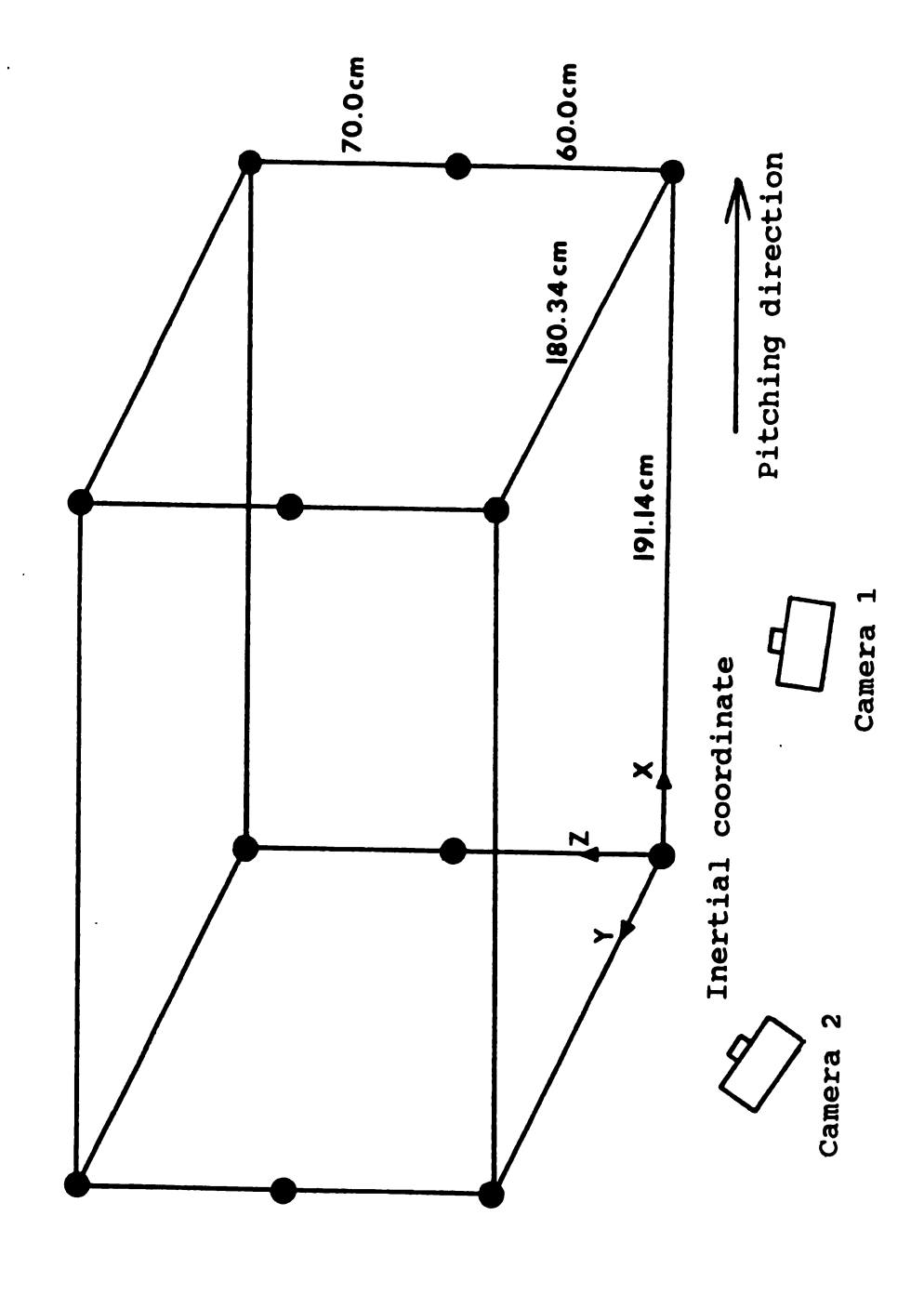


Figure 4-2. Calibration structure.

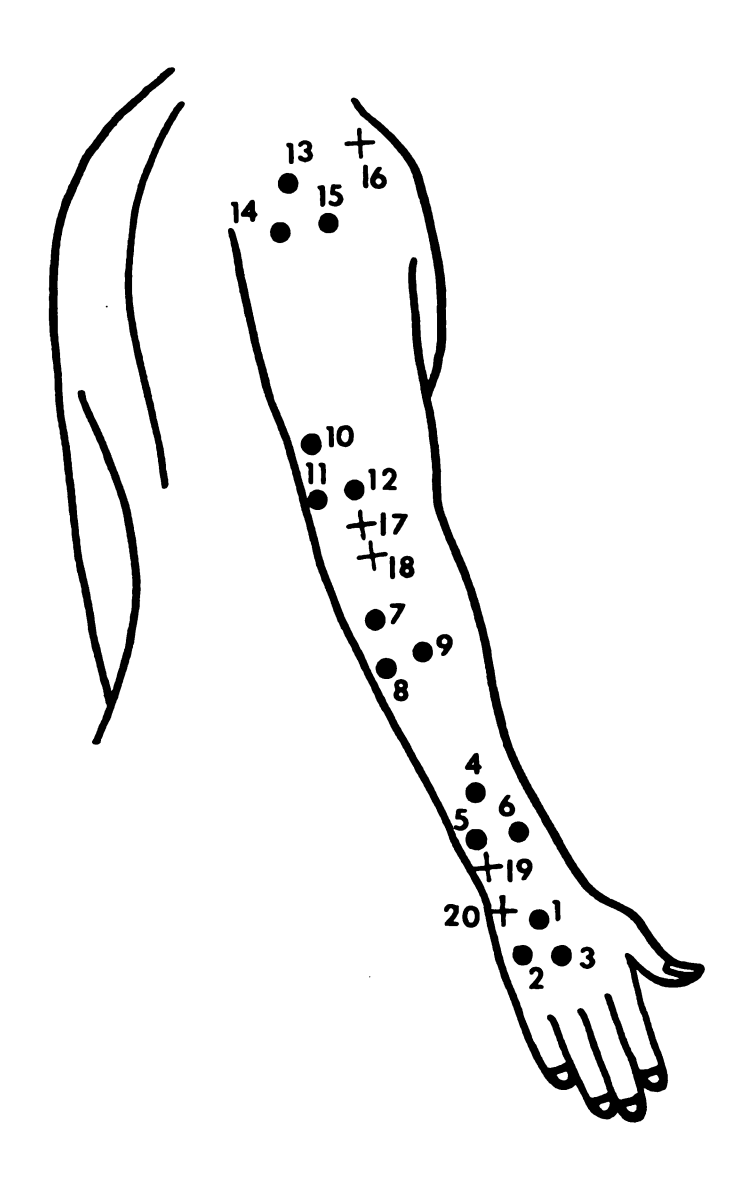


Figure 4-3. Targets on the upper extremity.

the two cameras was about 60 degrees. After several warmup pitches by the subject, overhand fast ball pitching motions were filmed by the two high speed 16 mm cine LOCAM cameras using Kodak 400 ASA color film and operating at 400 frames per second with 120 degree shutter angle. cameras were set identically and operated simultaneously to obtain time-matched position data. Filmed images were digitized using an Altek Datatab rear-projection system, coupled with an IBM personal computer to obtain planar position data from each camera. Slight time-unmatched data that may be mechanically generated in spite of identical setting and simultaneous operation of both cameras were time-matched by a linear interpolation method. Walton's program (JSW3D) was used to convert two sets of synchronized planar position data to three-dimensional position data (Walton, 1981). Raw three-dimensional position data were smoothed using Walton's program FILTER, which applies a low-pass Butterworth filtering technique.

Theoretically, angular orientation of a rigid body may be determined by three known targets placed on a rigid body. Even though human body segments contain soft tissues, they are commonly treated as rigid bodies. In situations where, body targets must be placed on the soft tissues, soft tissue motion may cause errors in the digitization of position data. Tracing targets from film showed that the relative locations of the upper arm and forearm targets placed on the proximal end were recognized to change

slightly during the pitching motion because a relatively large amount of muscle tissue exists in these areas.

Three targets (D₁₄, D₁₆, and D₁₇), placed on relatively immobile locations that formed a triangle as large as possible, were chosen to minimize the effects of soft tissue motion on the analysis of position data. Based on these three targets, two vectors, \overline{V}_1 and \overline{V}_2 and their vector product \overline{V}_y ($\overline{V}_y = \overline{V}_1 \times \overline{V}_2$), that was normal to both vectors, were formed (see Figure 4-4). One more vector \overline{V}_x , the product ($\overline{V}_y \times \overline{V}_z$) of \overline{V}_y crossed into \overline{V}_z was defined so that a film coordinate (X_1^f , Y_1^f , and Z_1^f) could have \overline{V}_x , \overline{V}_y , and \overline{V}_z axes at the origin D₁₆ as an orthogonal coordinate system.

The directions of axes of the film coordinate system were different from the directions of the axes of the bodyfixed coordinate system defined in Chapter III. necessary to rotate the film coordinate axes to the bodyfixed coordinate axes to compare simulation results with experimental results. A transformation matrix [E,] of the direction cosines, relating film coordinate axes to the inertial coordinate axes, could be easily computed by scalar products between axes of the inertial coordinates and the axes of the film coordinates. A transformation matrix $[E_R]$ of Euler angles relating the film coordinate to the body-fixed coordinate can be computed from the locations of the targets on the upper arm and the geometry of the upper arm as seen in Figures 4-4 and 4-5. Euler angles α , β , and γ in the order of rotation of ZYX convention are

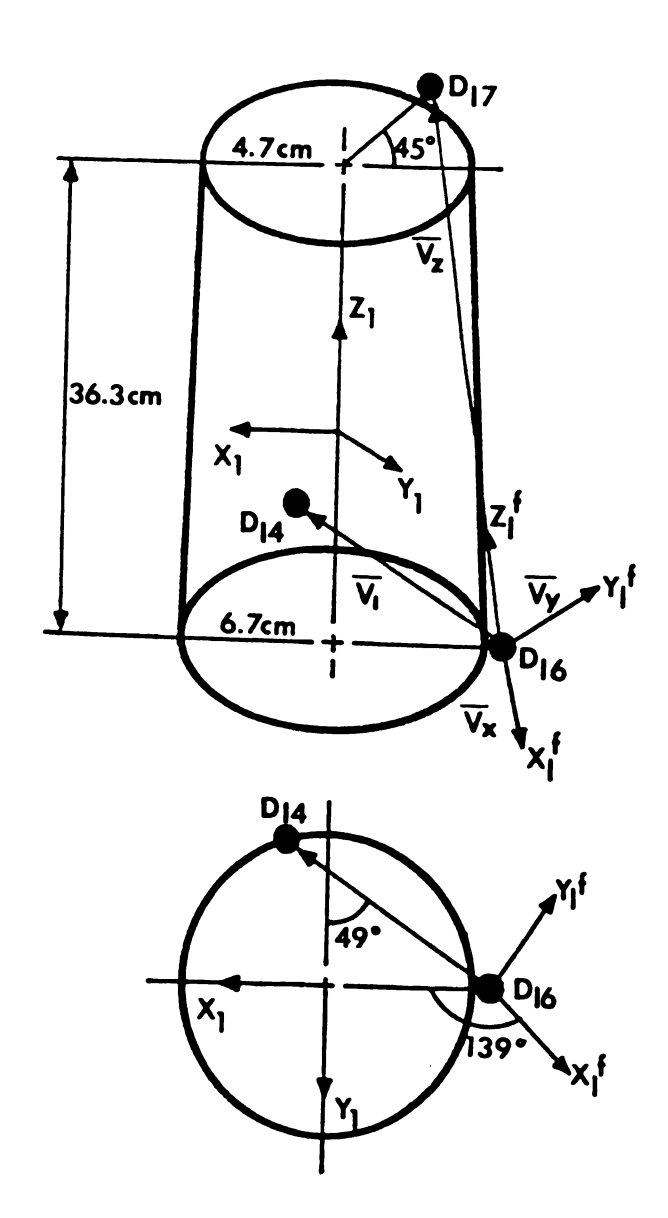


Figure 4-4. Geometry of the upper arm targets.

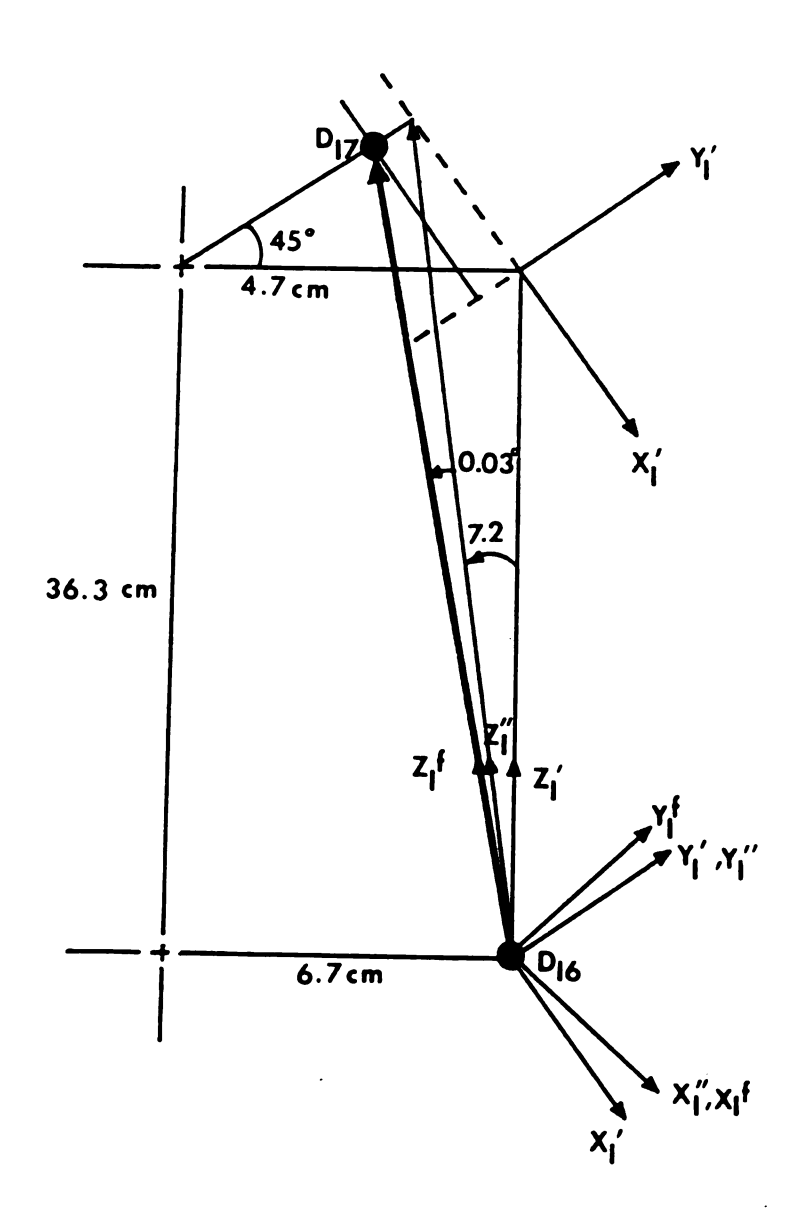


Figure 4-5. Spatial geometry of the upper arm targets.

 α = 139, β = -7.2, and γ = 0.03 degrees. Any position vector \overline{X}_{F} , relative to the film coordinate, can be converted to a position vector \overline{X}_{I} relative to the inertial coordinate or to a position vector \overline{X}_{B} relative to the body-fixed coordinate system by

$$\overline{X}_{F} = [E_{F}] \overline{X}_{1}, \qquad (4-1)$$

$$\overline{X}_{F} = [E_{B}] \overline{X}_{B} . \tag{4-2}$$

From equations 4-1 and 4-2, position vector \overline{X}_B , relative to the body-fixed coordinate system, was computed from the position vector \overline{X}_I , relative to the inertial coordinate system, and transformation matrix $[E_{BF}]$, directly relating the body-fixed coordinate system to the inertial coordinate system as follows:

$$\overline{X}_{B} = [E_{BF}] \overline{X}_{I} \tag{4-3}$$

where

$$[E_{BF}] = [E_{B}]^{-1}[E_{F}].$$

The transformation matrix relating a rotating coordinate system to a non-rotating reference frame may be formed in terms of Euler's angles or direction cosines. The transformation matrix $[E_1]$ of Euler's angles defined in Chapter III should be equivalent to the transformation matrix $[E_{BF}]$ of direction cosines. Then, Euler's angles

may be computed by equalizing respective terms of two transformation matrices (Nikravesh, 1988; Wittenburg, 1977) as in equation 4-4:

$$\sin\theta = -l_{13},$$

$$\cos\theta = \pm\sqrt{1 - \sin^2\theta},$$

$$\cos\phi = \frac{l_{11}}{\cos\theta},$$

where

 $\cos \psi = \frac{l_{33}}{\cos \theta},$

 l_{11} , l_{13} , and l_{33} are respective elements of transformation matrix $[E_{RF}]$ of direction cosines.

More practically, Euler angles can be computed by the two-argument tangent function that is an intrinsic function form of the FORTRAN language (Craig, 1986) as follows:

(4-4)

where

 l_{11} , l_{12} , l_{13} , l_{23} , and l_{33} are respective elements of transformation matrix $[E_{RF}]$.

If the rotation angle (θ) about y-axis is $\pm \pi$ / 2, a condition known as gimbal lock exists and the other Euler angles are undefined. The gimbal lock problem can be solved by setting one of the remaining angles equal to zero (Craig, 1986).

Polynomial equations for angular positions, velocities, and accelerations with respect to time were obtained from the least squares curve fitting method. The following are polynomial equations in radians and seconds for Euler angles, and their velocities and accelerations.

Derivation of these polynomial equations for tracking parameters was needed in simulation and optimization because the integration step size may be different from the film frame time interval.

Angular positions:

$$\phi(T) = -0.08889 + 13.98126T - 19.81561T^2 - 5657.01T^3$$

$$\theta$$
 (T) = 0.7597811 - 1.776727T + 764.9278T² - 10512.12T³

 $\psi(T) = 1.029547 - 0.2909322T + 158.9582T^2 - 6282.549T^3$ (4-6)
Angular velocities:

$$\dot{\phi}(T) = 12.5373 + 379.3696T - 44958.65T^2 + 431054.5T^3$$

$$\dot{\theta}$$
 (T) = 4.954282 - 73.77206T + 90123.87T² - 3536002.0T³
+ 3.401166E+07T⁴

$$\psi$$
(T) = -1.147039 + 662.0113T - 42593.05T²
+ 370858.3T³ (4-7)

Angular accelerations:

$$\ddot{\phi}(T) = 319.1234 - 217352.1T + 1.937653E+07T^{2}$$

$$- 7.288441E+08T^{3} + 8.828221E+09T^{4}$$

$$\ddot{\theta}(T) = 155.5996 + 148582.1T - 9787578.0T^{2}$$

$$+ 1.317554E+08T^{3}$$

$$\dot{\psi}(T) = 559.0472 - 200943.4T + 1.841427E+07T^{2}$$

$$- 7.109204E+08T^{3} + 8.697636E+09T^{4}$$
 (4-8)

The position vector of the mass center of the upper arm (OC), that was also the origin of body-fixed coordinates, relative to the inertial frame, was easily computed as follows:

$$\overline{OC} = \overline{OP} - [E_{BF}]\overline{CP}$$
 (4-9)

where

- \overline{CP} = internal position vector of D_{16} from the origin of the body-fixed coordinate, relative to the body-fixed coordinate and
- \overline{OP} = position vector of D₁₆ from the origin of the inertial coordinate, relative to the inertial frame.

Polynomial equations for the x, y, and z components of the position vector of the center of mass of the upper arm were

also obtained from the least squares curve fitting method.

The following polynomial equations are linear positions,

linear velocities, and linear accelerations of the upper arm
in metric units.

Linear positions:

$$X(T) = 1.120815 + 6.959321T - 9.703201T^2 - 1451.042T^3 + 15060.85T^4$$

$$Y(T) = 0.9062545 + 1.390025T + 26.57316T^2 - 943.8699T^3 + 8098.758T^4$$

$$Z(T) = 0.5310546 + 0.7901497T - 36.6773T^2 - 86.63342T^3 + 8063.237T^4$$
 (4-10)

Linear velocities:

$$\dot{X}(T) = 6.850571 - 52.93292T - 3217.349T^2 + 50774.79T^3$$

$$\dot{Y}(T) = 1.596527 + 47.5819T - 3167.259T^2 + 38831.24T^3$$

$$\dot{Z}(T) = 0.5353068 - 35.83658T - 4642.521T^2 + 192936.4T^3$$

$$- 1.744909E + 06T^4 \qquad (4-11)$$

Linear accelerations:

$$\ddot{X}(T) = -55.06328 - 3395.438T - 351517.0T^2$$

+ 2.238366E+07T³ - 2.845943E+08T⁴

$$\ddot{Y}(T) = 34.73928 - 3154.1734T - 199530.T^2$$

+ 1.146062E+07T³ - 1.305747E+08T⁴

$$\ddot{Z}(T) = -45.85297 - 7537.729T + 493753.6T^2$$

$$-4.432061E+06T^3 - 3.199947E+07T^4 \qquad (4-12)$$

2. Experimental trajectories

Experimental trajectories of the forearm and hand of the pitching arm were obtained from film analysis to compare with predicted angular trajectories that were determined by simulation and optimization in this chapter. Film coordinates of the forearm without radius, radius, and hand were rotated to the directions of respective body-fixed coordinates and moved to the respective origins of body-fixed coordinates in the same manner as described in the computation of the tracking parameters.

The flexion-extension angle at the elbow joint was the angle between the longitudinal axis, z_1 , of the body-fixed coordinate system of the upper arm and the longitudinal axis, z_2 , of the forearm as seen in Figure 3-4. The axis, z_1 , however, was not on the plane that was normal to the angular velocity vector of the elbow motion. The axis z_1^* , that was normal to the angular velocity vector, was obtained by a rotation of -8 degrees of the z_1 axis about the y_1 axis. Now, the angle of flexion-extension at the elbow joint was computed from the scalar product between axis z_1^* and z_2 axis.

The angle of forearm pronation-supination was obtained from the scalar product between the y_2 axis and the y_3 axis (see Figure 3-4).

The hand is very small in size relative to other body segments and moves fast in the baseball pitching motion.

It was reasoned that error might have occurred in obtaining

a body-fixed coordinate at the hand because the triad of targets was very close together and not clearly seen due to its size and speed. Therefore, only one target (D_3) , that presented the best view point during the whole acceleration phase of the baseball pitching motion, was digitized.

A vector, \overline{V}_h , that was obtained by subtracting D_{20} from D_3 , can be easily decomposed into a sum of two terms, the vector component of \overline{V}_h along the X_3 axis and the vector component of \overline{V}_h orthogonal to the X_3 axis. The wrist joint angle was computed by the scalar product between the Z_3 axis and a vector having a component of \overline{V}_h orthogonal to the X_3 axis.

D. Muscular Parameters

In order to incorporate Hatze's muscle model (1981) in the simulation of the acceleration phase of the baseball pitching motion, muscular parameters were determined prior to simulation and optimization. Hatze's muscle parameters may be categorized into three sets for convenience. The first set contains parameters that are common to human skeletal muscle and easily obtained from the literature. These are $\sigma = 1.531$, k = 0.0306, $c = 1.373 \times 10^{-4}$, $\delta = 10^{-8}$, s = 1, $k_2 = 10^{-4}$, $A_0 = 0.372$, B = 0.297, and $A_0' = 3.60$. The second set includes parameters that may have slightly different values from person to person. Because subject specific values are difficult to obtain and experimental equipment and facilities were not available to the current

study, subject values were based on parameter values suggested by Hatze (1981). Reasonable values for these parameters in human skeletal muscle are F^c / F = 1.33, $q_0 = 0.005$, $a_3 = 3.2$, $\check{z} = 1$, n = 14.3, $a_2' = 0.14$, c = 3.7, $a_3' = 0.105$, and v = 2.9. The third set is composed of parameters that are highly individual-oriented and must be directly measured from the subject. These are maximum isometric force (\bar{F}) , optimal muscle length $(\bar{1})$, maximum isometric extension of the tendinous series-elastic component $(\bar{\alpha})$, and the spread of the length-tension curve (S_t) .

To determine \overline{F} , S_{L} , $\overline{\alpha}$, and \overline{l} for the third set of muscle parameters, maximum isometric torques were measured with a simple instrument having a force transducer connected to an IBM personal computer and a frame designed to pull nearly at a right angle at any angular position of a joint. A 35 mm single lense reflex camera (Nikon N2020) and a video camera (Sony CCD-F70) were placed at a right angle to the intended joint motion. Maximum isometric torques, at various angles of flexion-extension at the elbow and the wrist joint and angles of pronation-supination of the forearm, were measured from the subject. Moment arms for experimental torques were measured from photographs taken at every measurement. Based on muscle moment arm, muscle length, muscle cross-sectional area derived from Amis' dissertation (1978), and the measured maximum isometric torque data, a computer program (ELPEST) written by Hatze

(1981) was modified. Also, the sum of squares of differences between predicted torques and measured torques was minimized by the Gauss-Newton-Marquardt method (Kuester and Mize, 1973) to determine parameter values \overline{F} , S_k , $\overline{\alpha}$, and \overline{L} .

An experimental apparatus was designed to measure passive elastic joint torques for elbow and wrist joint flexion-extension and forearm pronation-supination as a function of respective joint angles. The measuring frame consisted of a force transducer and an electric goniometer connected to an IBM personal computer and a circular plate that freely rotated in the horizontal plane. center of the subject's arm was adjusted to the axis of rotation of the plate. The subject's relaxed arm was slowly rotated by an examiner so that the viscous component of the passive joint torque was negligible. Based on passive elastic joint torque patterns obtained from the experiment, constants C_1 , C_2 , C_3 , C_4 , θ_1 , and θ_2 for elbow flexion-extension, wrist flexion-extension, and forearm pronation-supination (see Equation 3-19) were estimated by Marquardt's algorithm (Kuester and Mize, 1973) that minimizes a least squares objective function. Values of these constants are reported in Table 4-7.

Joint	C ₁	C ₂	C ₃	C ₄	^θ 1	θ2
elbow	0.488	1.686	0.475	4.076	1.00	2.00

Table 4-7. Constants of passive joint torque functions.

0.145 3.087 0.114 5.087 0.87 wrist 1.75 forearm 1.043 1.467 0.941 2.256 0.70 2.07

The coefficients of passive viscous torque at the elbow joint was adopted from Hayes and Hatze (1977). The values of the damping coefficient $C(\psi_2)$ for elbow joint ranged from 0.274 Nms/rad at an angular position of 0.56 rad to 0.057 Nms/rad at 1.55 rad and the coefficient value is given by :

$$C(\psi_2) = 0.545 - 0.562\psi_2 + 0.165\psi_2^2 \text{ (Nms/rad)}$$
 where

 ψ_2 = elbow joint angle.

The coefficient value may be different from person to However, the passive viscous torques at the elbow joint is relatively small within the middle range of passive motion compared to active muscular torque. Also note that the moment of inertia of the hand is very small and that the angular velocity of the hand in the baseball pitching motion is less than that of the forearm as reported in Chapter V. Therefore, passive viscous torque at the wrist joint may be ignored without much loss of accuracy.

II. SIMULATION

All anatomical, physiological, and motion-related constants and parameters were determined through experimentation or currently existing data gathered from the related literature. Initial values of ψ_2 , ϕ_3 , ψ_4 , ψ_2 , $\dot{\phi}_3$, and $\dot{\psi}_4$ were obtained from film analysis.

Theoretically, 76 first-order differential equations

(70 for the muscular system and 6 for the skeletal system)

can be simultaneously integrated by predicting 28 control

parameters (14 for rates of motor unit recruitment and 14

for motor unit stimulation rates) based on EMG data obtained

from the literature.

In Hatze's analysis of a kicking motion (1975), however, the control parameters of rate of motor unit recruitment and rate of motor unit stimulation provided identical results. Based on Hatze's result, Audu (1985) derived his muscle equations with one control parameter (rate of motor unit stimulation) under the assumption that both the rate of motor unit recruitment and the rate of motor unit stimulation are identical. The angular trajectories of the hip and knee in the kicking motion optimized by Audu's model, with the same parameter values and constants as in Hatze's kicking study (1975), turned out to be very similar to the results obtained by Hatze. Although it has not been proved whether or not the results from the rate of motor unit recruitment and the rate of motor unit stimulation in Hatze's muscle model are

identical, these two control parameters (between 0 and 1) were assumed to be the same in the current simulation study for simplification. Also, the angle of forearm pronation-supination was set to a constant as explained in Chapter V. These assumptions resulted in 64 first-order differential equations with 12 control parameters.

Simulation was performed in two ways: a) simulation of the skeletal system and b) simulation of the combined skeletal and muscular system. Simulation of the skeletal system, separated from the muscular system, was performed by predicting resultant joint torque patterns to find existing angular trajectories of the elbow and wrist joint and to investigate the roles of muscular torques at the elbow and wrist joint. This approach is common to most simulation studies (Gallenstein, 1973; Hubbard and Barlow, 1980; Ramey and Yang, 1981).

The muscular system adopted from Hatze's model (1981) is interrelated to the mathematical model of the musculoskeletal system used in this study through generalized forces (torques in this case), \overline{Q} , in equation 3-17 or 3-18. These generalized torques are equivalent to the respective summations of the active muscular torques computed from a) the active muscular forces, F^{SE} , in equation 3-33 and respective function of moment arms in equations 3-50 through 3-64, b) passive elastic torques, PET, in equation 3-19, and c) passive viscous torques, PVT, in equation 3-20.

In order to explain this interrelation between the muscular system and the skeletal system, a block diagram of the simulation with one muscle is shown in the Figure 4-6. The simulation of whole system, consisting of 12 prime muscles can be simply done by respective summation of gereralized forces to the respective generalized coordinates so that the final generalized forces can enter into the skeletal system.

The combined muscular and skeletal system was simultaneously simulated by predicting the patterns of control parameters that maximized the velocity of the hand at the release of the ball. These patterns of control parameters are used in optimization as starting values. This simulation was performed to avoid instability problems and to reduce the computing time in optimization as explained in the following section.

Fourth-order Runge-Kutta-Merson numerical method
(Lance, 1960; Bull, 1966; Hatze, 1981) was employed to
simultaneously integrate the system of differential
equations. The Runge-Kutta-Merson method is the one of
several modifications of Runge-Kutta method which is known
to be inherently stable for any type of differential
equations (Young, 1970; Mathews, 1987). The algorithm is
given as follows:

$$Y_{n+1} = Y_n + \frac{1}{2} (k_1 + 4k_4 + k_5)$$
 (4-13)

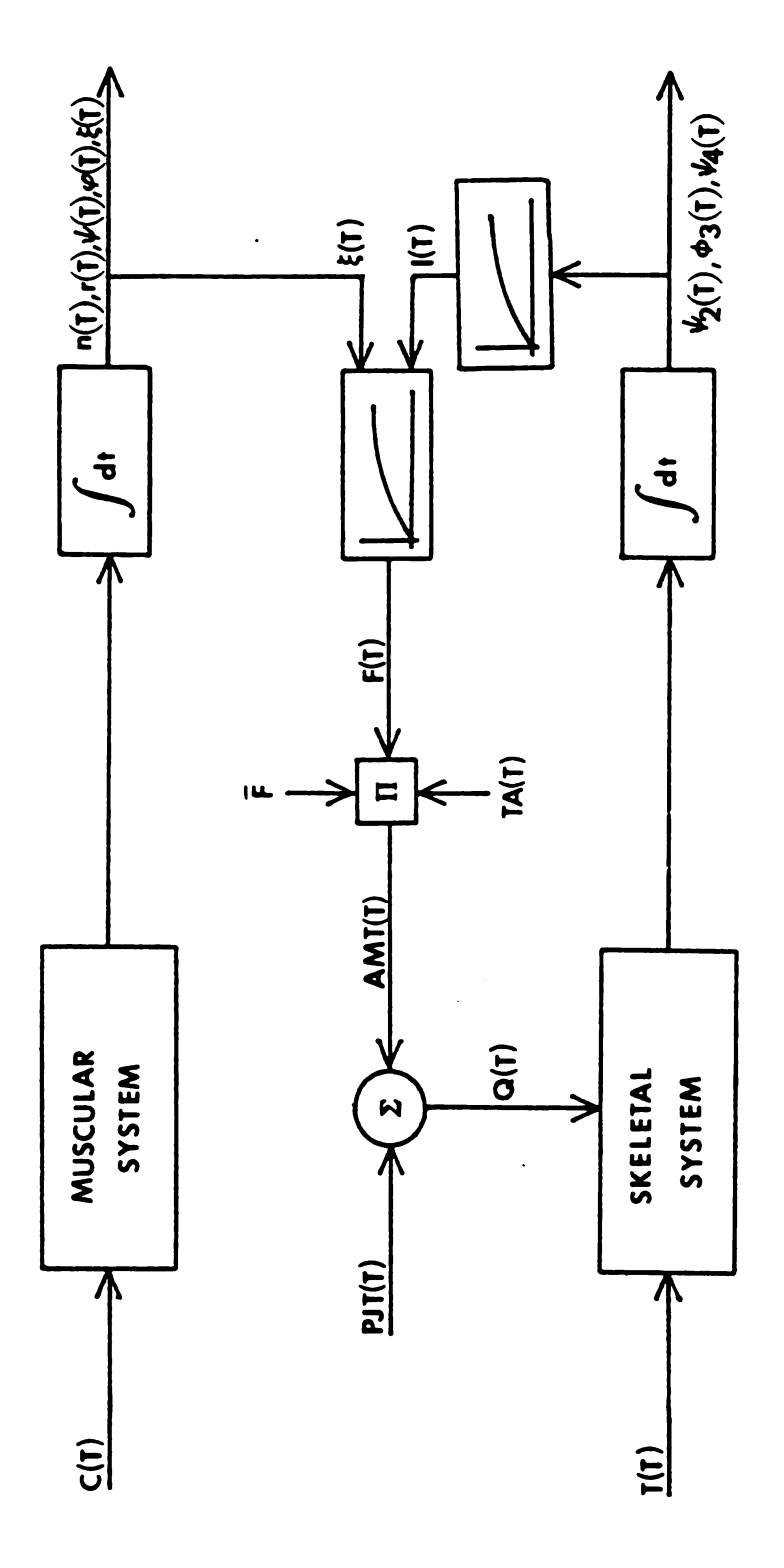


Figure 4-6. Simplified block diagram of the simulation of one muscle.

where

$$k_{1} = \frac{1}{3}hf(x_{n}, y_{n}),$$

$$k_{2} = \frac{1}{3}hf(x_{n} + \frac{1}{3}h, y_{n} + k_{1}),$$

$$k_{3} = \frac{1}{3}hf(x_{n} + \frac{1}{3}h, y_{n} + \frac{1}{2}k_{1} + \frac{1}{2}k_{2}),$$

$$k_{4} = \frac{1}{3}hf(x_{n} + \frac{1}{2}h, y_{n} + \frac{3}{8}k_{1} + \frac{9}{8}k_{3}),$$

$$k_{5} = \frac{1}{3}hf(x_{n} + h, y_{n} + \frac{3}{2}k_{1} - \frac{9}{2}k_{3} + 6k_{4}),$$

$$f(x, y) = dy / dx,$$

$$h = integration step size.$$

Simulation is a trial and error approach in predicting the input values for the best simulation results.

Simulation was performed again and again with different input patterns until the velocity of the hand at the release of the ball was considered to reach the peak.

III. OPTIMIZATION

The optimization problem in this study was to find the patterns of muscular control parameters that maximize the velocity (\overline{R}_4) of the hand at the release of the ball, subject to differential constraints for muscular and skeletal dynamics described in the previous chapter and constraints for angles and time. The final goal was to generate optimal angular trajectories of the elbow and wrist joint using these optimal patterns of control parameters.

The computer optimization software OPTDES.BYU

(developed at Brigham Young University) available at the engineering Hewlett-Packard (HP) Workstation (HP 9000/340 computer) of Michigan State University was used to solve this optimization problem. In order to implement this optimization problem utilizing OPTDES.BYU, reduce the computing time, and avoid instability problems, the optimization problem was considerably modified.

Control parameters in Hatze's muscle equations are onoff control (so-called bang-bang control). According to
Audu (1985), Hatze's muscle equations are unstable during
optimization and take enormous computing time. The
preliminary optimization run for this study showed the
lengthy computing time and instability problem.
Therefore, it was assumed that the patterns of control
parameters may be approximated by polynomial equations.

The acceleration phase of the baseball pitching motion occurs in one steady maximum effort within a very short period of time (less than 0.05 sec.). From the result of simulation and Audu's previous results (1985), it was decided that the patterns of control parameters for elbow flexors and extensors, and for wrist flexors and extensors may be approximated by the second or third order polynomial equations. Moreover, the patterns of control parameters within respective functional groups were considered to be similar. Therefore, in order to reduce the computing time, four elbow flexors and three wrist extensors that don't directly participate in the increase of the velocity of the

pitching hand were assumed to have the same control patterns within respective functional groups.

The total number of design variables was 28. These are the polynomial constants of the third order equations describing the seven muscles or muscle groups. The total number of design functions was 17. Fourteen design functions were needed to set the limit of magnitudes of control parameters. The remaining three design functions were final angles at the elbow and wrist joint, and the velocity of the hand that becomes an objective function.

The final optimization problem was to find the patterns of muscular control parameters that maximize the velocity (\bar{R}_4) of the pitching hand at the release of the ball, subject to 16 constraints. These constraints represent 16 of the design functions mentioned above. A generalized reduced gradient (GRG) algorithm was employed in this optimization study. The Runge-Kutta-Merson method for numerical integration was used as in simulation. Starting values were estimated from the simulation to reduce computing time and to avoid instability problems as mentioned in the previous section.

CHAPTER V

RESULTS AND DISCUSSION

I. EXPERIMENTAL RESULTS

A. Velocities of the Ball and Hand at the Release of the Ball

The velocity of the fast ball at release was 28.0 m/s. This velocity was slower than those of previous studies (average of 33.5 m/s from eight college pitchers, Feltner (1987); average of 33.8 m/s from 21 college varsity baseball team candidates, Logan, et al (1966)). The velocity of the hand of the subject in this study at the release of the ball was 19.60 m/s. Hereafter, the velocity of the hand at the release of the ball is used instead of the velocity of the ball at release because the velocity of the hand at the release of the ball could be easily computed from the model of the upper extremity during simulation and optimization.

There were several reasons that might explain why the velocity of the ball at its release was slower than those reported in other studies. The subject in this study was a retired major league baseball pitcher who was not currently active as a competitive pitcher. The laboratory setting, filming, body targets, and portable pitching mound

may also have influenced his pitching motion. It should be noted, however, that the purposes of this study were to mathematically model the upper extremity and to apply the model to the baseball pitching motion and not to kinematically analyze the pitching arm motion. Therefore, it was not very important whether pitching was performed by maximal effort or not because the pitching motion was to be examined in simulation and optimization.

B. Kinematics of the Elbow and Wrist Joints during the Acceleration Phase

From the start of the acceleration phase until the release of the ball, the elbow joint angle changed from -1.53 radians to -0.64 radians as shown in Figure 5-1 (see Figure 1-1 for an interpretation of elbow joint angle). The total change of the elbow joint angle, during the acceleration phase of fastball pitching, was 0.89 radians. This change in angle coincided with the average change in eight male intercollegiate varsity baseball pitchers reported by Feltner (1987). In Feltner's study, however, the average elbow joint angle changed from -1.24 radians, with 0.3 radians of standard deviation, to -0.35 radian, with 0.12 radians of standard deviation.

The experimental angular trajectory of the wrist joint motion is given in Figure 5-2. During the acceleration phase, the wrist joint angle changed 1.08 radians, from 0.90 radians to -0.18 radians. It should be noted by

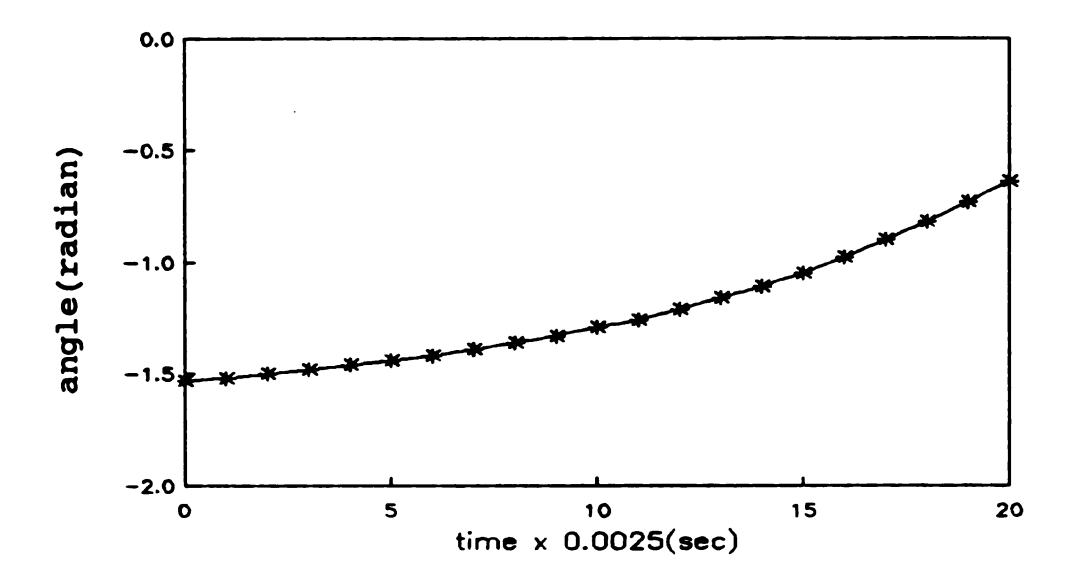


Figure 5-1. Experimental angular trajectory of the elbow joint during the acceleration phase.

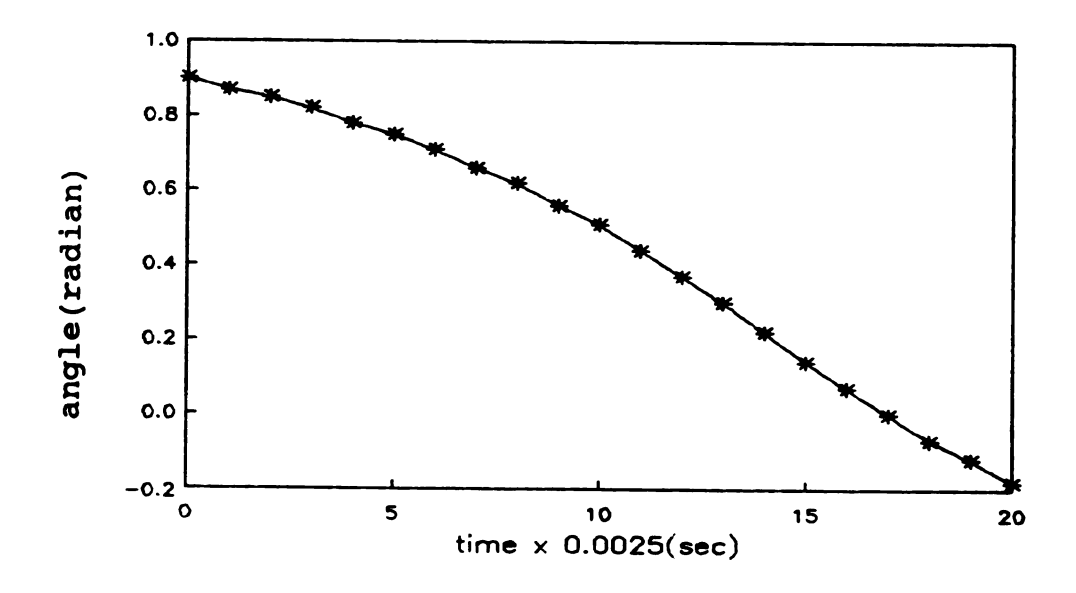


Figure 5-2. Experimental angular trajectory of the wrist joint during the acceleration phase.

definition (see definition of terms, Chapter I) that the wrist joint angle was beyond the neutral position.

However, the hand was nearly in straight alignment with the forearm at the release of the ball.

The patterns of angles and angular velocities at the elbow and wrist joints, in this study, were different than those reported in previous studies (Feltner, 1987; Gibson and Elliott, 1987). The elbow joint angle, in this study, increased relatively slowly throughout the acceleration phase. In the studies by Feltner (1987) and Gibson and Elliott (1987), the elbow joint angle sharply increased through the middle half of the acceleration phase. sharp increase in the elbow joint angle resulted in the occurrence of the peak angular velocity at the middle of the acceleration phase; whereas, the angular velocity in the current study increased slowly until just before the release of the ball. This can be seen in Figure 5-3.

The angular velocity at the wrist joint of the subject reached its maximum when nearly three fourth of the acceleration phase had been completed, then decreased until the release of the ball (see Figure 5-4). In the study by Gibson and Elliott (1987), the wrist joint angle of their subjects (Junior baseball pitchers) sharply increased in the second half of the acceleration phase and the angular velocity at the wrist joint increased nearly until the ball was released. Obviously, patterns of angles and angular velocities at the elbow and wrist joints in the studies by

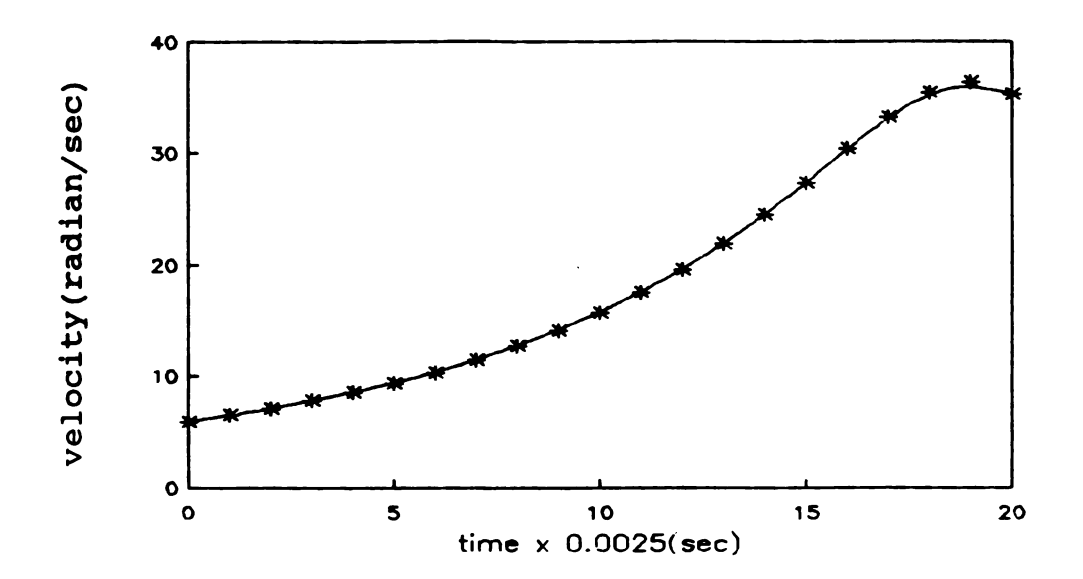


Figure 5-3. Experimental angular velocity at the elbow during the acceleration phase.

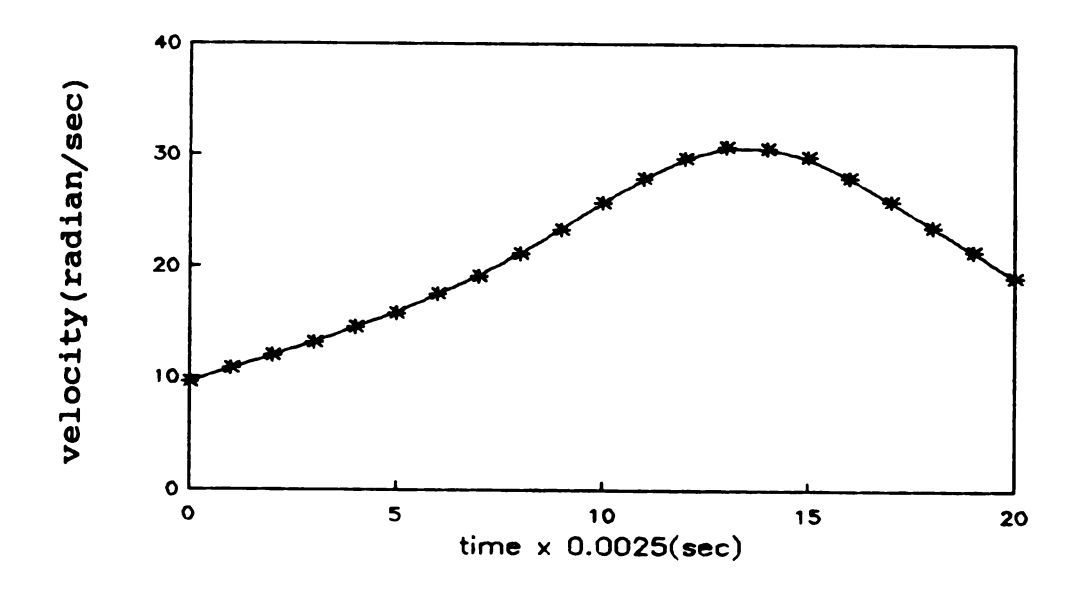


Figure 5-4. Experimental angular velocity at the wrist during the acceleration phase.

Feltner (1987) and Gibson and Elliott (1987) agree more closely to the so-called kinetic link principle mentioned in the Chapter II than the kinematic pattern obtained in the current study.

Another difference between the current study and Feltner's study (1987) was the performance time for the acceleration phase. The performance time for the acceleration phase in the current study was 0.05 seconds; whereas, the average time for the acceleration phase in Feltner's study was 0.032 seconds with a standard deviation of 0.008 seconds. Because there was a longer time period for the acceleration phase and because the patterns of angles and angular velocities at the elbow and wrist joints did not replicate the typical pattern of the kinetic link principle, it was inferred that the pitching arm of the subject was not fully accelerated. For these reasons, the subject's pitching motion may not have been well-In the section on simulation and coordinated. optimization results, patterns that may increase the velocity of the ball at release are generated by simulation and optimization.

An interesting point is that the maximum angular velocity at the wrist joint was lower than that of the elbow joint. This result is in agreement with the findings of Gibson and Elliott (1987) in their junior baseball pitchers. The hand can be quickly rotated at the wrist joint because the moment of inertia of the hand is relatively small.

However, Atwater (1979) pointed out that the so-called 'wrist snap', as a main contributor to the velocity of the ball at release, is a misconception. The primary role of wrist joint motion should be studied in the future because it is very important to know about how the wrist joint motion contributes to both the accuracy and the speed of the pitched ball.

C. Kinematics of the Forearm during the Acceleration

Phase

The forearm was at -1.8 radians at the start of the acceleration phase and supinated by 0.1 radians during the initial stage of the acceleration phase (see Figure 5-5).

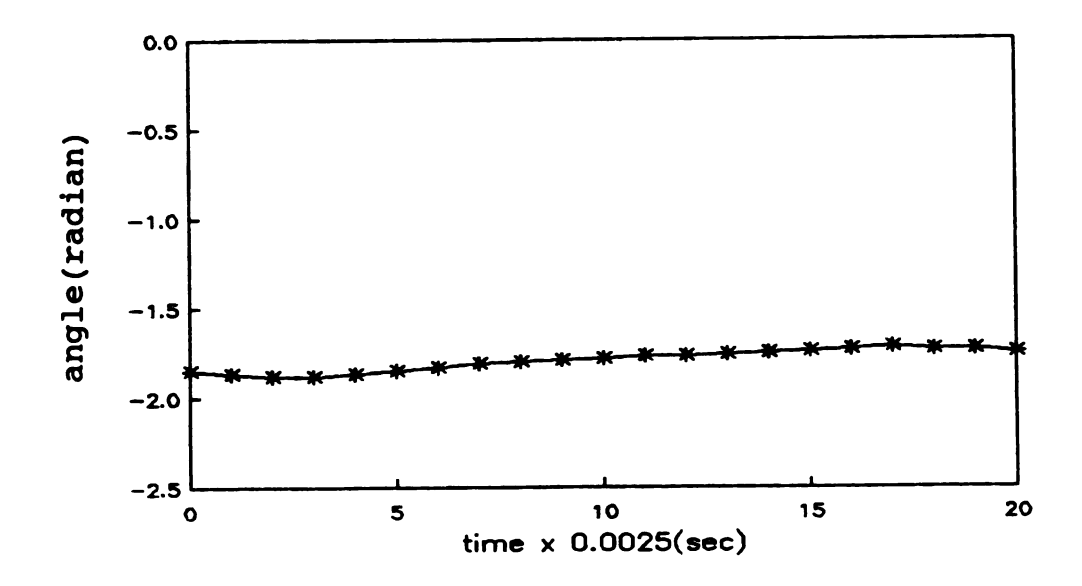


Figure 5-5. Experimental angular trajectory of the forearm for pronation-supination during the acceleration phase.

It should be mentioned again that the locations of the body targets were measured from projected film images. In an attempt to accurately locate body targets, many projected images from the film of the subject's pitching motion were repeatedly measured and averaged. Measurement error was likely to have been associated with the relatively small projected images and resulting vectors and the locations of body targets on soft tissue. With respect to the small range of forearm pronation-supination (approximately 0.1 radians), the proportion of measurement error was considered to be relatively large. this author was uncertain whether or not 0.1 radians of forearm rotation actually occurred in the acceleration phase of the baseball pitching motion. According to O'Brien (1990), the forearm pronation-supination may be negligible in the overhand fast ball pitching motion. Therefore. analysis of the angle of forearm pronation-supination was Instead, the angle was treated as omitted in this study. a constant (-1.85 radians). This was the average angle for the subject for forearm pronation-supination throughout the acceleration phase.

II. SIMULATION AND OPTIMIZATION RESULTS

The simulated angular trajectories of the elbow and wrist joints, which closely matched the respective experimental angular trajectories of the baseball pitching motion of the subject were generated from the mathematical

model of the upper extremity (see Figures 5-6, 5-7).

The experimental and the simulated angular trajectories for the elbow joint and for wrist joint were somewhat different, even though numerous simulations were performed to find simulated angular trajectories that closely matched their experimental trajectories. The hand velocity, obtained from the simulated angular trajectories of the elbow and wrist, was 16.45 m/s, about 3 m/s slower than that obtained from the experiment.

There were several possible sources of error that may have caused differences between experimental and simulated a) The differences may have been from trajectories. undetected computer coding errors. The computer program developed for this study was extremely lengthy (78 pages, with 25 lines per page). Use of computer software for symbolic mathematical manipulation, such as MATHEMATICA or MACSYMA, to remove the computer coding errors is recommended. b) Errors may have also been the result of the differences between the actual data obtained from the film and polynomial approximation in the process of computing tracking parameters. c) Errors may have been generated from the determination of the body-fixed coordinates computed from body targets placed on the upper extremity. The locations of these targets were measured from relatively small images of projected film. d) Some soft tissue and accompanying body target motion occurred during filming. e) Errors may have resulted from

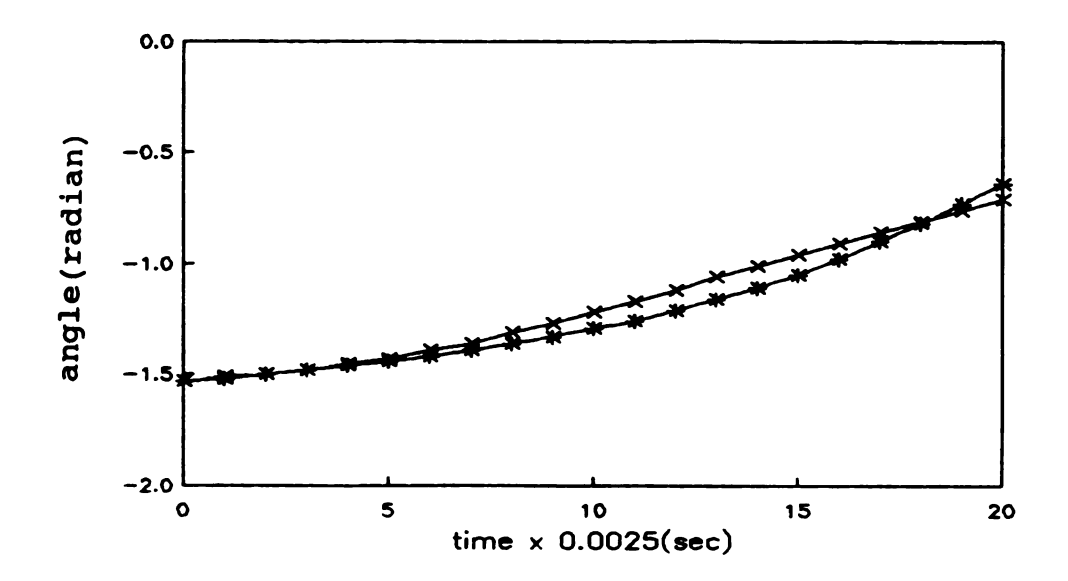


Figure 5-6. Simulated (x) and experimental (*) angular trajectories of the elbow joint during the acceleration phase.

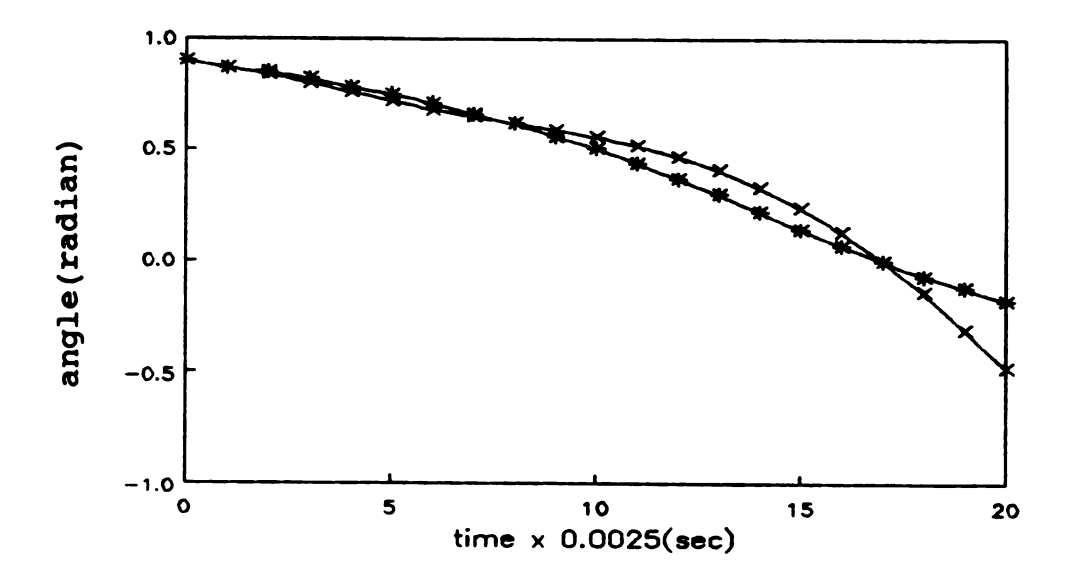


Figure 5-7. Simulated (x) and experimental (*) angular trajectories of the wrist joint during the acceleration phase.

assumptions made in this study to determine constants and parameters.

f) Differences may have resulted from accumulated computer rounding error. Addition and multiplication were numerously repeated.

In light of the fact that it is nearly impossible to model the upper extremity without assumptions, approximations, and measurement error, it is similarly unlikely that simulation will produce the exact patterns of experimental angular trajectories at the elbow and wrist joints. Therefore, the mathematical model of the human upper extremity created in this study is considered to reasonably simulate the experimental angular trajectories at the elbow and wrist in the pitching motion.

Figure 5-8 shows the resultant joint torque that was generated to predict the simulated angular trajectory at the elbow joint. By combining information from Figures 5-1 and 5-8, it is evident that the resultant elbow joint torque reached a maximum value of 36 Nm when the elbow angle was at -1.08 radians. This approximates the elbow angle of -1.18 radians where the subject had experimentally demonstrated a maximum isometric elbow extension torque of 40.7 Nm. This torque pattern also agreed with the results of Hunsicker (1955) and Elkins et al., (1951) who measured the isometric elbow extension strength from 55 male subjects, and 10 male and 14 female subjects, respectively. According to studies of arm strength reported by Amis (1978), the maximum isometric elbow joint torques published occurred at the

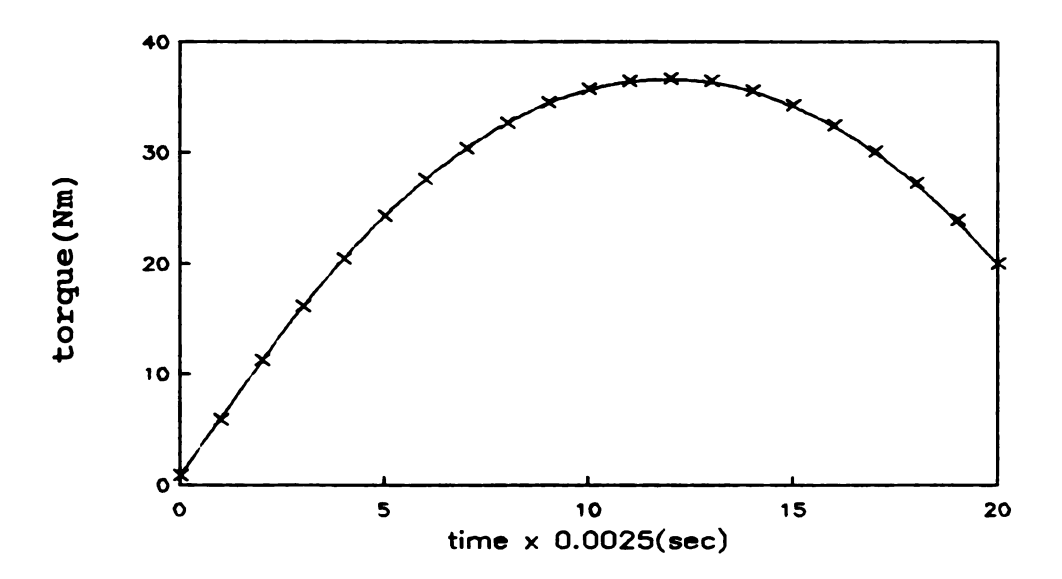


Figure 5-8. Simulated resultant elbow joint torque during the acceleration phase.

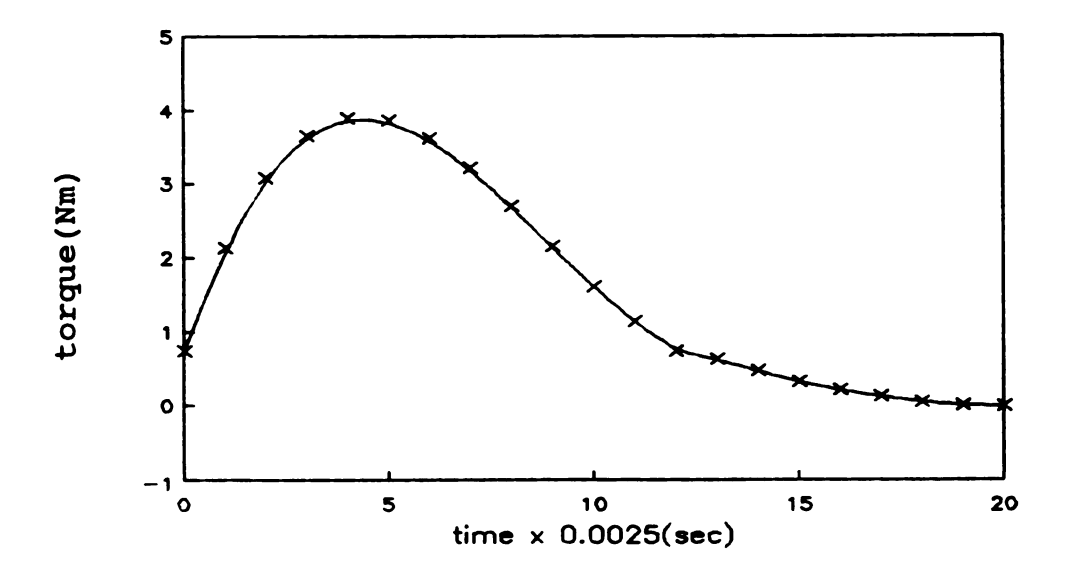


Figure 5-9. Simulated resultant wrist joint torque during the acceleration phase.

elbow angles between -1.05 radians and -1.57 radians (Provins, 1955; Currier, 1972).

Figure 5-9 shows the resultant joint torque that was generated to predict the simulated angular trajectory of the wrist joint. By combining information from Figures 5-2 and 5-9, it is evident that the resultant wrist joint torque reached a maximum value of 3.8 Nm when the wrist joint angle was at 0.64 radians. This approximates the wrist angle of 0.55 radians where the subject had previously demonstrated a maximum isometric wrist flexion torque of 11.7 Nm.

After reaching maximum torque, the resultant wrist joint torque sharply decreased until the release of the ball. As the point of release of the ball was approached, the simulated resultant wrist joint torque approached zero. It can be interpreted that the antagonistic muscle action by the wrist extensor muscles caused a decrease in resultant torque and a decrease in wrist joint angular velocity at release (see Figure 5-4 and 5-9). This may result in an increase in accuracy of the pitched ball and a prevention of injury.

Figures 5-10 and 5-11 contain the optimal angular trajectories for the elbow and wrist joints obtained from simulation and optimization. Similarly, Figures 5-12 and 5-13 contain the resultant torque patterns that generated these optimal angular trajectories. Control parameters for the elbow extensor, elbow flexor, wrist flexor, and

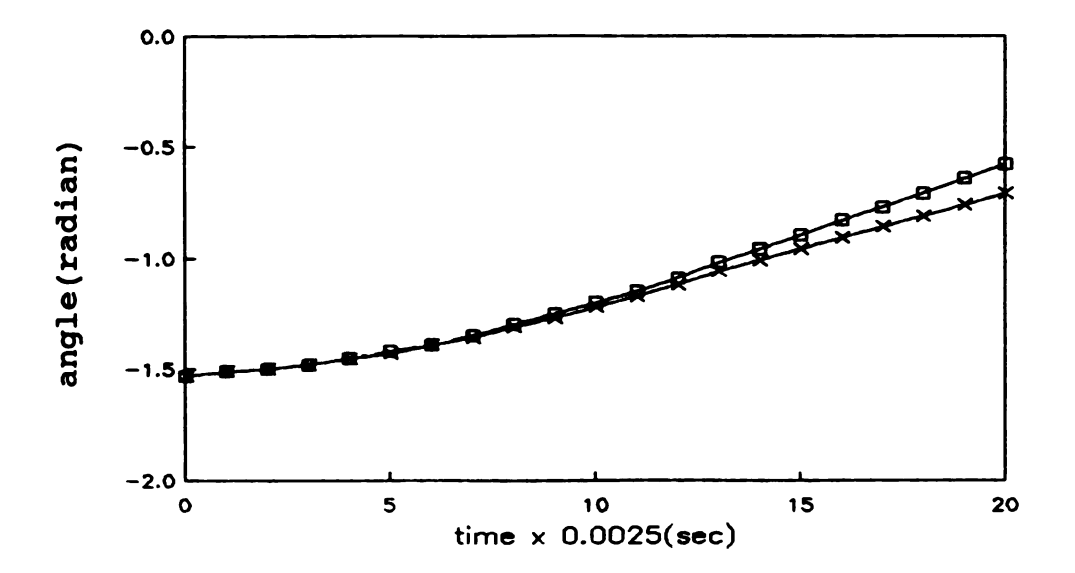


Figure 5-10. Optimal ([]) and simulated (x) angular trajectories of the elbow joint during the acceleration phase.

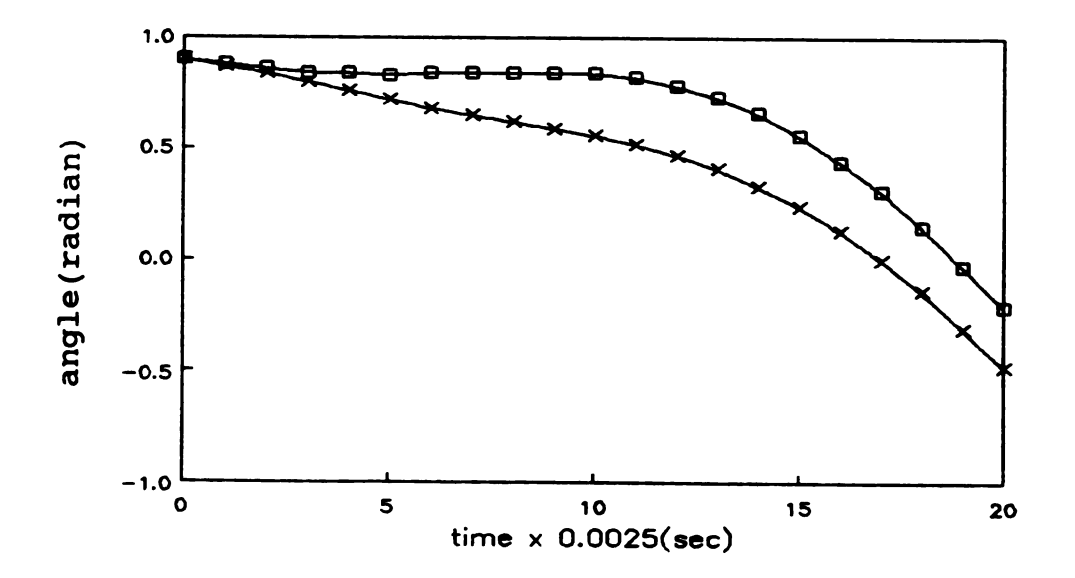


Figure 5-11. Optimal (\square) and simulated (x) angular trajectories of the wrist joint during the acceleration phase.

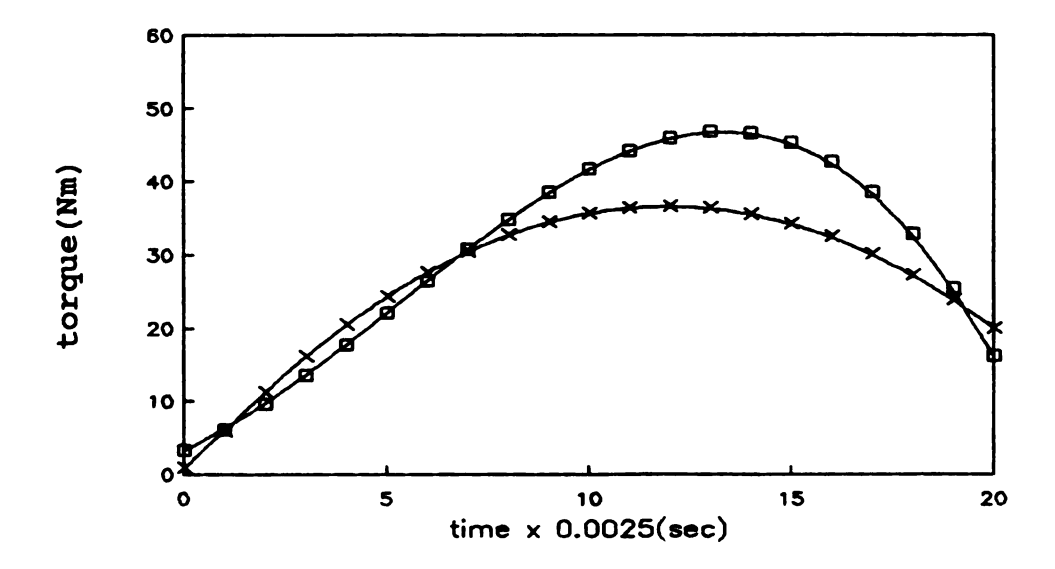


Figure 5-12. Simulated resultant elbow joint torque (x) and optimal resultant elbow joint torque (\(\sigma\)) for optimal angular trajectory of the elbow joint during the acceleration phase.

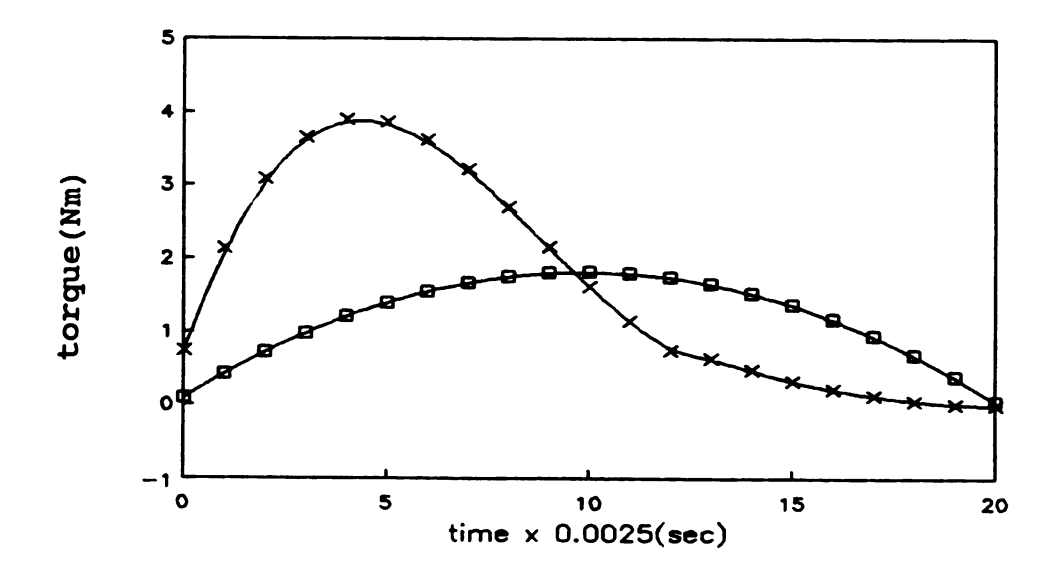


Figure 5-13. Simulated resultant wrist joint torque (x) and optimal resultant wrist joint torque (\(\pi\)) for optimal angular trajectory of the wrist joint during the acceleration phase.

wrist extensor muscles are shown in the Figure 5-14 through 5-17. The patterns of control parameters of each functional group for the elbow flexion-extension and wrist flexion-extension were nearly identical.

Theoretically, there may exist only one optimal trajectory of the pitching arm that maximizes the velocity of the ball at release. Hatze (1975), who studied the kicking motion, however, stated that there are near-optimal trajectories in the vicinity of the exact optimal trajectory. Therefore, the optimal trajectory is somewhat arbitrary in a complex system and should encompass a certain range of trajectories.

Under the condition that the tracking parameters, initial and final angles and performance time (0.05 sec), are predetermined, this author was unable to obtain dramatic changes in the angular trajectory of the elbow joint and accompanying ball velocity, from the experimental angular trajectory toward an angular trajectory that resulted in increased hand velocity at the release of the ball.

As seen in Figure 5-10, as long as the initial and the final angles and performance time were preset to the values obtained from the experiment, the optimal angular trajectory of the elbow joint was very similar. The hand velocity at the release of the ball from the optimal trajectory of the elbow joint was only 1.0 m/s faster than that of the experimental angular trajectory.

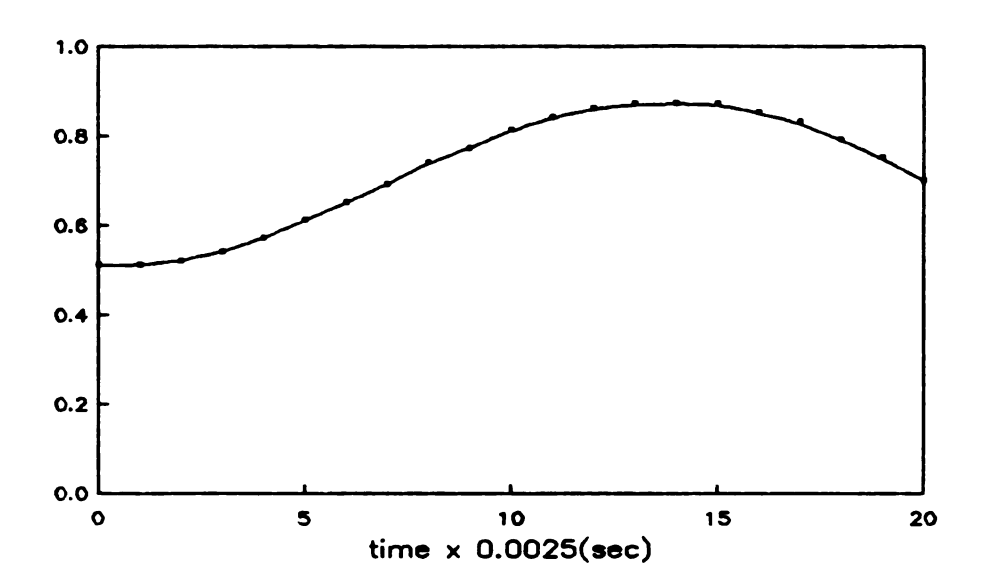


Figure 5-14. Control parameter pattern of the elbow joint extensor muscles during the acceleration phase.

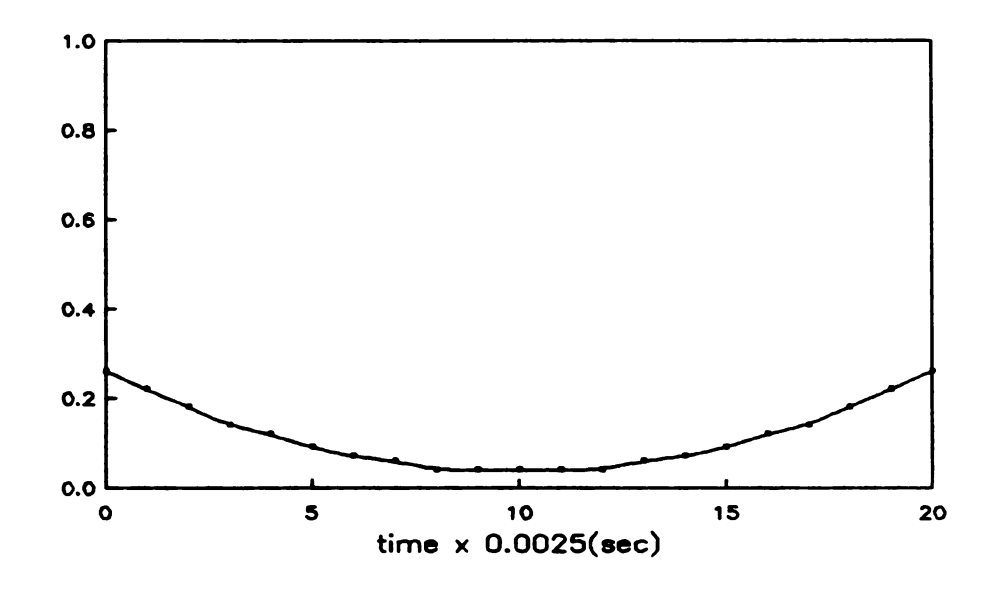


Figure 5-15. Control parameter pattern of the elbow joint flexor muscles during the acceleration phase.

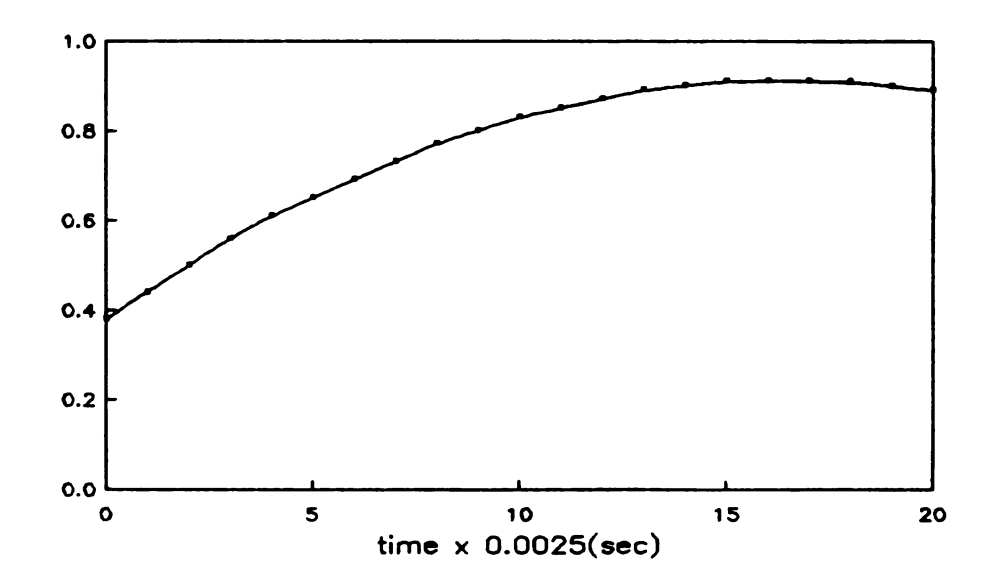


Figure 5-16. Control parameter pattern of the wrist joint flexor muscles during the acceleration phase.

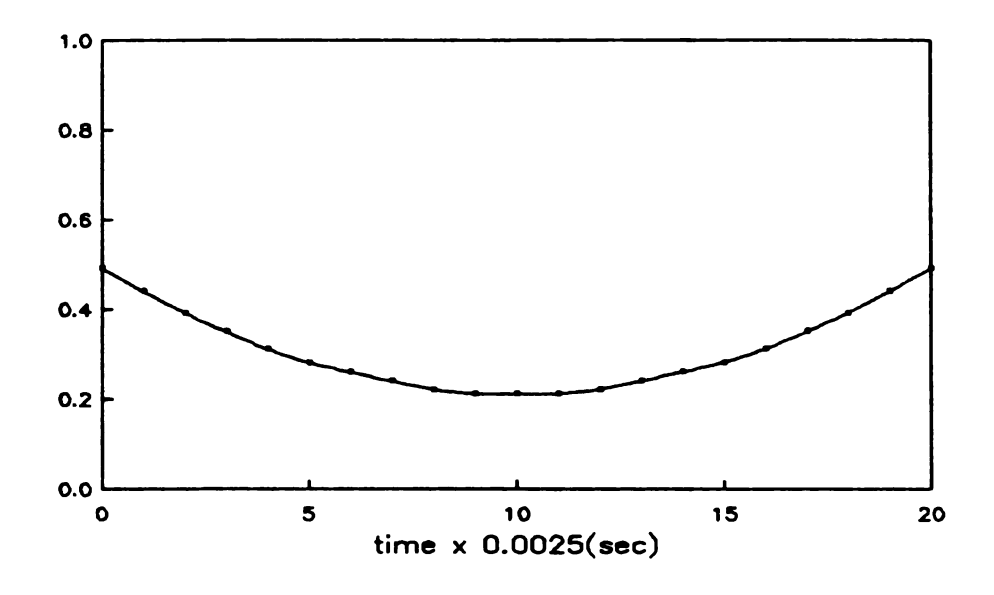


Figure 5-17. Control parameter pattern of the wrist joint extensor muscles during the acceleration phase.

From simulation and optimization, it was possible to find an optimal angular trajectory of the wrist joint that was different from the experimental angular trajectory of the wrist joint. The hand velocity at the release of the ball from the optimal angular trajectory of the wrist joint was 2.0 m/s faster than that of the experimental angular trajectory. Obviously, the hand segment was influenced less from tracking parameters than the forearm segment that is directly connected to the upper arm.

As mentioned earlier, the angular velocity of the hand was slower than that of the forearm, even though the hand can theoretically have a higher angular velocity than the For these reasons, it was possible to obtain an forearm. optimal angular trajectory of the wrist joint that was quite different from the experimental angular trajectory of the wrist joint. However, the primary role of the hand in the overhand fastball pitch has not been clearly determined whether it is to control the accuracy of the pitch or it is to impart speed to the ball. In baseball pitching, the ball accuracy and the ball speed are both very important. According to Hatze (1975), accuracy and speed of motion are incompatible, or at least very difficult to achieve simultaneously. Controlling of the ball in baseball pitching is a very complicated phenomenon governed by the neural system. It should be investigated further.

In addition to elbow and wrist joint trajectories, the contributions of other body parts and the performance time

may function to influence the optimal angular trajectory of the pitching arm in baseball. The tracking parameters that described the contributions of other body parts to the velocity of the ball were obtained from high speed three-dimensional cinematography and used as input to the simulation and optimization. Thus, the remaining variable that could be manipulated was performance time.

It was decided to test the acceleration phase time of 0.0325 seconds, that had been obtained by Feltner (1987) as an average for eight collegiate pitchers. Figures 5-18 and 5-19 are angular trajectories of the elbow and wrist joints, simulated with an acceleration phase time of 0.0325 Figure 5-20 and 5-21 are the resultant joint seconds. torques that generated these angular trajectories. The shorter performance time (0.0325 sec.), using the same tracking parameters, needed considerably greater joint torque to match the final angle of the hand at the release of the ball to that of the experimental angular trajectory (see Figures 5-12,5-13,5-20 and 5-21). The hand velocity at the release of the ball was increased by approximately 2 m/sec from that obtained from the experimental angular trajectory.

In order to investigate the roles of the elbow and wrist joint muscles on the angular trajectory of the pitching arm, it was hypothesized that if the resultant joint torques at the elbow and/or wrist joints were set to zero, their angular trajectories would be only due to the

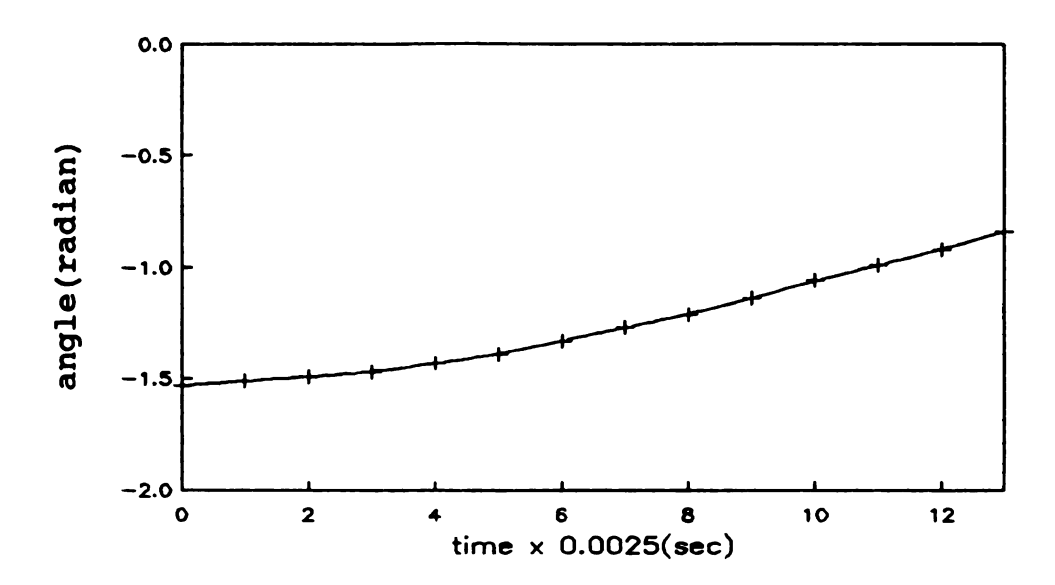


Figure 5-18. Predicted angular trajectory of the elbow joint during an acceleration phase of 0.0325 seconds.

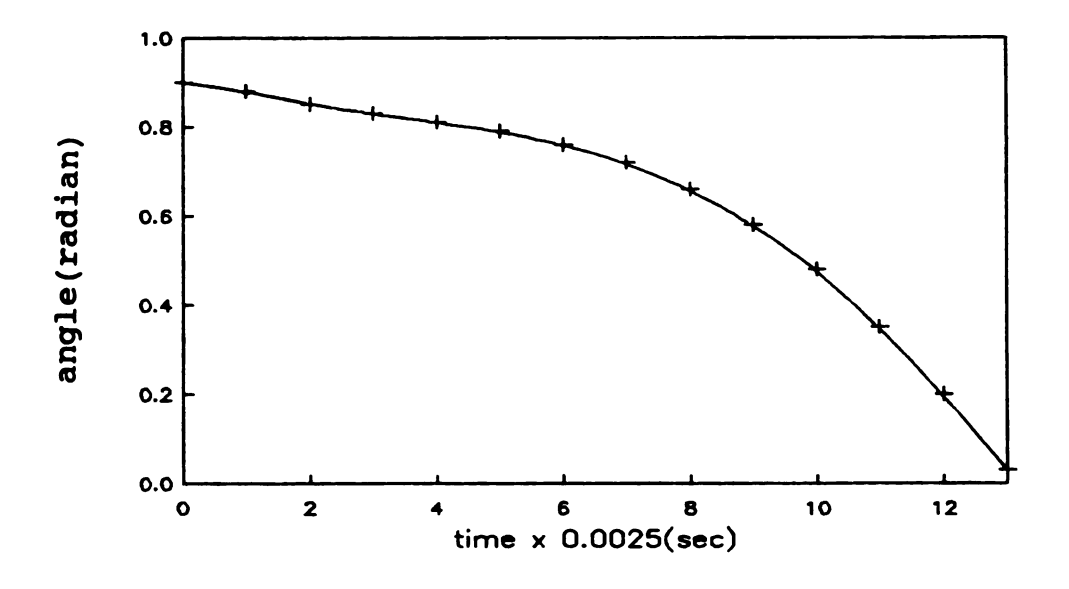


Figure 5-19. Predicted angular trajectory of the wrist joint during an acceleration phase of 0.0325 seconds.

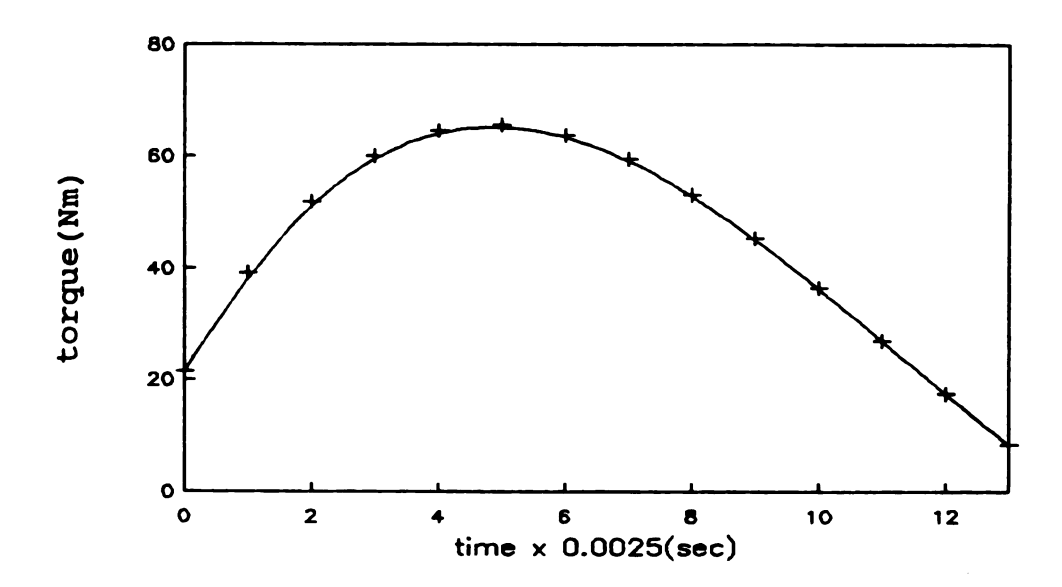


Figure 5-20. Predicted resultant elbow joint torque during an acceleration phase of 0.0325 seconds.

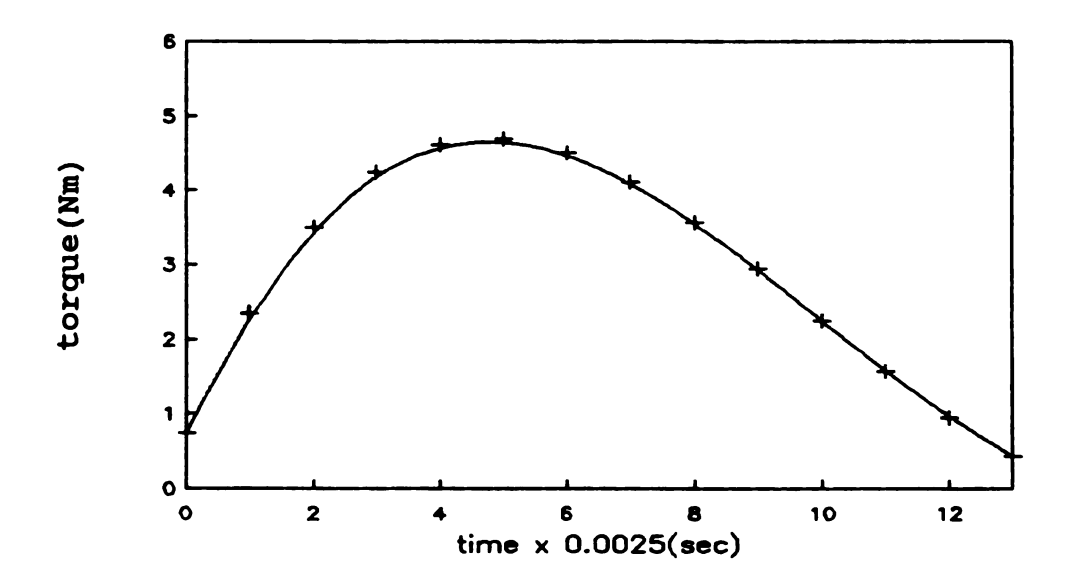


Figure 5-21. Predicted resultant wrist joint torque during an acceleration phase of 0.0325 seconds.

contribution of other body parts and the ballistic movement of the pitching arm itself. Figures 5-22 and 5-23 are the simulation results when the respective resultant joint torques at the elbow and at the wrist joint were set to zero. Figures 5-24 and 5-25 are the angular trajectories of the elbow and wrist when the resultant joint torques of both the elbow and the wrist joints were set to zero.

In the case when only the elbow joint resultant torque was set to zero, the total change of the elbow angle was 0.47 radians, from -1.53 radians to -1.06 radians, and the hand velocity at the release of the ball was 13 m/s. In the case where only the resultant wrist joint torque was set to zero, the wrist joint angle changed 0.19 radians, from 0.9 radians to 0.71 radians, and the hand velocity at the release of the ball was approximately 16 m/s. With both the elbow and wrist joint resultant torques set to zero, the elbow and wrist joint angles changed respectively 0.5 radians, from -1.53 radians to -1.03 radians, and 0.21 radians, from 0.9 radians to 0.69 radians and the hand velocity at the release of the ball was 12 m/s.

From these simulation results, it was thought that the elbow extensor muscles and/or the wrist flexor muscles were not the major contributors to the hand velocity. With the resultant elbow joint torque set to zero, the forearm was flexed about the half of the total angle obtained in the experimental results. With the resultant wrist joint torque set to zero, the hand was flexed about one sixth of

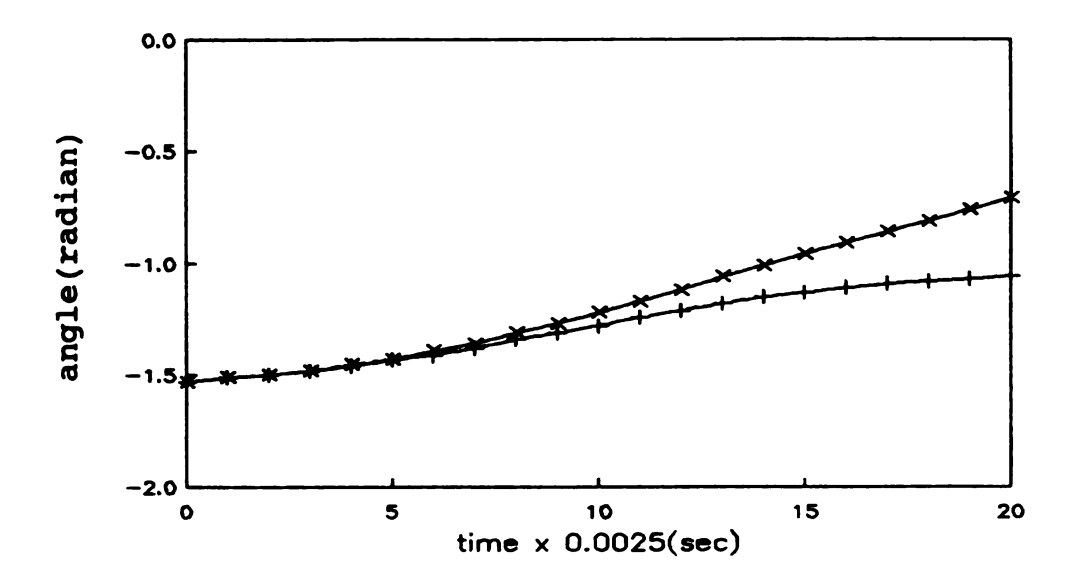


Figure 5-22. Simulated angular trajectory (x) of the elbow joint and predicted angular trajectory (+) of the elbow joint with the resultant elbow joint torque set to zero.

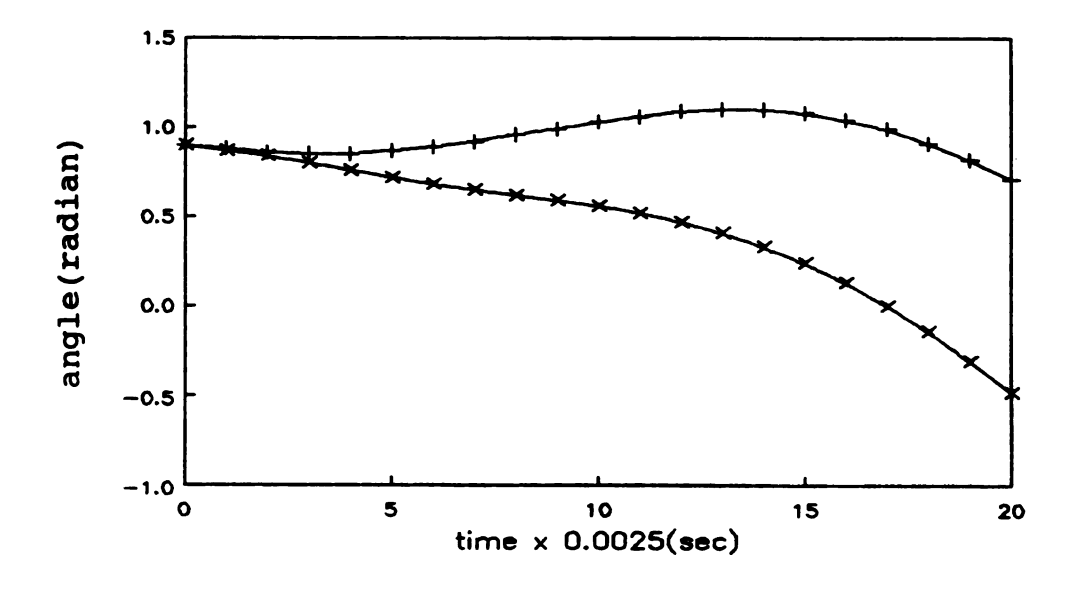


Figure 5-23. Simulated angular trajectory (x) of the wrist joint and predicted angular trajectory (+) of the wrist joint with the resultant wrist joint torque set to zero.

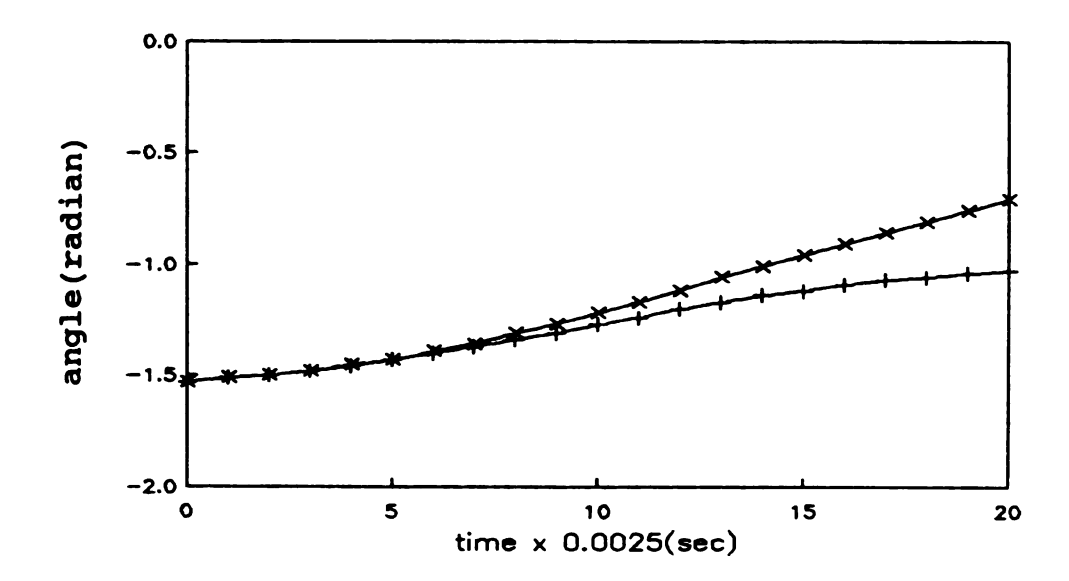


Figure 5-24.Simulated angular trajectory (x) of the elbow joint and predicted angular trajectory (+) of the elbow joint with the resultant joint torques of both the elbow and wrist joints set to zero.

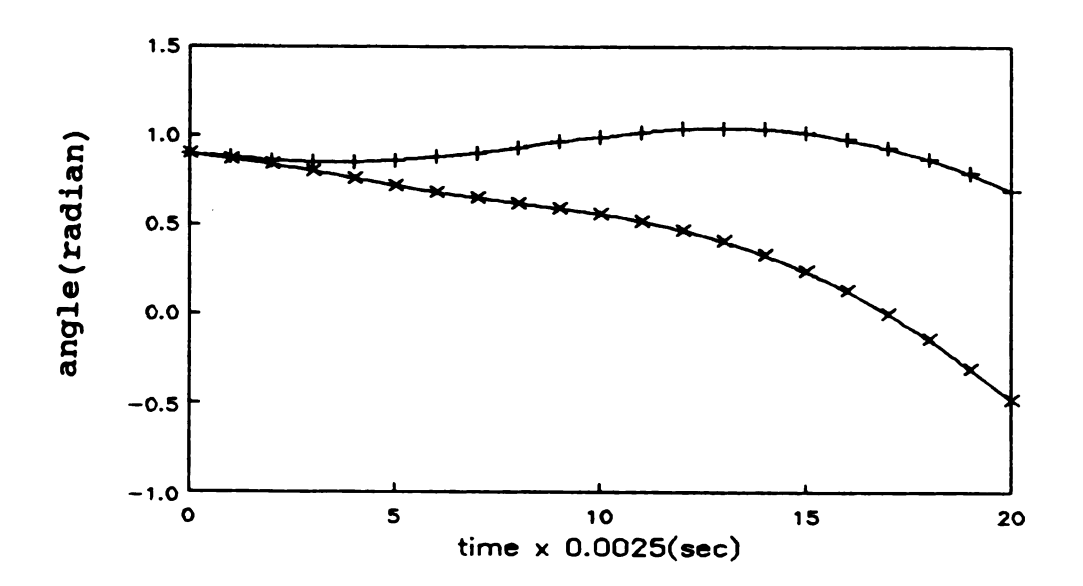


Figure 5-25.Simulated angular trajectory (x) of the wrist joint and predicted angular trajectory (+) of the wrist joint with the resultant joint torques of both the elbow and wrist joints set to zero.

the total angle obtained in the experimental results. The hand velocity at the release of the ball, however, was approximately 80 percent of the experimental result with the resultant elbow joint torque set to zero, approximately 95 percent of the experimental result with the resultant wrist joint torque set to zero, and approximately 75 percent with both the resultant elbow and wrist joint torques set to zero.

The baseball pitching motion is accomplished by a sequential interaction of the all body parts, through a link system from the foot to the pitching hand. The current study fully supported the findings of Feltner (1987). Through his detailed kinematic analysis he concluded that elbow extension in the acceleration phase was due mainly to the trunk rotation, and not to the activity of the elbow extensor muscles.

Conclusion

The purposes of the study were to create a mathematical model of the human upper extremity and to apply the model to the acceleration phase of the fast baseball pitching motion. Angular trajectories at the elbow and wrist joints in the fast baseball pitching were generated experimentally by a three-dimensional cinematographic technique and theoretically by simulation and optimization techniques.

The mathematical model was applied to generate

a) angular trajectories that closely matched the

experimental trajectories at the elbow and wrist joint and b) optimal angular trajectories that maximize the velocity of the hand at the release of the ball. The mathematical model was also used to investigate the roles of elbow and wrist joint muscles in baseball pitching. The model of the human upper extremity, created in this study was considered to closely simulate the experimental angular trajectories at the elbow and wrist joint in the pitching motion.

Under the condition that the tracking parameters, initial and final angles, and performance time were predetermined, this author was unable to obtain dramatic changes in the experimental angular trajectory of the elbow joint toward an angular trajectory that resulted in increased hand velocity at the release of the ball. From simulation and optimization, it was possible to find an optimal angular trajectory of the wrist joint that was different from its experimental angular trajectory.

With the resultant elbow joint torque set to zero, the forearm flexed to about the half of the total flexion obtained in the experimental results. With the resultant wrist joint torque set to zero, the hand flexed to about one sixth of the total flexion obtained in the experimental results. The hand velocity at the release of the ball, however, was approximately 80 percent of the experimental result when the resultant elbow joint torque was set to zero, approximately 95 percent of the experimental result

when the resultant wrist joint torque was set to zero, and approximately 75 percent of the experimental result when both the resultant elbow and wrist joint torques were set to zero.

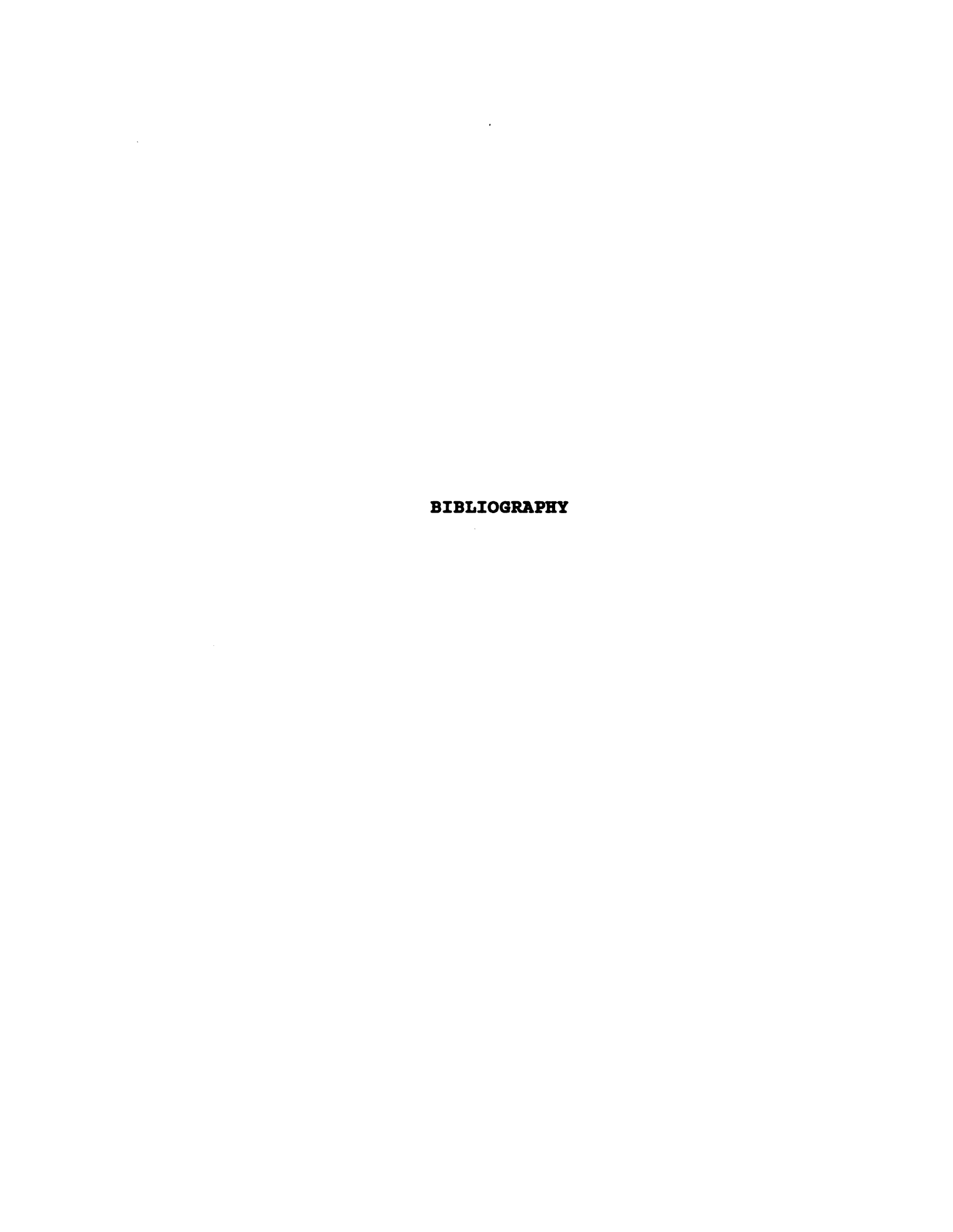
Velocity of the ball at release in pitching is primarily generated by body parts other than the upper extremity. From the results of this study, it was concluded that the primary contribution of the elbow and wrist joints were to position the hand so that the velocity and accuracy of the pitched ball could be maximized. The optimal angular trajectory of the pitching arm depends heavily on the motion of the other body parts connected to the upper arm through the gleno-humeral joint. Therefore, the optimal angular trajectory of the pitching arm that can be obtained from simulation and/or optimization is not the true optimal angular trajectory unless the motion of the other body parts is optimal.

III.RECOMMENDATIONS

Simulation and/or optimization as a method of solving the direct dynamics problem can be theoretically applied to open the black box that has not been opened via the inverse dynamics approach. In this study, however, many things remained untouched because of the limitations of time, financial support, experimental equipment, and accumulated knowledge. Further simulation and/or optimization research should be carried out to discover the causes of

individual differences in the performances of sports skills and ways to maximize an athlete's ability. The following are recommendations to assist in this process.

- 1. Anatomical parameters such as muscle fiber angle, muscle cross-sectional area, and muscle-tendon length should be measured directly from living subjects, using advanced medical instruments such as NMR.
- 2. Data collection via three-dimensional filming should be investigated to find out the range of error associated with soft tissue motion that may largely influence position data.
- 3. All muscles(prime and secondary) should be included in the muscular system to determine their roles in a model before developing a simplified model.
- 4. Tolerances of errors in the approximations of the insertions of muscles that occupy a broad area should be investigated.
 - 5. Various pitching motions should be studied.
- 6. Joint stability should be investigated to prevent injuries that commonly occur in the baseball pitching.
- 7. A muscle model that can recognize individual differences of motor control should be developed.



BIBLIOGRAPHY

- Aleshinsky, S. Y. and Zatsiorsky, V. M. (1978). Human locomotion in space analyzed biomechanically through a multi-link chain model. <u>Journal of Biomechanics</u>, Vol.11, pp 101-108.
- Amis, A. A., Dowson, D., Unsworth, A., Miller, J., and Wright, V. (1977). An examination of the elbow articulation with particular reference to variation of the carrying angle. <u>Engineering in Medicine</u>, Vol. 6, pp 76-80.
- Amis, A. A. (1978). <u>Biomechanics of the Upper Limb and Design of an Elbow Prosthesis</u>. University of Leeds, Doctoral Dissertation.
- Amis, A. A., Dowson, D., and Wright, V. (1979). Muscle strengths and musculo-skeletal geometry of the upper limb. Engineering in Medicine, Vol.18, pp 41-48.
- An, K. N., Kwak, B. M., Chao, E. Y., and Morrey, B. F. (1983). Determination of muscle and joint forces across human elbow. In Kwak, B. M. (ed.), 1983 Advances in Bioengineering. ASME pp 70-71.
- An, K. N., Morrey, B. F., and Chao, E. Y. (1985).

 Kinematics of the elbow. In Winter, D. A. (ed.),

 Biomechanics IX-A. Human Kinetics Pub., Champain,

 Illinois. pp 154-159.
- An, K. N., Hui, F. C., Morrey, B. F., Linscheild, R. L., and Chao, E. Y. (1981). Muscle across the elbow joint: A biomechanical analysis. <u>Journal of Biomechanics</u>, Vol.14, No. 10, pp 659-669.
- An, K. N., Takahashi, K., Harrigan, T. P., and Chao, E. Y. (1984). Determination of muscle orientations and moment arms. <u>Journal of Biomechanical Engineering</u>, Vol. 106, pp 280-282.
- Anderson, M. B. (1979). Comparison of muscle patterning in the overarm throw and tennis serve. Research

 Ouarterly, Vol. 50, pp 541-553.

- Andrews, J. G. and Youm, Y. (1979). A biomechanical investigation of wrist kinematics. <u>Journal of Biomechanics</u>, Vol.12, pp 83-93.
- Atwater, A. E. (1979). Biomechanics of overarm throwing movements and of throwing injuries. In Hutton, R. S. & Miller, D. I. (eds.), Exercise and Sport Sciences Review, Vol.7, pp 43-85.
- Audu, M. L. (1985). Optimal Control Modeling of Lower Extremity Musculoskeletal Motion. Case Western Reserve University, Doctoral Dissertation.
- Audu, M. L. and Davy, D. T. (1986). The influence of muscle model complexity in musculoskeletal motion modeling. <u>Journal of Biomechanical Engineering</u>, Vol.107, pp 147-157.
- Basmajian, J. V. and Latif, A. (1957). Integrated actions and functions of the chief flexors of the elbow. The <u>Journal of Bone and Joint Surgery</u>, Vol.39-A, pp 1106-1118.
- Bernstein, B. A., Salzgeber, O. A., Parlenko, P. P., and Gurvich, N. A. (1936). Determination of location of the centers of gravity and mass of the limbs of the living human body (In Russian). All-Union Inst. Exptl. Med., Moscow.
- Bloem, J. L., Kieft, G. J., Bos, C. F. M. and Rozing, P. M. (1988). In. Falke, T. H. M. (ed.), Essentials of Clinical MRI, Martinus Nijhoff Pub., Boston. pp 219-228.
- Boone, D. C., and Azen, S. P. (1979). Normal range of motion of joints in male subjects. <u>The Journal of Bone and Joint Surgery</u>, Vol.61-A, pp 756-759.
- Bouisset, S., Lestienne, F., and Maton, B. (1976). Relative work of main agonists in elbow flexion. In Komi, P. V. (ed.), Biomechanics V-A. University Park Press, Boltimore. pp 272-279.
- Brand, P. W. (1985). Clinical Mechanics of the Hand. The C.V. Mosby Co., St. Louis, Missouri.
- Braune, W. and Fischer, O. (1889). Über den schwerpunkt des menschlichen korpers mit rucksicht auf die austrutung des deutschen infanteristen. Abh. d. Math.-Phys. cl. d. k. Sachs. Gesselsch. der Wiss, Vol. 26, pp 561-672. In Korgman, W. M. and Johnston, F. E. (eds.), Human Mechanics-Four Monographs Abridged. Wright-Patterson air Force Base, Ohio, 1963. (AMRL-TDR-63-123).

- Brumbaugh, R. B., Crowninshield, R. D., Flair, W. F. and Andrews, J. G. (1982). An in-vivo study of normal wrist kinematics. <u>Journal of Biomechanical Engineering</u>, Vol. 104, pp 176-181.
- Bull, G. (1966). Computational Methods and ALGOL. George G. Harrap and Co., London.
- Chao, E. Y. and Rim, K. (1973). Application of optimization principles in determining the applied moments in human leg joints during gait. <u>Journal of Biomechanics</u>, Vol.6, pp 497-510.
- Chao, E. Y. and Morrey, B. F. (1978). Three-dimensional rotation of the elbow. <u>Journal of Biomechanics</u>, Vol.11, pp 57-73.
- Chao, E. Y., An, K. N., Askew, L. J., and Morrey, B. F. (1980). Electrogoniometer for the measurement of human elbow joint rotation. <u>Journal of Biomechanical Engineering</u>, Vol.102, pp 301-310.
- Chow, C. K. and Jacobson, D. H. (1971). Studies of human locomotion via optimal programming. <u>Mathematical</u> Biosciences, Vol.10, pp 239-306.
- Chow, C. K. and Jacobson, D. H. (1974). An optimal programming study of human gait. Human Locomotor Engineering. Institution of Mechanical Engineering, London. pp 103-110.
- Clauser, C. E., McConville, J. T. and Young, J. W. (1969). Weight, Volume, and Center of Mass of Segments of the Human Body. Wright-Patterson Air Force Base, Ohio. (AMRL-TR-69-70).
- Clemente, C. D. (1987). Anatomy: A regional atlas of the human body (3rd ed.). Urban & Schwarzenberg, Baltimore.
- Cnockaert, J. C., Lensel, G., and Pertuzon, E. (1975).

 Relativecontribution of individual muscles to the isometric contraction of a muscular group. <u>Journal of Biomechanics</u>, Vol.8, pp 191-197.
- Cochran, G. B. (1982). Biomechanics of the elbow-forearm complex. In Wadsworth, T. G., and Fowler, S.B. (eds.), The Elbow. Churchill Livingstone, New York. pp 31-47.

- Cooper, J. M., and Glassow, R. B. (1976). Overarm patterns. In Cooper, J. M. and Glassow, R. B. (eds.), Kinesiology. The C.V. Mosby Co., St. Louis, Missouri. pp 135-150.
- Craig, J. J. (1986). Introduction to Robotics. Addison-Wesley Pub. Co., Massachusetts.
- Crowninshield, R. D. (1978). Use of optimization techniques to predict muscle forces. <u>Journal of Biomechanical Engineering</u>, Vol.100, pp 88-92.
- Crowninshield, R. D., and Brand, R. A. (1981). A physiologically based criterion of muscle force prediction in locomotion. <u>Journal of Biomechanics</u>, Vol.14, pp 793-801.
- Currier, D. P. (1972). Maximum isometric tension of the elbow extensors at varied positions. <u>Physical Therapy</u>, Vol. 52, pp 1043-1049.
- Davy, D. T. and Audu, M. L. (1987). A dynamic optimization technique for predicting muscle forces in the swing phase of gait. <u>Journal of Biomechanics</u>, Vol.20, pp 187-202.
- Dempster, W. T. (1955). Space Requirements of the Seated Operator. Wright-patternson Air Force, Base, Ohio. (WADC-TR-55-159).
- Dillman, C. J. (1970). Muscular torque patterns of the leg during the recovery phase of sprint running. Pennsylvania State University, Doctoral Dissertation.
- Dillman, C. J. (1971). A kinetic analysis of the recovery leg during sprint running. In Cooper, J. M. (ed.), Selected Topics on Biomechanics. Athletic Institute, Chicago.
- Dillman, C. J. (1985). Overview of the United States Olympic committee sports medicine biomechanics program. In The Elite Athlete. Butts, N. K., Gushiken, T. T., and Zarins, B. (eds.), Life Enhancement Pub., Champain, Illinois. pp 35-80.
- Dvir, Z., and Berme, N. (1978). The shoulder complex in elevation of the arm; A mechanism approach. <u>Journal of Biomechanics</u>, Vol.11, pp 219-225.
- Ekenstam, F. W., Palmer, A. K., and Glisson, R. R. (1984). The load on the radius and ulna in different positions of the wrist and forearm. <u>Acta Orthop. Scand</u>, Vol.55, pp 363-365.

- Elkins, E. C., Ledan, U. M. and Wakim, K. G. (1951).

 Objective recording of the strength of normal muscles.

 Arch. Phys. Med., Vol. 32, pp 639-647.
- Elliott, B., Marsh, T., and Blanksby, B. (1986). A three-dimensional cinematographic analysis of the tennis serve. <u>International Journal of Sport Biomechanics</u>, Vol.2, pp 260-271.
- Engin, A. E. (1979). Passive resistive torques about long bone axes of major human joints. <u>Aviation, Space, and Environmental Medicine</u>, Vol. 50, pp 1052-1057.
- Engin, A. E. (1979). On the biomechanics of major articulating human joints. In Akkas, N. (ed.), Progress in Biomechanics. Sijthoff & Noordhoff. pp 157-188.
- Engin, A. E., and Chen, S. M. (1986). Statistical data base for the biomechanical properties of the human shoulder complex-I. Kinematics of the shoulder complex. <u>Jornal of Biomechanical Engineering</u>, Vol.108, pp 215-221.
- Engin, A. E., and Chen, S. M. (1986). Statistical data base for the biomechanical properties of the human shoulder complex-II. Passive resistive properties beyond the shoulder complex sinus. <u>Journal of Biomechanical Engineering</u>, Vol.108, pp 222-227.
- Engin, A. E., and Chen, S. M. (1987). Kinematic and passive resistive properties of human elbow complex. <u>Journal of Biomechanical Engineering</u>, Vol.109, pp 318-323.
- Feltner, M. and Dapena, J. (1986). Dynamics of the shoulder and elbow joints of the throwing arm during a baseball pitch. <u>International Journal of Sport Biomechanics</u>, Vol.2, pp 235-259.
- Freimanis, A. K. (1989). Personal communication. Department of Radiology, Michigan State University.
- Frigo, C. and Pedotti, A. (1978). Determination of muscle length during locomotion. In Asmussen, E. and Jørgebsen, K. (eds.), Biomechanics VI-A. University Park Press, Baltimore, Maryland.
- Fung, Y. C., Perrone, N., and Anliker, M. (1972).

 Biomechanics: Its foundation and objectives. Prentice-Hall, Inc., New Jersey.
- Fung, Y. C. (1981). Biomechanics: mechanical properties of living tissue. Springer-Verlag, New York.

- Gallenstein, J. (1973). Analysis of swinning motions. <u>Human</u>
 <u>Factors</u>, Vol.15, No.1, pp 91-98.
- Ghosh, T. K. and Boykin, W. H. (1976). Analytic determination of an optimal human motion. <u>Journal of Optimization Theory and Applications</u>, Vol.19, pp 327-346.
- Gibson, B. J., and Elliott, B. (1987). A three dimensional cinematographic analysis of junior baseball pitchers.

 <u>Journal of Human Movement Studies</u>, Vol.13, pp 363-375.
- Goldstein, H. (1981). Classical Mechanics. Addison-Wesley Pub., Massachusetts.
- Gowan, I. D., Jobe, F. W., Tibone, J. E., Perry, J., and Moynes, D. R. (1987). A comparative electromyographic analysis of the shoulder during pitching. The American Journal of Sports Medicine, Vol. 15, pp 586-590.
- Hanavan, E. P. (1964). A mathematical model of the human body. Technical Report. AMRL-TR-64-102. Wright-Patterson Air Forces Base, Ohio.
- Hardt, D. E. (1978). Determining muscle forces in the leg during normal human walking-an application and evaluation of optimization methods. <u>Journal of Biomechanical Engineering</u>, Vol.100, pp 72-78.
- Harless, E. (1962). The Static Moments of the Component Masses of the Human Body. 1860. Wright-patterson Air Force Base, Ohio. (FTD-TT-61-295).
- Harms, S. E. and Greenway, G. (1988). Musculoskeletal System in Magnetic Resonance Imaging. In Stark, D. D. and Bradley, W. G. (eds.), Magnetic Resonace Imaging. pp 1323-1433.
- Hatze, H. (1975a). A Control Model of Skeletal Muscle and its Application to a Time Optimal Bio-motion.
 University of South Africa, Doctroal Dissertation.
- Hatze, H. (1975b). A new method for the simultaneous measurement of the moment of inertia, the damping coefficient and the location of the centre of mass of a body segment in situ. <u>European Journal of Applied Physiology</u>, Vol. 34, pp 217-226.
- Hatze, H. (1976). A method for describing the motion of biological systems. <u>Journal of Biomechanics</u>, Vol.9, pp 101-104.

- Hatze, H. (1977a). The relative contribution of motor unit recruitment and rate coding to the production of static isometric muscle force. <u>Biological Cybernetics</u>, Vol.27, pp 21-25.
- Hatze, H. (1977b). A complete set of control equations for the human musculo-skeletal system. <u>Journal of Biomechanics</u>, Vol. 10, pp 799-805.
- Hatze, H. (1980). A mathematical model for the computational determination of parameter values of anthropomorphic segments. <u>Journal of Biomechanics</u>, Vol.13, pp 833-843.
- Hatze, H. (1981a). A comprehensive model for human motion simulation and its application to the take-off phase of the long jump. <u>Journal of Biomechanics</u>, Vol. 14 No. 3, pp 135-142.
- Hatze, H. (1981b). Estimation of myodynamic parameter values from observations on isometrically contracting muscle groups. <u>European Journal of Physiology</u>, Vol.46, pp 325-338.
- Hatze, H. (1981c). Myocybernetic Control Models of Skeletal Muscle(Characteristics and Application). University of South Africa, Pretoria.
- Hatze, H. (1983). Computerized optimization of sports motions: An overview of possibilities, methods and recent developments. <u>Journal of Sports Sciences</u>, Vol.1, pp 3-12.
- Hatze, H. (1984). Dynamics of the musculoskeletal system. In Perren, S. M., and Schneider, E. (eds.), Biomechanics: Current Interdisciplinary Research. Martinus Nijhoff Pub., Boston. pp 15-25.
- Hay, J. G. (1978). The Biomechanics of Sports Techniques. Prentice-Hall, Englewood Cliffs, New Jersey.
- Hayes, K. C. and Hatze, H. (1977). Passive visco-elastic properties of the structures spanning the human elbow joint. <u>European Journal of Applied Physiology</u>, Vol.37, pp 265-274.
- Hillman, B. J., Neu, C. R., Winkler, J. D., Aroesty, J., Rettig, R. A., and Williams, A. P. (1986). Diffusion of Magnetic Resonance Imaging into Clinical Practice. Rand Health Insurance Experiment Series, R-3392-HHS. Rand Pub., Santa Monica, California.

- Högfors, C., Sigholm, G., and Herverts, P. (1987).

 Biomechanical model of the human shoulder-I. Elements.

 Journal of Biomechanics, Vol.20, pp 157-166.
- Hubbard, M. and Barlow, D. A. (1980). A multiple segment pole vault model with optimization of vaulter inputs and its use in coaching. In Cooper, J. M. and Haven, B. (eds.), Biomechanics: symposium proceedings. Indiana University.
- Huiskes, R., van Campen, D. H., and de Wijn, J. R. (1982). Perface in Biomechanics: Principles and Applications. Martinus Nijhoff Pub., Boston.
- Hull, M. L., Gonzalez, H. K., and Redifield, R. (1988).

 Optimization of pedaling rate in cycling using a muscle stress-based objective function. <u>International Journal of Sport Biomechanics</u>, Vol.4, pp 1-20.
- Hunsicker, P. (1954). Arm Strength at Selected Degrees of Elbow Flexion. WADC Tech. Report 54-548.
- Ikegawa, S., Tsunoda, N., Yata, H., Matsuo, A., and Fukunga, T. (1987). The absolute muscle strength of various muscle groups. In Jonsson, B. (ed.), Biomechanics X-A. Human Kinetics Pub., Champaign, Illinois, pp 519-521.
- Jackson, K. M., Joseph, J., and Wyard, S. J. (1977). Squential muscular contraction. <u>Journal of Biomechanics</u>, Vol.10, pp 97-106.
- Jensen, R. H. and Davy, D. T. (1975). An investigation of muscle lines of action about the hip: A centroid line approach vs the straight line approach. <u>Journal of Biomechanics</u>, Vol.8, No.2, pp 103-110.
- Jobe, F. W., Tibone, J. E., Perry, J., and Moynes, D. (1983). An EMG analysis of the shoulder in throwing and pitching a preliminary report, The American Journal of Sports Medicine, Vol.11, pp 3-5.
- Jobe, F. W., Radovich, D., Moynes, T. J., and Perry, J. (1984). An EMG analysis of the shoulder in pitching. The American Journal of Sports Medicine, Vol.12, pp 218-220.
- Jöris, H. J. J., van Muyen, A. J. E., van Ingen Schenau, G. J., and Kemper, H. C. G. (1985). Force, velocity and energy flow during the overarm throw in femal handball players. <u>Journal of Biomechanics</u>, Vol.18, pp 409-414.
- Kapanji, I. A. (1982). The Physiology of the Joints. Vol. 1
 Upper limb. Churchill Livingstone, New York.

- Kent, B. E. (1971). Functional anatomy of the shoulder complex. <u>Physical Therapy</u>, Vol.51, pp 867-887.
- Kieft, G. J. and Bloem, J. L. (1988). In Falke, T. H. M. (ed.), Essentials of Clinical MRI. Martinus Nijhoff Pub., Boston. pp 197-202.
- King, A. I. (1984). A review of biomechanical models.

 <u>Journal of Biomechanical Engineering</u>, Vol.106,
 pp 97-105.
- Kreighbaum, E. and Barthels, K. M. (1985). A qualitative approach for studying human movement. Biomechanics (7th ed.), MacMillan Pub., New York. pp 205-214.
- Kuester, J. L. and Mize, J. H. (1973). Optimization techniques with Fortran. McGraw-Hill Book Co., New York.
- Lance, G. N. (1960). Numerical Methods for High Speed Computers. Iliffe and Sons, London.
- Langer, D. F. and Hemami, H. (1985). Dynamics, control and simulation of the jump of a quadruped. <u>Mathematical Biosciences</u>, Vol.75, pp 257-277.
- Langrana, N. A. (1981). Spatial kinematic analysis of the upper extremity using a biplanar videotaping method.

 <u>Journal of Biomechanical Engineering</u>, Vol.103, pp 11-17.
- Lindner, E. (1971). The phenomenon of the freedom of lateral deviation in throwing (Wurfseitenfreiheit). In Vredenbregt, J., and Wartenweiler, J. (eds.), Medicine & Sport Vol.6, Biomechanics II, University Park Press, Baltimore. pp 240-245.
- Logan, G. A., McKinney, W. C., Rowe, W., and Lumpe, J. (1966). Effect of resistance through a throwing range of motion on the velocity of a baseball. <u>Perceptual and Motor Skills</u>, Vol. 23, No. 1, pp 25-34.
- Logan, G. A. and McKinney, W. C. (1970). Elbow joint motion. Anatomic Kinesiology (2nd ed), Wm.C.Brown Co., Dubugue, Iowa. pp 171-186.
- Lohman, T. G., Roche, A. F., and Martorell, R. (1988).
 Anthropometric Standardization Reference Manual.
 Human Kinetics Books, Champaign, Illinois.
- London, J. T. (1981). Kinematics of the elbow. <u>The Journal</u> of Bone and Joint Surgery, Vol.63-A, pp 529-535.

- MacConail, M. A. (1941). The mechanical anatomy of the carpus and its bearings on some surgical problems.

 <u>Journal of Anatomy</u>, Vol. 75, pp 166-175.
- Martin, P. E., Mungiole, M., Marzke, M. W. and Longhill, J. M. (1989). The use of magnetic resonance imaging for measuring segment inertial properties. <u>Journal of Biomechanics</u>, Vol. 22, No. 4, pp 367-376.
- Mathews, J. H. (1987). Numerical Methods for Computer Science, Engineering, and Mathematics. Prentice Hall, Englewood Cliffs, New York.
- Mansour, J. M. and Audu, M. L. (1986). The passive elastic moment at the knee and its influence on human gait.

 <u>Journal of Biomechanics</u>, Vol.19, pp 369-373.
- Morrey, B. F. and Chao, E. Y. (1976). Passive motion of the elbow joint. <u>The Journal of Bone and Joint Surgery</u>, Vol.58-A, pp 501-508.
- Moynes, D. R., Perry, J., Antonelli, D.J., and Jobe, F.W. (1986). Electromyography and motion analysis of the upper upper extremity in sports. <u>Physical Therapy</u>, Vol.66, pp 1905-1911.
- Mueller, K. J. and Buehrle, M. (1987). Comparison of static and dynamic strength of the arm extensor muscles. In Jonsson, B. (ed.), Biomechanics X-A. Human Kinetics Pub., Champaign, Illinois, pp 501-505.
- Nigg, B. M. (1982). Perspectives in biomechanics applied to sport and physical education. In Huiskes, R., van Campen, D. H., and de Wijn, J. R. (eds.), Biomechanics: principles and applications. Martinus Nijhoff Pub., Boston. pp 19-30.
- Nikravesh, P. E. (1988). Computer-Aided Analysis of Mechanical Systems. Prentice Hall, Englewood Cliffs, New Jersey.
- O'brien, D. J. (1990). Personal Communication.
 Machigan State University.
- Otahal, S. (1971). A method of measuring some kinetic properties of voluntary muscle activity. In Vredenbregt, J. and Wartenweiler, J. (eds.), Medicine & Sport, Vol.6, Bimechanics II., University Park Press, Baltimore. pp 181-184.

- Panjabi, M. (1979). Validation of mathematical models.

 <u>Journal of Biomechanics</u>, Vol.12, pp 238.
- Pappas, A. M., Zawacki, R. M., and Sullivan, T. J. (1985).

 Biomechanics of baseball pitching. <u>The American</u>

 <u>Journal of Sports Medicine</u>, Vol.13, pp 216-222.
- Patriarco, A. G., Mann, R. W., Simon, S. R., and Mansour, J. M. (1981). An evaluation of the approaches of optimization models in the prediction of muscle forces during human gait. <u>Journal of Biomechanics</u>, Vol.14, pp 513-525.
- Pauly, J. E., Rushing, J. L., and Scheving, L. E. (1967). An electromyographic study of some muscles crossing the elbow joint. Anatomical Record, Vol.159, pp 47-54.
- Pedotti, A., Krishnan, V. V., and Stark, L. (1978).

 Optimization of muscle force sequencing in human locomotion. <u>Mathematical Biosciences</u>, Vol.38, pp 57-76.
- Peindl, R. D. and Engin, A. E. (1987). On the biomechanics of human shoulder complex-II. Passive resistive properties beyond the shoulder complex sinus. <u>Journal of Biomechanics</u>, Vol.20, pp 119-134.
- Plagenhoef, S. C. (1966). Methods for obtaining kinetic data to analyze human motions. Research Quarterly, Vol.37, pp 103-112.
- Plagenhoef, S. C. (1968). Computer programs for dotaining kinetic data on human movement. <u>Journal of Biomechanics</u>, Vol.1, No.3, pp 221.
- Plagenhoef, S. C. (1971). Patterns of Human Motion-A cinematographic analysis. Prencite-Hall, Englewood Cliffs, New Jersey.
- Pletta, D. H. and Frederick, D. (1964). Engineering Mechanics: Statics and Dynamics. Ronald Press Co., New York.
- Provins, K. A. and Salter, N. (1967). Maximum torque exerted about the elbow joint. <u>Journal of Applied Physiology</u>, Vol.7, pp 393-398.
- Ramey, M. R. and Yang, A. T. (1981). A simulation procedure for human motion studies. <u>Journal of Biomechanics</u>, Vol.14, No.4, pp 203-213.
- Rasch, P. J. and Burke, R. K. (1978). Movement of elbow and radio-ulnar joints. Kinesiology and Applied Anatomy. Lea & Febiger, Philadelphia. pp 222-241.

- Redfield, R. and Hull, M. L. (1986). Prediction of pedal forces in bicycling using optimization methods. <u>Journal of Biomechanics</u>, Vol. 19, No. 7, pp 523-540.
- Remizov, L. (1984). Biomechanics of optimal flight in skijumping. <u>Journal of Biomechanics</u>, Vol.17, pp 167-171.
- Richardson, A. B. (1983). Overuse syndromes in baseball, tennis, gymnastics, and swimming. <u>Clinics in Sports Medicine</u>, Vol.2, pp 379-390.
- Rodrigue, D. and Gagnon, M. (1983). The evaluation of forearm density with axial tomography. <u>Journal of Biomechanics</u>, Vol. 16, No. 11, pp 907-913.
- Roth, K. (1984). NMR-Tomography and-Spectroscopy in Medicine. Springer-Verlag, New York.
- Seireg, A. and Arvikar, R. J. (1973). A mathematical model for evaluation of forces in lower extremities of the musculo-skeletal system. <u>Journal of Biomechanics</u>, Vol.6, pp 313-326.
- Seireg, A. and Arvikar, R. J. (1975). The prediction of muscular load sharing and joint forces in the lower extremities during walking. <u>Journal of Biomechancis</u>, Vol. 8, pp 89-102.
- Seireg, A. and Arvikar, R. J. (1989). Biomechanical analysis of the musculoskeletal structure for medicine and sports. Hemisphere Pub., New York.
- Selin, C. (1959). An analysis of the aerodynamics of pitched baseballs. Research Quarterly, Vol. XXX, pp 232-240.
- Shiba, R. and Sorbie, C. (1985). Axis of flexion-extension of humero-ulna joint. In Kashiwagi, D. (ed.), Elbow Joint. Excerpta medica, New York. pp 19-24.
- Shoup, T. E. (1984). Applied Numerical Methods for the Microcomputer. Prentice-Hall, Englewood Cliffs, New Jersey.
- Sisto, D. J., Jobe, F. W., Moynes, D. R., and Antonelli, D. J. (1987). An electromyographic analysis of the elbow in pitching. The American Journal of Sports Medicine, Vol.15, pp 260-263.
- Springings, E. J. (1986). Sport biomechanics data collection modeling and inplementation stages of development.

 <u>Canadian Journal of Sports Science</u>, Vol.13, No.1, pp 3-7.

- Tajima, T. (1985). Functional anatomy of the elbow joint. In kashiwagi, D. (ed.), Elbow Joint(Proceeding of the Int. seminar, Kobe, Japan). Excerpta Medica, New York. pp 3-24.
- Tolbert, J. R., Blair, W. F., Andrews, J. G., and Crowninshield, R. D. (1985). The kinetics of normal and prosthetic wrists. <u>Journal of Biomechanics</u>, Vol.18, pp 887-897.
- Torzilli, P. A. (1982). Biomechanics of the elbow. In Inglis, A. E. (ed.), American academy of orthopaedic surgeons symposium on total joint replasement of the upper extremity. The C.V. Mosby, St. Louis, Missouri. pp 150-168.
- Travill, A. (1962). Electromyographic study of the extensor apparatus of the forearm. <u>Anatomical Record</u>, Vol. 144, pp 373-376.
- Van Leemputte, M., Spaepen, A. J., Willemx, E. J. (1987). Effect of the contraction history on the forcevelocity relation of elbow flexors. In Jonsson, B. (ed.), Biomechanics X-A. Human Kinetics Pub., Champaign, Illinois. pp 271-276.
- Van Zuylen, E. J., van Velzen, A., and van Der Gon, J. J. D. (1988). A biomechanical model for flexion torques of human arm muscles as a function of elbow angle. <u>Journal of Biomechanics</u>, Vol.21, No.3, pp 183-190.
- Vidic, B. and Suarez, F. R. (1984). Photographic Atlas of the Human Body. The C. V. Mosby Company. St. Louis, Missouri.
- Walton, J. S. (1981). Close-range Cine-photogrammetry: A generalized technique for quantifying gross human motion. Pennsylvania State University, Doctral Dissertation.
- Whiting, W., Puffer, J. C., Finerman, G. A., Gregor, R. J., and Maletis, G. B. (1985). Three-dimensional cinematographic analysis of water polo throwing in elite performers. <u>American Journal of Sports Medicine</u>, Vol. 13, pp 95-98.
- Wickstrom, R. L. (1983). Fundamental motor patterns. Lea & Febiger, Philadelphia.
- Wittenburg, J. (1977). Dynamics of Systems of Rigid Bodies. B. G. Teubner, Stuttgart.

- Yoon, Y. S. and Mansour, J. M. (1982). The passive elastic moment at the hip. <u>Journal of Biomechanics</u>, Vol.15, pp 905-910.
- Youm, Y., Sprague, B. L., and Flatt, A. E. (1976). Moment arm analysis of the prime wrist movers. In Komi, P. V. (ed.), Int. series on biomechanics Vol.1A, Biomechanics V-A. University of Park Press, Baltimore. pp 355-365.
- Youm, Y., McMurtry, R. Y., Flatt, A. E., and Gillespie, T. E. (1978). Kinematics of the wrist. <u>Journal of Bone Joint and Surgery</u>, Vol. 60-A, pp 423-431.
- Youm, Y. (1980). Biomechanics of human elbow joint. Advances in Bioengineering. pp 83-86.
- Youm, Y., Dryer, R. F., Thambyrajah, K., Flatt, A. E., and Sprangue, B. L. (1979). Biomechanical analyses of forearm pronation-supination and elbow flexion-extension. <u>Journal of Biomechanics</u>, Vol.12, pp 245-255.
- Young, R. D. (1970). A three-dimension Mathematical Model of an Auto Mobil Passenger. Texas Transportation Institute, Research Report 140-2. College station, Texas.
- Zahalak, G. I. and Heyman, S. J. (1979). A quantitative evaluation of the frequency-response characteristics of active human skeletal muscle in vivo. <u>Journal of Biomechanical Enineering</u>, Vol.101, pp 28-37.
- Zajac, F. E. and Gordon, M. E. (1989). Determining muscles force and action in multi-articular movement. <u>Exercise</u> and <u>Sport Sciences Reviews</u>, Vol. 17, pp 187-230.
- Zatsiorsky, V. M. (1978). The present and future of biomechanics of sports. In Landry, F., and Orban, W. A. R. (eds.), Biomechanics of Sports and Kinanthropometry. Symposia Specialists Inc. pp 11-17.
- Zatsiorsky, V. M. and Seluyanov, V. (1983). The mass and inertia characteristics of the main segments of the human body. In Matsui, H. and Kobayashi, K. (eds.). Biomechanics VIII-B. Human Kinetics, Champaign, Illinois.
- Zatsiorsky, V. M. and Seluyanov, V. (1985). Estimation of the mass and inertia characteristics of the human body by means of the best predictive regression equations. In Winter, D. A., Norman, R. W., Wells, R. P., Hayes, K. C. and Patla, A. E. (eds.), Biomechanics IX-B. Human Kinetics. Champaign, Illinois.

Zollinger, R. L. (1973). Mechanical analysis of windmill fast pitch in women's softball. The Research Ouarterly, Vol.44, pp 290-300.

MICHIGAN STATE UNIV. LIBRARIES
31293007620218